SOME DIELECTRIC AND FAR-INFRARED STUDIES OF DISPERSION

A THESIS SUBMITTED BY

C. K. McLellan

IN PARTIAL FULFILLMENT OF THE REQUIREMENTS OF THE DEGREE

OF

Doctor of Philosophy

TO

THE UNIVERSITY OF MANITOBA

WINNIPEG, MANITOBA

MAY, 1977

COPY NUMBER: 2

SOME DIELECTRIC AND FAR-INFRARED STUDIES OF DISPERSION

BY

C.K. MCLELLAN

A dissertation submitted to the Faculty of Graduate Studies of the University of Manitoba in partial fulfillment of the requirements of the degree of

DOCTOR OF PHILOSOPHY

TABLE OF CONTENTS

ABSTRACT

Studies have been carried out on some dielectric and far-infrared absorptions and their associated dispersions, with particular emphasis on the processes observed in the far-infrared region between 10 and 200 cm^{-1} frequency. The initial work on pure liquid halobenzenes, benzonitrile and 1,1,1-trichloroethane using microwave-frequency Michelson interferometers and a Grant cell was aimed at measuring the parameter ε_∞, being the high-frequency limiting value of the complex dielectric permittivity, and thereby the magnitude of the far-infrared dispersion, $(\varepsilon_\infty - n_D^2)$. This work led to the conclusion that these parameters may not be derived with sufficient accuracy from a Cole-Cole analysis of the experimental data since there is considerable overlap of the absorptions due to dielectric relaxation and the far-infrared absorption processes.

Characterization of the dielectric relaxations observed in solutions of polar solutes dissolved in atactic polystyrene was undertaken through a study of aromatic molecules containing the rotatable acetyl substituent group and of some analogous rigid molecules. Preparations of these solutions as solid disks and the dielectric measurements using a General Radio 1615-A capacitance bridge and a Hewlett-Packard Q-meter with appropriate temperature-controllable cells have been described. The enthalpy barrier to intramolecular

rotation of the acetyl group was found to be in the range 29 to 31 kJ mol^{-1}; the entropy of activation was 20 to 40 $JK^{-1}mol^{-1}$ in acetophenone and like molecules, estimated by application of the Eyring equation to the dielectric data.

Far-infrared studies were conducted to take advantage of the considerable reduction of the rate of molecular relaxation in polystyrene matrix solutions compared to that in dilute solutions in liquid benzene. The absorption spectra of four molecules including two rod-like substituted biphenyls showed clear broad bands in the 40 to 80 cm^{-1} range very similar to those found in benzene solutions. It was concluded that the far-infrared broad band absorption is due to a type of molecular motion separate from that of dielectric absorption, and is not merely a continuation of the dielectric absorption. Further, the far-infrared absorption did not appear sensitive to the nature of the solvent nor to the rate of molecular relaxation, for the intensity, frequency, and bandwidth of the absorption band were not altered very much on passing from benzene to polystyrene as solvent. Similar results have been obtained from a very cold polystyrene matrix solution and from the supercooled liquid phase of n-propylbenzene.

Acknowledgements

The research which provided the material for this thesis was carried out at Lakehead University, Thunder Bay, Ontario under the direction of Dr. S. Walker, Chairman of my thesis advisory committee, for whose constant guidance and frequent helpful suggestions I wish to express my sincere thanks. I should like to thank also Drs. C. E. Burchill, E. M. Kartzmark, R. Wallace and C. W. Searle of my advisory committee for their assistance.

I am indebted to my fellow students and to the staff of the Chemistry Department, particularly Dr. N. Weir, of Lakehead University for frequent informative discussions. Thanks are due also to Mr. B. K. Morgan for his considerable technical assistance throughout the course of this work.

Financial support for this work was provided by the National Research Council of Canada, which assistance is acknowledged with thanks.

Finally, I wish to express my gratitude to my wife, Betty, for her constant support and encouragement which has allowed me to pursue my studies and research interests.

CHAPTER I

Introduction

DIELECTRIC ABSORPTION

The measurement of the dielectric properties of materials has been employed for some time in investigations both of molecular structure and of molecular motion. Very low frequency dielectric data may be used to calculate the permanent dipole moment of a molecule, which may be related to its structure. The major use of dielectric properties has been in the study of the frequency dependence of the complex dielectric permittivity,

$$\varepsilon^* = \varepsilon' - i\varepsilon'' \qquad \text{I-1}$$

where ε', the real part, is commonly called the dielectric constant (even though it is not a constant), ε'', the imaginary part, is called the dielectric loss factor, and $i = \sqrt{-1}$. For a simple dipolar system, the frequency dependence of this complex quantity may be expressed[1] by Eqn. I-2.

$$\frac{\varepsilon^* - \varepsilon_\infty}{\varepsilon_0 - \varepsilon_\infty} = \frac{1}{1 + i\omega\tau} \qquad \text{I-2}$$

where ε_0 is the low-frequency limiting value of ε^*,

ε_∞ is the high-frequency limiting value of ε^*,

ω is the angular frequency in rad s^{-1},

and τ is the characteristic relaxation time in s.

Combining Equations I-1 and I-2 and separating into real and imaginary parts by rationalization yields the Debye-Pellat

$$\frac{\varepsilon' - \varepsilon_\infty}{\varepsilon_0 - \varepsilon_\infty} = \frac{1}{1 + (\omega\tau)^2} \qquad \text{I-3}$$

$$\frac{\varepsilon''}{\varepsilon_0 - \varepsilon_\infty} = \frac{\omega\tau}{1 + (\omega\tau)^2} \qquad \text{I-4}$$

Equations I-3 and I-4. By inspection it may be seen that for the limiting case $\omega \to 0$, $\varepsilon' \to \varepsilon_0$ and $\varepsilon'' \to 0$, while as $\omega \to \infty$, $\varepsilon' \to \varepsilon_\infty$ and $\varepsilon'' \to 0$ again. The maximum value of ε'' occurs for $\omega = 1/\tau$ and has the value $(\varepsilon_0 - \varepsilon_\infty)/2$, and at this frequency, $\varepsilon' = \varepsilon_\infty + (\varepsilon_0 - \varepsilon_\infty)/2 = (\varepsilon_0 + \varepsilon_\infty)/2$. A plot of ε' versus the natural logarithm of angular frequency is sigmoidal in shape, decreasing from ε_0 at $\ln(\omega) \to -\infty$ through the inflection point of $\varepsilon' = (\varepsilon_0 + \varepsilon_\infty)/2$ at $\ln(\omega) = -\ln(\tau)$ to the asymptotic value ε_∞ as $\ln(\omega) \to \infty$. The plot of ε'' versus $\ln(\omega)$ is somewhat bell-shaped with the maximum value $(\varepsilon_0 - \varepsilon_\infty)/2$ at $\ln(\omega) = -\ln(\tau)$ and decreases asymptotically to zero as ω becomes either very small or very large.

Elimination of the frequency and relaxation time variables from Eqns. I-3 and I-4 yields Eqn. I-5 which is the basis of the Cole-Cole complex plane plot.

$$\left[\varepsilon' - \frac{\varepsilon_0 + \varepsilon_\infty}{2}\right]^2 + (\varepsilon'')^2 = \left[\frac{\varepsilon_0 - \varepsilon_\infty}{2}\right]^2 \qquad \text{I-5}$$

The plot of ε'' versus ε' is thus a semicircle with radius $(\varepsilon_0 - \varepsilon_\infty)/2$ and centre at $((\varepsilon_0 + \varepsilon_\infty)/2, 0)$. Thus, if ε' and ε'' are measured experimentally for several values of frequency, the Cole-Cole plot may be prepared and a semicircle drawn through the points to extrapolate the graph to obtain an estimate of ε_∞. As is the case in most extrapolation procedures, this estimate is likely to be more accurate if experimental points on the graph are available close to the extrapolated end of the curve (in this case, this means values measured at very high frequencies).

If more than one relaxation process is involved in the dielectric absorption, the analysis of experimental data becomes more complicated. The simplest case here occurs when there are only two distinct relaxation processes, and for this situation Budó has proposed[2] that Eqns. I-3 and I-4 may be modified to include a weighted sum of two terms, one for each process, yielding Eqns. I-6 and I-7.

$$\frac{\varepsilon' - \varepsilon_\infty}{\varepsilon_0 - \varepsilon_\infty} = \frac{C_1}{1 + (\omega\tau_1)^2} + \frac{C_2}{1 + (\omega\tau_2)^2} \qquad \text{I-6}$$

$$\frac{\varepsilon''}{\varepsilon_0 - \varepsilon_\infty} = \frac{C_1\omega\tau_1}{1 + (\omega\tau_1)^2} + \frac{C_2\omega\tau_2}{1 + (\omega\tau_2)^2} \qquad \text{I-7}$$

In these equations, C_1 and C_2 are normalizing constants such that $C_1 + C_2 = 1$, and τ_1 and τ_2 are the characteristic relaxation times for the two processes. Iterative computer programs are available which vary trial values of C_1, C_2, τ_1, τ_2 and ε_∞ to obtain the best fit of experimentally-measured values of ε' and ε'' as a function of ω to values calculated from Eqns. I-6 and I-7. In principle this approach may be extended to more than two terms in the summations, but in practice it is often difficult to meet the requisite conditions and such a procedure is seldom attempted.

When neither Debye-Pellat nor Budó analysis is suitable, it is common practice in dielectrics work to employ an empirical relationship for the analysis of experimental data, such as the Cole-Cole equation, the Cole-Davidson equation, or the Fuoss-Kirkwood equation. Cole and Cole [3] modified Eqn. I-2 to obtain Eqn. I-8, which may be rationalized [1] to yield Eqn. I-9 and Eqn. I-10:

$$\frac{\varepsilon^* - \varepsilon_\infty}{\varepsilon_0 - \varepsilon_\infty} = \frac{1}{1 + (i\omega\tau_0)^{1-\alpha}} \qquad \text{I-8}$$

where $i = \sqrt{-1}$

$$\frac{\varepsilon' - \varepsilon_\infty}{\varepsilon_0 - \varepsilon_\infty} = \frac{1 + (\omega\tau_0)^{1-\alpha} \sin(\alpha\pi/2)}{1 + 2(\omega\tau_0)^{1-\alpha} \sin(\alpha\pi/2) + (\omega\tau_0)^{2(1-\alpha)}} \qquad \text{I-9}$$

$$\frac{\varepsilon''}{\varepsilon_0 - \varepsilon_\infty} = \frac{(\omega\tau_0)^{1-\alpha} \cos(\alpha\pi/2)}{1 + 2(\omega\tau_0)^{1-\alpha} \sin(\alpha\pi/2) + (\omega\tau_0)^{2(1-\alpha)}} \qquad \text{I-10}$$

where in these equations, τ_0 is the mean, or most probable, relaxation time, and α is known as the Cole-Cole distribution parameter which may take values $0 \leq \alpha < 1$. For $\alpha = 0$, the equations reduce to the Debye-Pellat Eqns. 1-2, 1-3 and 1-4. For non-zero values of α, the Cole-Cole complex plane plot of ε'' versus ε' retains the semicircular form, but the centre lies below the ε' axis on a line drawn in the positive ε' direction from ε_∞ but rotated in a clockwise direction about this point by the angle $\alpha\pi/2$ radians.

Davidson and Cole[4] found that the frequency dependence of the complex dielectric permittivity of some systems could be described by Eqn. I-11 which may be rationalized[5] to Eqns. I-12 and I-13.

$$\frac{\varepsilon^* - \varepsilon_\infty}{\varepsilon_0 - \varepsilon_\infty} = \frac{1}{(1 + i\omega\tau)^h} \qquad \text{I-11}$$

$$\frac{\varepsilon' - \varepsilon_\infty}{\varepsilon_0 - \varepsilon_\infty} = \cos^h(\phi)\cos(h\phi) \qquad \text{I-12}$$

$$\frac{\varepsilon''}{\varepsilon_0 - \varepsilon_\infty} = \cos^h(\phi)\sin(h\phi) \qquad \text{I-13}$$

where $i = \sqrt{-1}$

and $\phi = \arctan(\omega\tau)$

In these equations the parameter h may take values $0 < h \leq 1$, with h = 1 corresponding to the Debye Eqn. I-2. The shape of the complex plane plot described by these equations is a skewed arc (i.e., not symmetrically semicircular) with the maximum value of ε'' occurring to the right of the centre of the arc (i.e., at lower frequencies and higher values of ε'). This is often taken to indicate that the dielectric absorption arises from a relaxation mechanism which involves co-operative motion of the surroundings of the dipolar molecule.

FAR-INFRARED ABSORPTION

The theories and equations outlined above appeared adequate to describe the dielectric behaviour of polar molecules. However, in 1950 Whiffen [6] reported that, for six non-polar liquids expected to exhibit no dielectric loss, values of $\tan \delta = \varepsilon''/\varepsilon'$ increased linearly with frequency. He considered four possible sources of the observed absorption, concluding that it was due to the existence of small temporary electric dipole moments induced in the molecules by distortions resulting from bi-molecular collisions. He noted that the relaxation time estimated from the data was of the order of 1×10^{-12} s, similar to the estimated frequency of bimolecular collisions.

In 1957 van Eick and Poley [7] reported data for the polar molecules, chlorobenzene and bromobenzene, which indicated that the value of ε_∞ was significantly larger than the square of the refractive index measured at the sodium D line. According to the Maxwell equations, the complex dielectric permittivity is equal to the square of the complex refractive index. Further, the difference between the refractive indices of a liquid measured above and below the frequencies at which normal infrared absorptions occur is considerably smaller

than the differences observed by van Eick and Poley. Therefore, it appeared that there must be some additional dispersion, and hence an associated absorption, located between the microwave frequency region and the low-frequency infrared region in which fundamental bending vibrations were known to occur. Moreover, van Eick and Poley had found that the magnitude of this dispersion appeared to be strongly temperature dependent.

For a time in the early 1960's there was some discussion as to whether or not the difference between ε_∞ and $(n_D)^2$ could be accounted for by the known infrared absorption bands. In 1965, three pieces of information were reported which clarified the issue at least in part. Garg et al.[8] reported that new high-frequency microwave equipment confirmed the existence of non-zero dielectric loss factors for four nominally non-polar liquids. Gebbie et al.[9] noted that, at 29.7 cm^{-1} frequency, the ε' values of four monohalobenzenes were significantly lower than could be predicted from use of the Debye-Pellat equations based on lower-frequency microwave measurements. This indicated that there was, indeed, some extra dispersion process operative at frequencies above those at which dielectric absorptions were known to occur. Then Chantry and Gebbie[10] published the far-infrared absorption spectra in the range 10 to 400 cm^{-1} for liquid and solid phases of pure chlorobenzene, the spectra having been obtained

by Fourier transformation of interferometric data. The liquid showed a broad, featureless absorption centred near 45 cm^{-1}, while the solid showed two sharp peaks at 36 and 57 cm^{-1}. From the similarity of frequencies they suggested that the liquid-phase absorption arose from a "pseudo-lattice". One year later, Bradley et al.[11] published similar results for both chlorobenzene and carbon disulphide.

Dielectric measurements reported by Hassell and Walker[12], Santraelli et al.[13] and Crossley and Walker[14] suggested that there might be a high-frequency absorption process in several liquid systems with relaxation times of the order of the frequency of bimolecular collisions. Chamberlain et al.[15] reported that both polar and non-polar liquids exhibited a definite absorption at a frequency of 29.7 cm^{-1}. In 1967, Gabelnick and Strauss[16] reported that liquid carbon tetrachloride exhibited an absorption peak near 40 cm^{-1} with an associated very short relaxation time and small dipole moment, and that the moment of inertia estimated from this frequency was considerably less than that of the whole molecule. They also found that this absorption peak was absent in the gaseous phase and concluded that it must be a property of the liquid phase, and not of the molecule itself.

Chantry et al.[17] studied pure solid and liquid phases of

three non-polar molecules of different shapes in the far-infrared region, finding that all three liquids gave absorption bands at frequencies similar to those found in the crystalline lattices. They suggested that a liquid molecule is entrapped in a pseudo-lattice of neighbours which induce in the trapped molecule a small dipole, the magnitude and direction of which alter as the pseudo-lattice oscillates. These authors pointed out that the "point dipole" treatment common in dielectrics theories is inappropriate to far-infrared absorptions since the inductive forces they postulated operate over distances of the order of the separation between molecules.

Davies et al.[18] noted a number of features emerging from their investigation of the far-infrared absorptions exhibited by polar liquids, both pure and in dilute solutions. The absorptions were much more intense than could be accounted for by the high-frequency tail of the dielectric relaxation processes as described by the full Debye theory, in which the effect of the molecular moment of inertia is taken into account. The absorption bands were broader than the Debye theory predicts for a relaxational process. The intensities of the absorptions appeared to be related to the magnitude of the permanent molecular dipole moment. Finally, the absorption bands appeared relatively insensitive to the nature of the solvent used for solution measurements but were affected by temperature. A decrease in sample temperature produced a sharper peak which shifted to higher frequency.

Davies et al.[19] also examined several non-polar liquids, finding that all exhibited an absorption in the far-infrared region. The intensity of these absorptions was increased if the molecule was more flexible or if it contained more polar bonds. They concluded that the absorptions in non-polar liquids were probably composed of a superposition of overlapping rotational-translational resonance modes. Garg et al.[20] assigned the absorptions observed in non-polar liquids to molecules possessing a multipole-induced dipole and trapped temporarily in a cage of neighbours for times of the order of the time between molecular collisions.

Kroon and van der Elsken[21] investigated the effects of temperature and solvent on the absorptions of several polar molecules. They found that the major portion of the absorption could be accounted for by an equation developed by Gordon[22] for pure rotations in the liquid phase and suggested that the remainder should be assigned to translational motion. They felt that the band shifts with altered temperature were due to the temperature dependence of the relative importance of these two processes. Jain and Walker[23] studied several polar and non-polar molecules in liquid phase and found that the observed absorption intensities did not agree with predictions based on Gordon's formula. They concluded that the rotational model was inadequate on its own, even though rotational motion could be involved as suggested by the fact that there was a strong correlation between

the maximum absorption intensity and the quotient μ^2/I, where μ is the permanent molecular dipole moment and I is the molecule's average moment of inertia for rotations.

Bulkin[24] argued that the molecular cage concept was not involved in far-infrared absorption since his investigation of polar solutes in a range of non-polar solvents showed that the absorption intensity was proportional to concentration and therefore apparently insensitive to the solvent polarity. He favoured a mechanism of vibrations of dipole-dipole complexes.

Studies of guest molecules in clathrates,[25,26] which may be regarded as providing a well-defined model cage, were interpreted to indicate that absorptions in the far-infrared region were due both to dipoles induced during translational motion of the guest and to hindered rotational motion of the guest. Davies et al.[27] concluded that the absorptions by non-polar molecules were primarily of collisional origin and involved the polarizabilities of the more readily accessible groups within the molecules, whereas those in polar molecules were dominated by absorptions of a resonance character which involved movement of molecular and/or group dipole moments.

In 1968 Brot et al.[28] reported that the absorption spectra of some solid phases of tert-butyl chloride were similar to those of

the pure liquid, and that only the cold solid phase in which no molecular rotation is possible showed a separation into two peaks of the absorption band. The author of the present work has examined the effect of temperature on several molecules in pure liquid and solid phases.[29,30] In general, both the maximum absorption intensity and the frequency at which this was found increased smoothly as temperature was decreased in the liquid phase. For some almost spherical molecules molecular rotation occurs in the warmer solid phases until at a lower temperature a phase transition takes place to a non-rotator solid. The far-infrared absorption spectra of these rotator solid phases were very similar to those of the corresponding liquid phases, with no sudden change of band intensity or frequency on their passing through the liquid-rotator solid phase change. Only in the non-rotator solids were the absorption spectra different, in these cases the spectra being composed of one or more intense narrow bands due to translational motions. This behaviour was exhibited also by the non-polar molecule, carbon tetrachloride.

THE HILL MODEL

In 1963, Hill[31] proposed a model in which a polar solute molecule was temporarily trapped in a cage of nearest neighbours. As it rotated, it encountered potential energy minima involving, for example, dipolar forces and steric factors. Such a molecule could undergo reorientation characterized by a longer relaxation time, and/or oscillations about its equilibrium position at one potential energy minimum, characterized by a shorter relaxation time. She stated that the potential energy barriers between minima must be greater than the thermal energy, kT, so that the effect would not be obscured by considerable switching between minima. Hill surmised that molecules which exhibit a rotator solid phase would not meet this criterion and therefore would not exhibit any absorption in the far-infrared region. At that time the available dielectric evidence suggested that for several molecules of this type there was no disagreement between ε_∞ and $(n_D)^2$, which indicated that there should not be any absorption at frequencies above the microwave region. As outlined in the preceding section, this suggestion pertaining to rotator solid phases has proved to be inadequate.

From her model, Hill developed Eqn. I-14:

$$\frac{\varepsilon_\infty - n^2}{\varepsilon_o - n^2} = \frac{1 + i\omega\tau\,(2kT/I\omega_o^{\,2})\,(a - ib)}{1 + i\omega\tau} \qquad \text{I-14}$$

where $i = \sqrt{-1}$

$$a = \frac{1 - (\omega/\omega_o)^2}{[\,1 - (\omega/\omega_o)^2\,]^{\,2} + (r\omega/\omega_o)^2}$$

$$b = \frac{r\omega/\omega_o}{[\,1 - (\omega/\omega_o)^2\,]^{\,2} + (r\omega/\omega_o)^2}$$

I is the molecular moment of inertia,

ω_o is the natural frequency of the oscillation,

and r is a damping coefficient.

For high frequencies Hill made the approximation $\omega/\omega_o \ll 1$ and obtained Eqn. I-15, from which ω_o may be calculated since all other quantities are measurable.

$$\frac{\varepsilon_\infty - n^2}{\varepsilon_o - n^2} = \frac{2kT}{I\omega_o^{\,2}} \qquad \text{I-15}$$

For the halobenzenes Eqn. I-15 predicts ω_o values in the range 17 to 33 cm^{-1}, while the observed frequency at the peak of the broad band absorption of pure chlorobenzene at T = 300K is 45 cm^{-1}.

In 1968, Hill [32] considered qualitatively a liquid model composed of a continuous distribution of damped resonance systems by taking an algebraic sum of only three overlapping absorption curves of equal amplitude. She noted that the frequency predicted by Eqn. I-15 was greater than that found for the maximum absorption coefficient in the overlap model, which in turn was greater than the frequency of maximum dielectric loss factor, where the dielectric loss factor may be calculated from the optical absorption coefficient, α, via Eqn. I-16:[33]

$$\varepsilon'' = \frac{n\alpha}{2\pi\bar{\nu}} \qquad \text{I-16}$$

where ε'' is the dielectric loss factor at frequency $\bar{\nu}$ cm^{-1}, α is the optical absorption coefficient, and n is the refractive index at this frequency.

In 1969, Hill[34] considered the types of absorption and refractive index curves which might result from assuming a continuous distribution of resonance frequencies. Both Debye and Gaussian

distribution functions were used to describe this distribution, and both gave satisfactory comparisons with experimental data, provided that the damping coefficient was close to unity. She concluded that it was possible to account for the observed far-infrared absorptions with a model of a distribution of resonance systems, but that it was difficult, and perhaps impossible, to discern from experimental data the exact form of the distribution function.

In a 1971 paper, Hill[35] examined the far-infrared absorption to be expected for a dipolar molecule in the liquid phase from a theoretical treatment based on an autocorrelation function of the angular velocity of the molecule with characteristic time τ_1 for the Debye relaxation process and τ_2 for the effect of the moment of inertia of the molecule. She showed that the high-frequency absorption process causes the total absorption band in the far-infrared region to decrease in intensity to values less than could be predicted from the Debye theory, even when this latter theory includes terms to take into account the moment of inertia. The conclusion was that it is not possible to estimate the shape and intensity of the absorption band due solely to the high-frequency process by simply subtracting from the observed band that portion due to molecular relaxational processes.

Leroy et al.[36] applied an autocorrelation function treatment to the problem and derived several equations which may be employed to describe the observed far-infrared spectra. They were able to confirm experimentally an interesting prediction of their theories concerning the Cole-Cole plot for a dilute solution of 1,1,1-trichloroethane in n-hexane. At very high frequencies the ε'' versus ε' plot deviates from the semicircular form. As frequency increases (and the dielectric loss factor, ε'', decreases), the value of the real component, ε', of the complex dielectric permittivity first decreases and then increases again. As a result, the limiting value, ε_∞, is in fact larger than could be predicted by the simple semicircular extrapolation of the Cole-Cole arc.

Minami and Ohno [37] and Higasi et al. [38] have applied auto-correlation function treatments to far-infrared absorptions by polar rod-like molecules in the liquid state, based on a model akin to that of Hill. Likewise, Haffmans and Larkin [39] and Larkin[40] have considered the cases of polar spherical molecules. In all of these, if a square well model was used for the shape of the potential energy minimum encountered by the librating species, the angle through which a nearly spherical molecule may librate was of the order of 35^0. For a disk-like molecule such as iodobenzene the angle

is about 10^{0}, and for less symmetric species the libration angle may be even less. If a damped harmonic oscillator model was used instead of the square well, agreement between theory and experimental data depended upon the choice of theoretical parameters such as the damping coefficient and on the form of an assumed distribution of resonance frequencies. In either case, however, examination of that portion of the total absorption band in the far-infrared region due only to the librational motions of the molecules is rather difficult because this absorption is overlapped by a part of the dielectric absorption.

THE PRESENT WORK

It is clear from the literature that existing dielectric theories could not account for the broad band absorption in far-infrared spectra. This absorption did not appear to exist in the low-pressure gaseous phase, and the absorptions found in non-rotator solid phases appeared to be entirely different from the broad, featureless absorption band found in liquids. Moreover, solid phases in which molecular rotations are possible exhibit a broad band absorption much like those of liquid phases, irrespective of whether or not the molecules possess a permanent molecular electric dipole moment. This suggests that the process responsible for the broad band absorption involves molecular rotational motion and the influence of neighbouring molecules.

The origin of the broad band absorptions observed in the far-infrared region is frequently discussed in the literature in terms of a model advanced by Hill. This approach suggests that the absorptions are not a mere continuation of a dielectric absorption which is described inadequately by existing dielectric theories, but are due to a different process. The process is small-angle librations of a molecule within a potential energy well provided

by a cage of neighbouring molecules. The depth and width of the well and the damping coefficient for resonance in the well may vary with time as the cage geometry is altered through molecular collisions.

The Kramers-Kronig relationship, Eqn. I-17, relates absorption of energy from an applied field as a function of frequency to dispersion; that is, to the change in dielectric constant (which is the change in the square of the refractive index, according to the Maxwell equations).[41] This equation is not restricted to any specific model. It is therefore completely general.

$$\Delta\varepsilon' = \varepsilon_o - \varepsilon_\infty = \frac{2}{\pi}\int_0^\infty \frac{\varepsilon''(\nu)}{\nu}\, d\nu \qquad \text{I-17}$$

$$= \frac{2}{\pi}\int_{-\infty}^{\infty} \varepsilon''(\nu)\; d(\log_e \nu)$$

If there are two absorption processes, each makes its own contribution to the total dispersion $\Delta\varepsilon'$. These may be determined from Eqn. I-17 by separating the integration on the right hand side into two parts,

each of which represents an integration for absorption due solely to one of the processes. This may lead to some confusion as to the meaning of the parameter ε_∞. In this work, the following definition is made: ε_∞ is taken as the limiting high-frequency value of the dielectric permittivity due solely to the dispersion which results from dielectric relaxation. The dispersion associated with the absorptions found in the far-infrared region, in the "normal" infrared region, and all the way to the visible light region collectively amount to a "residual dispersion", $(\varepsilon_\infty - n_D^2)$, where n_D is the refractive index of the sample measured at the sodium D line frequency. Within the accuracy of estimating ε_∞ from dielectric property measurements, the dispersion contributed by "normal" infrared absorptions due to molecular vibrations is negligible compared to this total residual dispersion.[7] Thus the quantity $(\varepsilon_\infty - n_D^2)$ is a good approximation for the dispersion due solely to the broad band absorption in the far-infrared region.

The results of van Eick and Poley[7] indicated that the residual dispersion altered sharply with a change in temperature. Later studies of the broad band absorption showed no such sudden change within the liquid phase. An examination of this discrepancy has been undertaken, the results being reported in Chapter III. These data provided an opportunity to examine the usefulness of the parameter ε_∞ from dielectrics measurements, and hence of the

quantity ($\varepsilon_\infty - n_D^2$), in attempts to understand the far-infrared broad band absorption. On the basis of this investigation it was decided to approach the question from a different direction. Chapter IV reports investigations of the dielectric properties of solutions of polar molecules in polystyrene. This material has provided the information required to undertake the investigation reported in Chapter V of the far-infrared broad band absorption of some polar solutes in a polystyrene matrix in which the rate of molecular relaxation is considerably reduced from that of liquid phase samples. In addition, a study of n-propylbenzene as a super-cooled liquid has been undertaken in which the molecular relaxation was likewise very much slower than at room temperature. In these samples the contribution to total far-infrared absorption band intensity due to dielectric relaxation is therefore reduced so that it has been possible to establish that there is a separate absorption band in the far-infrared region independent of the dielectric absorption. Some features of this absorption are discussed, and suggestions made concerning the usefulness of this sample preparation technique for further research.

REFERENCES

1. C. P. Smyth, "Dielectric Behaviour and Molecular Structure", McGraw-Hill Book Co., Inc., New York, New York, U.S.A., (1955), pp. 54-56 and 68-69.

2. A. Budó, Phys. Z., 39, (1938), p. 706.

3. K. S. Cole and R. H. Cole, J. Chem. Phys., 9, (1941), p. 341.

4. D. W. Davidson and R. H. Cole, J. Chem. Phys., 19, (1951), p. 1484.

5. N. E. Hill, W. E. Vaughan, A. H. Price and M. Davies, "Dielectric Properties and Molecular Structure", Van Nostrand Reinhold Co., London, England, (1969), p. 55.

6. D. H. Whiffen, Trans. Faraday Soc., 46, (1950), p. 124.

7. A. J. van Eick and J. Ph. Poley, Appl. Sc. Res., 6B, (1957), p. 359.

8. S. K. Garg, H. Kilp and C. P. Smyth, J. Chem. Phys., 43, (1965), p. 2341.

9. H. A. Gebbie, N. W. B. Stone, F. D. Findlay and E. C. Pyatt, Nature, 205, (1965), p. 377.

10. G. W. Chantry and H. A. Gebbie, Nature, 208, (1965), p. 378.

11. C. C. Bradley, H. A. Gebbie, A. C. Gilby, V. V. Kechin and J. H. King, Nature, 211, (1966), p. 839.

12. W. F. Hassell and S. Walker, Trans. Faraday Soc., 62, (1966), p. 861.

13. V. A. Santarelli, J. A. MacDonald and C. Pine, J. Chem. Phys., 46, (1967), p. 2367.

14. J. Crossley and S. Walker, Can. J. Chem., 46, (1968), p. 847.

15. J. E. Chamberlain, E. B. C. Werner, H. A. Gebbie and W. Slough, Trans. Faraday Soc., 63, (1967), p.2605.

16. H. S. Gabelnick and H. L. Strauss, J. Chem. Phys., 46, (1967), p. 396.

17. G. W. Chantry, H. A. Gebbie, B. Lassier and G. Wyllie, Nature, 214, (1967), p. 163.

18. M. Davies, G. W. F. Pardoe, J. E. Chamberlain and H. A. Gebbie, Trans. Faraday Soc., 64, (1968), p. 847.

19. _____ Chem. Phys. Lett., 2, (1968), p. 411.

20. S. K. Garg, J. E. Bertie, H. Kilp and C. P. Smyth, J. Chem. Phys., 49, (1968), p. 2551.

21. S. G. Kroon and J. van der Elsken, Chem. Phys. Lett., 1, (1967), p. 285.

22. R. G. Gordon, J. Chem. Phys., 38, (1963), p. 1724.

23. S. R. Jain and S. Walker, J. Phys. Chem., 75, (1971), p. 2942.

24. B. J. Bulkin, Helv. Chim. Acta, 52, (1969), p. 1348.

25. J. C. Burgiel, H. Meyer and P. L. Richards, J. Chem. Phys., 43, (1965), p. 4291.

26. P. R. Davies, Dicuss. Faraday Soc., No. 48, (1969), p. 181.

27. M. Davies, G. W. F. Pardoe, J. E. Chamberlain and H. A. Gebbie, Trans. Faraday Soc., 66, (1970), p. 273.

28. C. Brot, B. Lassier, G. W. Chantry and H. A. Gebbie, Spectrochim. Acta, 24A, (1968), p. 295.

29. C. K. McLellan, M. Sc. Thesis, Lakehead University, Thunder Bay, "P", Ontario, Canada, P7B 5E1, (1971).

30. C. K. McLellan and S. Walker, J. Chem. Phys., 61, (1974), p. 2412.

31. N. E. Hill, Proc. Roy. Soc., 82, (1963), p. 723.

32. _____ Chem. Phys. Lett., 2, (1968), p. 5.

33. See reference 5, p. 300.

34. N. E. Hill, J. Phys., A 2, (1969), p. 398.

35. _____ J. Phys. C: Solid St. Phys., 4, (1971), p. 2322.

36. Y. Leroy, E. Constant, C. Abbar and P. Desplanques, Adv. Mol. Relax. Proc., 1, (1967-68), p. 273.

37. R. Minami and A. Ohno, J. Phys. Soc. Japan, 35, (1973), p. 1730.

38. K. Higasi, R. Minami, H. Takahashi and A. Ohno, J. Chem. Soc. Faraday II, 69, (1973), p. 1579.

39. R. Haffmans and I. W. Larkin, J. Chem. Soc. Faraday II, 69, (1972), p. 1729.

40. I. W. Larkin, J. Chem. Soc. Faraday II, 69, (1973), p. 1278.

41. K. D. Möller and W. G. Rothschild, "Far-Infrared Spectroscopy", Wiley-Interscience, division of John Wiley and Sons, Inc., New York, New York, U. S. A., (1971), p. 419.

CHAPTER II

Experimental Procedures

INTRODUCTION

When a material of dielectric constant ε completely fills the space between the two plates of an ideal capacitor, the dielectric constant is defined by the simple ratio :

$$\varepsilon = C/C_o \qquad \text{II-1}$$

where C is the capacitance when the space is filled with the material, and C_o is the capacitance measured when there is a perfect vacuum between plates. In fact, however, ε is not a constant. It is a frequency-dependent complex quantity, and it is therefore preferable to name it the complex dielectric permittivity, defined as :

$$\varepsilon^* = \varepsilon' - i\varepsilon''$$

where $i \sqrt{-1}$. II-2

Let us connect to the capacitor a sinusoidal varying potential of maximum amplitude E_o and frequency ω rad s^{-1} described by Eqn. II-3:

$$E = E_o\, e^{i\omega t} = E_o(\cos\omega t + i \sin\omega t) \qquad \text{II-3}$$

The current flowing in the circuit is given by Eqn. II-4 :

$$I = E\omega C = E\omega C_o \ (\varepsilon' - i\varepsilon'') \qquad \text{II-4}$$

We see that the current has two components as a result of the complex dielectric permittivity. The imaginary component, $E\omega C_o\varepsilon''$, is in phase with the applied potential and therefore causes consumption of electrical power given by the dot product $EI = E^2\omega C_o\varepsilon''$. The real component, $E\omega C_o\varepsilon'$, is 90^o out of phase with the applied potential, and therefore does not cause any electrical work to be done. These two currents are often referred to as the loss current and charging current, respectively. If we define δ as the angle between the total current and the charging current axis, then

$$\tan \delta = \frac{E\omega C_o\varepsilon''}{E\omega C_o\varepsilon'} = \frac{\varepsilon''}{\varepsilon'} \qquad \text{II-5}$$

MICROWAVE-FREQUENCY MEASUREMENTS

Let an electromagnetic wave of angular frequency ω radians per second be propagated in the positive X direction through a medium of propagation coefficient γ defined as:

$$\gamma = \alpha + i\beta \qquad \text{II-6}$$

If the time-varying potential described as in Eqn. II-3 is E_1 at a reference plane $x = 0$, then the potential at the position $x = x$ is E_2 given by Eqn. II-7.

$$\begin{aligned} E_2 &= E_1 e^{-\gamma x} \\ &= E_o e^{-\gamma x} e^{i\omega t} \\ &= E_o e^{-\alpha x} e^{i(\omega t - \beta x)} \\ &= E_o e^{-\alpha x}\left[\cos(\omega t - \beta x) + i \sin(\omega t - \beta x)\right] \end{aligned} \qquad \text{II-7}$$

It is apparent that, compared to the potential E_1 at $x = 0$, the potential E_2 has been altered in both phase and magnitude. The maximum amplitude of the potential has been reduced by the factor $e^{-\alpha x}$, and the phase has been altered by βx radians. For these reasons, α is termed the attenuation coefficient, in units of neper

cm^{-1}, and β is the phase coefficient, in units of rad cm^{-1}. If the wavelength of the electromagnetic radiation is λ_d in the dielectric medium of propagation coefficient γ, then the periodic nature of the field dictates that $\beta = 2\pi/\lambda_d$. The relationships between the experimentally-measurable quantities α and β and the desired complex dielectric permittivity are provided by Eqns. II-8 and II-9[1]

$$\varepsilon' = \frac{\lambda_o^2}{\lambda_d^2}\,(1-\alpha^2/\beta^2) \qquad \text{II-8}$$

$$\varepsilon'' = \frac{2\lambda_o^2\alpha}{\lambda_d^2\beta} = \frac{\lambda_o^2\alpha}{\pi\lambda_d} \qquad \text{II-9}$$

where λ_o is the wavelength of the radiation in vacuum.

Experimentally, the measurement of the attenuation coefficient, α, is made using a detector crystal and metered amplifier calibrated on the so-called "square law"; that is, the meter indicates the differences in power, in units of decibels, between the electric fields at the positions $x = 0$ and $x = x$. Now the power at any position x is proportional to the square of the potential at that position. Therefore, Eqns. II-10 and II-11

which respectively define the units neper and decibel, lead to Eqn. II-12[2]:

$$\text{Number of nepers} = \log_e(E_1/E_2)$$

$$= \tfrac{1}{2}\log_e(P_1/P_2) \qquad \text{II-10}$$

$$\text{Number of decibels} = 10 \log_{10}(P_1/P_2) \qquad \text{II-11}$$

$$\text{Number of decibels} = 10 \log_{10}(e) \times \log_e(P_1/P_2)$$

$$= 20 \log_{10}(e) \times \text{Number of nepers} \qquad \text{II-12}$$

Therefore, there are 8.6858896 decibels in one neper.

MICROWAVE INTERFEROMETERS

Dielectric measurements at wavelengths of approximately 0.4 and 0.2 cm (in vacuum) were carried out using a microwave version of the familiar Michelson interferometer. The system has been fully described in the literature.[3] Briefly, the signal source consisted of a Baytron model 1V-80/G harmonic generator and crystal fed by a Philips YK1010 klystron tube operated at a frequency of 71.0×10^9 s^{-1}, as measured by a precision resonant cavity type frequency meter. The output of the klystron tube was modulated by a 1 kHz square wave applied to the reflector voltage supply. The 142 GHz signal was split into two equal parts by a microwave ring circulator which takes the place of a beam splitter in an optical interferometer, one half passing to a reference arm consisting of a calibrated attenuator and a variable-position short circuit of the impedance transform type, and the other half passing to the sample cell via an antenna horn and a dielectric collimating lens. The sample cell was a stainless steel tube fitted with a teflon window at the bottom and lined with a sleeve of carbon-impregnated teflon (to reduce reflections from the walls) of inner diameter 1.0 inches. A silver-plated reflecting surface the plane of which was normal to the axis of the cell was movable along the axis by a micrometer drive system.

In operation, the cell was filled with the liquid sample to a level such that the reflecting surface was always within the liquid column, and the liquid allowed to come to thermal equilibrium at a temperature determined by that of a thermostatically-controlled circulating fluid flowing through a jacket around the cell. This temperature was measured by a thermocouple placed in a small well in the jacket. For low-temperature work the circulating fluid was automotive antifreeze mixed with water, according to the manufacturer's instructions, to yield a solution with a freezing point of $-48^{o}C$. This solution has the advantages of being non-flammable and non-corrosive to cell parts and the circulating pump.

In making measurements with the microwave interferometer, the frequency source was first adjusted for maximum power output at the desired frequency. Then the relative orientations of the antenna horn, dielectric collimating lens, and cell were adjusted to give the maximum standing wave ratio between maxima and minima as the cell reflecting surface was moved along the cell axis. In order to minimize the standing wave created by reflections from the cell window, the position of the reference arm short circuit was adjusted so that the standing wave in the cell arm produced a node at the window. This condition was met when the standing wave ratio was maximized as a function of the reference arm short

circuit position.

A detector crystal mounted in the fourth arm of the ring circulator provided a signal to a calibrated microwave power meter. This crystal/meter system was first calibrated against a precision rotary vane attenuator placed in the microwave waveguide. Therefore, one is able to measure the power at the maxima and minima of the standing wave produced by the electromagnetic waves reflected from the cell reflecting surface. Of course, both the amplitude and wavelength of this wave are altered by the complex dielectric permittivity of the liquid solution in the cell, which is the basis of this measurement technique. The power levels at the maxima and minima of the standing wave pattern and the positions of the minima were recorded and submitted for processing to a computer program.

The apparatus for measurements at 71.0 GHz was exactly the same as the foregoing except that the harmonic generator was not used since the klystron tube provided the required frequency directly. In both of these microwave interferometers the measurements are made in a free space environment as far as the sample is concerned. That is, the sample and the electromagnatic radiation passing through it are not confined in a space which is small compared to the wave-

length of the radiation, as would have been the case if the sample were contained in a section of waveguide. However, there is a finite limit to the diameter of the sample column. To check whether this affected the operation of the system, measurements were made of the wavelength of the radiation in an empty cell and in the cell filled with a low-loss liquid of known dielectric constant (cyclohexane, fractionally distilled and dried over sodium wire). Similar measurements of the free-space wavelength were made using a very large diameter reflecting surface mounted on a micrometer drive without the cell. In all cases, the wavelength was in excellent agreement with the frequency meter used to measure the output of the klystron tube, indicating that the system does, in fact, operate as a free-space system.

THE GRANT CELL

Dielectric measurements at low microwave frequencies (below 2 GHz) were made using a Grant cell similar to that described by Grant and Keefe.[4] The cell used for the present study is shown diagramatically in Fig. II-1. Basically, the cell consists of a length of rigid coaxial line terminated by a short circuit and mounted vertically so that the space between inner and outer conductors may be filled with the liquid sample. A jacket containing a circulating fluid surrounds the outer conductor for temperature control. The centre conductor is made of two lengths of telescoping tubing, the upper half stationary and the lower half movable via a micrometer drive system. A small hole near the middle of the lower half allows a probe to protrude a short distance into the sample.

There are two circuits connected with the operation of the Grant cell. Input power is supplied to the cell via a connector at the top from a signal generator (in this case, a Rohde and Schwarz model SLRD) and impedance-matching trombone line. The frequency of the generator was monitored with a Rohde and Schwarz model WAL frequency meter. Within the cell, the reflection of electromagnetic waves from the short circuit termination produces a standing wave whose amplitude and wavelength are determined by the complex dielectric

Key to Figure II-1 on facing page

IC Input connector from signal generator (General Radio type 874, locking)

SB Teflon support blocks for centre conductor (note vent holes bored through)

OC Outer conductor (silver tubing)

ICS Inner conductor, stationary upper portion (silver tubing)

ICM Inner conductor, moving lower portion (silver tubing)

P Probe protruding slightly from inner conductor

SF Sample fill/drain tube

SCR Silver contact rings for short circuit connection from outer to inner conductors

TS Teflon seal

CS Cone seal (teflon)

PC Probe cable to detector and SWR meter

M Micrometer arm for moving lower portion of inner conductor

CLI Circulating liquid inlet for temperature control

J Jacket for circulating liquid

CLO Circulating liquid outlet

Note: Total length of the cell from the top of the input connector to the bottom of the cone seal was approximately 65 cm.

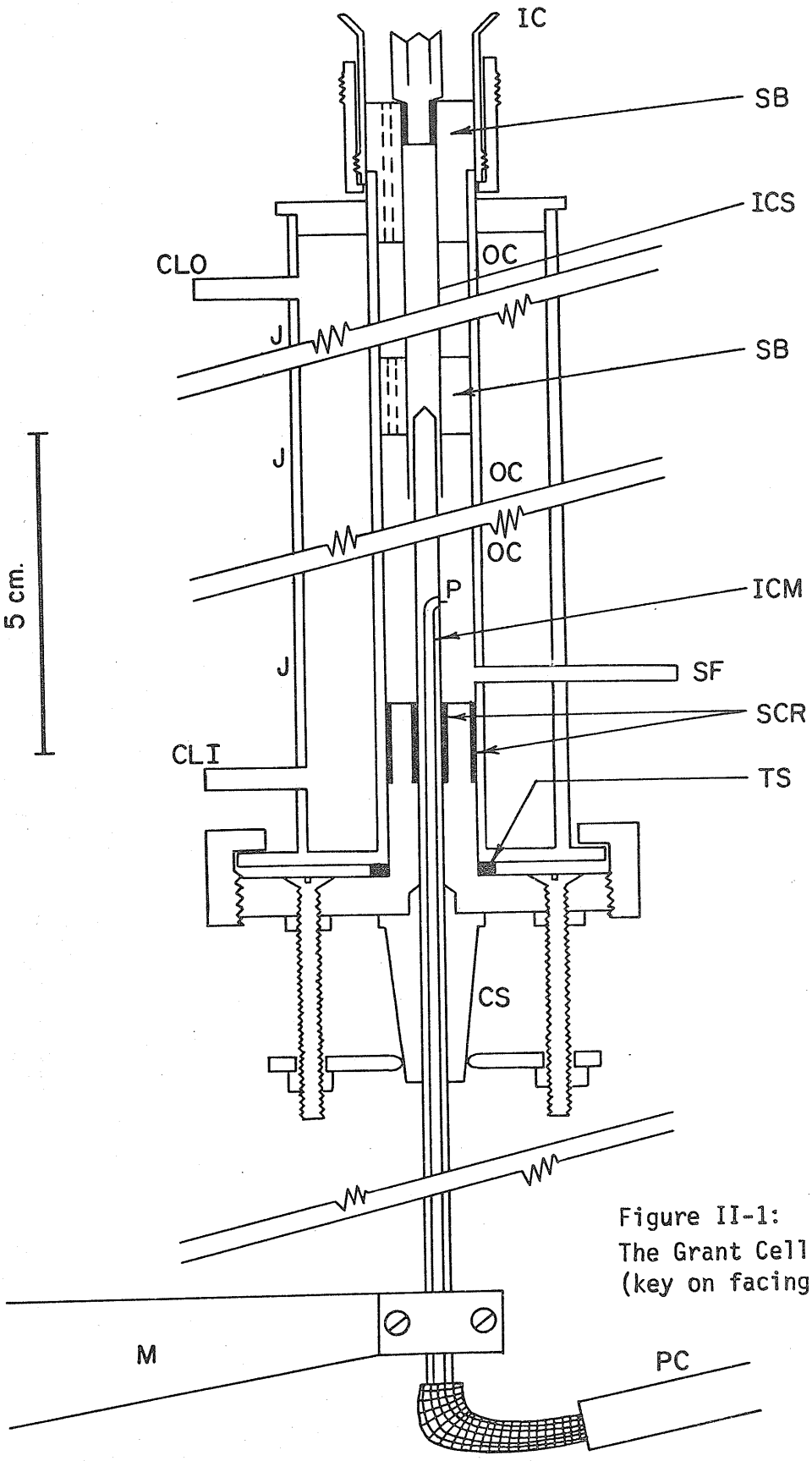

Figure II-1:
The Grant Cell
(key on facing page)

permittivity of the liquid sample. This standing wave is sampled by the probe protruding from the inner conductor, which is the input signal for the second (measuring) circuit.

The circuits used in the present study differed somewhat from those employed by Grant and his colleagues. In the present system the signal generator produced a microwave signal which was amplitude-modulated at a frequency of 1 kHz. The probe output was fed through a Hewlett-Packard detector crystal model 423A(NEG) equipped with a model 11523A matching load resistor so that its output was the 1 kHz square wave with an amplitude related to that of the probe signal by the square law. The detector signal was amplified and displayed by a Hewlett-Packard model 415E Standing Wave Ratio meter. An impedance-matching device was mounted in the probe line to optimize its performance. All cable connectors were General Radio type 874 (locking) to reduce leakage of electromagnetic radiation, which might cause errors in the measurements.

Grant and Keefe[4] have shown that the attenuation coefficient, α, may be obtained from Eqn. II-13 for medium-loss liquids (defined as $\alpha x_0 \leq 0.35$, where x_0 is the position of the first minimum of the standing wave with respect to the short circuit plane).

$$r = \frac{\sinh(\alpha x_1)}{\cosh(\alpha x_2)} \qquad \text{II-13}$$

where $r = V_1/V_2$ is the inverse voltage standing wave ratio,

x_2 is the position of the maximum to the short circuit side of the minimum, and

x_1 is the position of the minimum.

Thus, it is necessary to measure the positions of the maxima and minima in the standing wave pattern, the inverse voltage standing wave ratio at each minimum, and the position of the short circuit plane. This latter quantity may be deduced from the internal consistency of the minima positions if there are several minima in the observations, or may be measured separately by making measurements on a liquid of low dielectric loss.

The voltage standing wave ratio at a minimum may be measured simply by reading on the SWR meter the ratio of powers in the minimum and its associated maximum, but this procedure is prone to two errors which may be quite large for medium loss liquids. The first is that it depends on the detector crystal to obey the square law

exactly over very large variations of input signal. The second is that, for medium loss liquids, the power at a maximum displaced from the minimum is altered by the attenuation coefficient of the sample. Therefore, the preferred technique is the so-called "half power" system, outlined for example by Cross.[5] If the voltage in the standing wave pattern at a position y cm. away from the minimum is p times that at the minimum, then the inverse voltage standing wave ratio, r, is given by Eqn. II-14:

$$r = \frac{\sin(\pi y/\lambda_d)}{\sqrt{p^2 - \cos^2(\pi y/\lambda_d)}} \qquad \text{II-14}$$

where λ_d is the wavelength in the dielectric medium.

The name "half power" applied to this technique comes from the fact that it is usually used by determining that value of the variable y which produces a power level exactly twice that of the minimum (i.e., 3.01 decibels above the minimum). In this case, $p^2 = 2$, since the power ratio is the square of the voltage ratio, p. However, any value of p may be chosen. In fact, a smaller value of p may be preferable for the present case of medium-loss liquids (provided of course that it may be measured accurately) since the deviation of the shape of the standing wave minimum from the parabolic form assumed in the derivation of Eqn. II-14 becomes

more pronounced as larger values of p (and therefore of y) are sampled, and in medium-loss liquids the standing wave ratio minimum is rather shallow (i.e., y is larger for a given value of p) compared to what is found in low-loss liquids, as may be seen from Eqns. II-13 and II-14.

STATIC DIELECTRIC CONSTANTS

The static dielectric constant, ε_0, is the low-frequency limiting value of the real part of the complex dielectric permittivity. For the pure liquid benzonitrile, this parameter was measured using a Wiss.-Techn. Werkstatten Dipolmeter model DM01 fitted with a WTW model MFL3 cell. The measurement was conducted at a frequency of 2 MHz. The temperature of the sample was controlled by circulation of the automotive antifreeze solution described in the "Microwave Interferometers" section of this chapter, and measured by inserting a small thermocouple directly into the sample immediately before and after a measurement. The system was calibrated at the desired temperature with three liquids, the static dielectric constants of which were obtained from reference tables. This calibration procedure was carried out at the same time as the measurements on the unknown (benzonitrile) to avoid the possibility that the system calibration might change from one day to the next.

The static dielectric constants of the four halobenzenes and of 1,1,1-trichloroethane were measured by a General Radio type 1615A capacitance bridge connected via a rigid adapter to a WTW model MFL2/s cell. The measurement frequency was 2 kHz, and temperature control and measurement were the same as in the case of benzonitrile. For the halobenzenes, seven calibration liquids were

employed; for 1,1,1-trichloroethane, three liquids were used for calibration of the measurement system.

REFRACTIVE INDICES

An Abbe refractometer was used to measure the refractive indices of the liquid samples at the D line of sodium in the visible light region. Again, a circulating liquid flowing around the refractometer prism was used to obtain the desired temperatures.

POLYSTYRENE MATRIX SAMPLE PREPARATIONS

Solutions of solutes in polystyrene were prepared in the following manner to produce solid disks. The desired weight of solute was placed in a ceramic crucible, and to this was added the required weight of polystyrene pellets. This mixture was then dissolved in trans-1,2-dichloroethylene, a non-polar solvent, and the crucible placed in a drying oven at approximately 375K. As the dichloroethylene solvent evaporated, the crucible was removed periodically from the oven and its contents stirred with a stainless steel spatula to ensure that the remaining solution was uniform. When the mixture had lost enough dichloroethylene to attain the consistency of chewing gum, the crucible was removed from the oven and allowed to cool so that it could be handled. Then the viscous mass was gently pried away from the crucible walls and rolled into a flat disk. This disk was placed on a teflon sheet in a vacuum oven at approximately 360K, and the pressure reduced by a single-stage rotary pump. This caused the plastic mass to expand a great deal into a foam as the remaining dichloroethylene evaporated under the vacuum oven conditions. After about ten minutes the oven was returned to atmospheric pressure, the sample removed (the sample shrank as the pressure was raised), and several deep score marks were cut in each side of the disk to facilitate the escape of dichloroethylene from the interior of the sample. The sample was returned

to the vacuum oven and the process repeated. After the second scoring of the sample, it was returned to the oven for at least one hour for evaporation of the last traces of dichloroethylene. The resultant sample was weighed, and, if there was any suspicion that some dichloroethylene remained, it was returned to the oven for further treatment until no further weight loss was noted. None of the samples in the present study gave evidence that this process led to loss of the desired solute from the matrix. For example, the matrix material containing acetophenone was left under a vacuum for twenty-four hours at 360K with no weight loss.

In a few cases where the boiling point of the solute was low (e.g. below about 400K). the procedure was altered. In these cases no trans-1,2-dichloroethylene was used. Instead, the desired weight of polystyrene was dissolved directly in a large excess of the liquid which was to become the solute, and the evaporation process carried out as before, except that the final evaporation in the vacuum oven was halted when the total sample weight indicated that the matrix contained the desired amount of solute.

The matrix material was placed in a stainless steel die equipped with polished tungsten carbide faces, and a heating sleeve placed around the die. The latter was heated to a temperature necessary

to melt the matrix material, power being supplied from a controller which measured the die temperature via a thermocouple. The temperature used depended on the solute concentration, being about 410K for pure polystyrene, about 400K for matrices containing 3% by weight solute, and about 385K for ones with 10% solute. Heating was accomplished in 20 to 30 minutes. The sample was then pressed by applying a force of 5 tons to the moving element of the die. Then the heating sleeve was raised out of the way and a stream of air from a fan directed onto the die to cool it down to room temperature in about 30 minutes. The die was disassembled and the moving element pressed out of the die collar by application of a force of about 2 tons. The edges of the sample, a disk of diameter 2.0 inches, were lightly smoothed with a sharp knife blade, and the sample thickness measured with a micrometer at ten points to yield an average value. The sample weight was recorded, and from this weight and the weights of solute and polystyrene originally used, the molar concentration of the solute was calculated.

Samples of pure solids were prepared by grinding the solid with a mortar and pestle, placing the powder in the die, and pressing it at room temperature with a force of 30 tons. Similar measurements of disk weight and thickness allowed the concentrations of the pure solids to be calculated.

THE GENERAL RADIO BRIDGE

The model 1615-A capacitance bridge manufactured by the General Radio Company allows measurement of the capacitance and conductivity of a sample to be made at frequencies ranging from 50 to 10^5 s^{-1} if it is used in conjunction with their model 1310-B sine wave signal generator and model 1232-A tuneable amplifier/null detector. For the present study it was found that the addition of an oscilloscope facilitated these measurements. The signal generator output was split, part going to the capacitance bridge input terminals and the other part used to supply the horizontal deflection signal of the oscilloscope. The amplified bridge unbalance signal from the output terminals of the model 1232-A detector was used as the vertical deflection signal for the oscilloscope, a small capacitor being placed in the ground lead of this connection to avoid the possibility that ground loop currents might introduce errors. The pattern on the oscilloscope was thus a 1:1 Lissajous figure whose vertical amplitude reflected the magnitude of the bridge imbalance. More importantly, the tilt angle of the pattern could be correlated to the direction of the imbalance of both the capacitance and conductivity controls so that the imbalance could be corrected easily to achieve the desired null condition. Two other advantages accrued owing to the use of the oscilloscope. At low frequencies, environmental noise makes a contribution to the total signal displayed

by the null detector meter. The oscilloscope pattern allows one to see more easily the average value of the signal to judge whether null balance has been achieved. In addition, at these frequencies the transformer core in the capacitance bridge may become saturated if high signal power is supplied from the generator, and this condition is indicated on the oscilloscope by a severe distortion of the Lissajous figure. Therefore, the oscilloscope allows the user to set the signal generator output to the maximum possible level without causing errors due to transformer core saturation.

The frequency scale of the signal generator was calibrated against the power line frequency (60 s^{-1}) by Lissajous figure comparisons with an oscilloscope for several output frequencies.

The capacitor measured by the General Radio bridge consisted of the polystyrene matrix disk clamped between electrodes. The electrode assembly is shown in Fig. II-2. It was a three-terminal assembly with an outer diameter of 2.0 inches. The low electrode had a diameter of approximately 1.5 inches and was surrounded by a guard ring electrode of outer diameter 2.0 inches. This type of electrode assembly reduces considerably any errors caused by fringing of the electric field at the edges of the measurement area. It was used in such a way that the capacitance measured is solely that between the high and low electrodes.

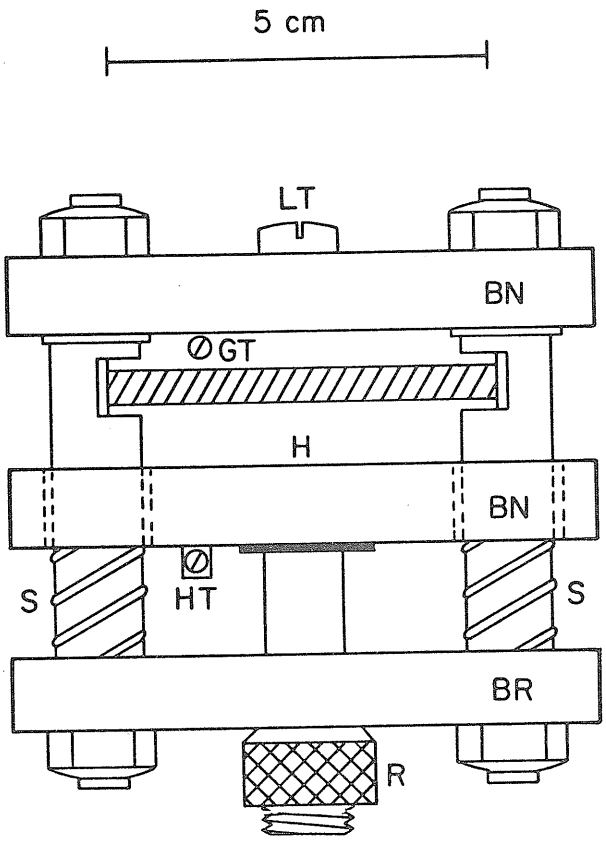

Figure II-2: Three-terminal electrode assembly for dielectric measurements on solid disks.

Key: LT Low electrode connection terminal

BN Boron Nitride insulating support plates

GT Guard ring connection terminal

H High electrode

HT High electrode connection terminal

BR Brass support plate

R Release nut

S Steel clamping springs

The electrode assembly was mounted in an aluminum chamber which could be sealed off from the atmosphere. Two sealed tubes allowed connections to the electrodes, and two more tubes allowed the chamber to be purged with dry nitrogen gas and then maintained at a slight positive pressure to prevent the entry of atmospheric moisture during low-temperature measurements. The chamber was equipped with a heating coil of nichrome wire wrapped around its exterior. The heater resistance was about 2 ohms, so that a 12 volt supply provided a heating power of about 70 watts. Power to the heater winding was provided by a Beckmann/RIIC model TEM-1 indicating proportional controller which sensed the chamber temperature via a small thermocouple placed in a well in the chamber wall. Cooling of the chamber was accomplished by placing on its flat top a container of liquid nitrogen. To maintain a stable temperature, an appropriate number of sheets of paper were inserted between the chamber and the liquid nitrogen container so that the heater current was about 2 amps, corresponding to a power of about 8 watts. Measurement of the sample in this cell was carried out only after the sample had reached thermal equilibrium with the chamber case, as judged by stability of the capacitance and conductivity readings. From the changes in these readings from one measurement temperature to another, it was estimated that the sample temperature at equilibrium was constant to within $\pm$ 0.1K.

The measurement temperature was read from the indicating dial of the controller. This dial was calibrated against an accurate temperature standard to be accurate to the limits of reading the scale, which was ± 0.5 K. Late in the experimental program the acquisition of a Hewlett-Packard model 2802A platinum resistance thermometer allowed measurement of temperatures to an accuracy of ±0.1 K.

The General Radio bridge measures the capacitance and conductivity of the capacitor consisting of the sample between the high and low electrodes. These quantities may be related to the components of the complex dielectric permittivity by Eqns. II-15 and II-16:[6]

$$\varepsilon' = C/C_o \qquad \text{II-15}$$

$$\varepsilon'' = G/\omega C_o \qquad \text{II-16}$$

where C = capacitance of the system,

C_o = capacitance if sample is replaced by air,

G = conductivity of the system, and

$\omega = 2\pi f$ = angular frequency of the applied field.

Measurement of C_o would require that the electrodes be arranged exactly as they were when they contained the sample, but without the

sample. This is difficult. Instead, the C_o value may be calculated from Eqn. II-17:[7]

$$C_o = \frac{0.2244A_1}{d_1} \qquad \text{II-17}$$

$$= \frac{0.08842A_2}{d_2}$$

where A_1 = effective area of the plates in in.^{2}

A_2 = effective area in cm ^{2}

d_1 = spacing of the plates in in.

d_2 = spacing in cm

C_o is the capacitance in units of picofarads.

Combining Eqns. II-15, II-16 and II-17 leads to Eqns. II-18 and II-19 which are more convenient for the handling of experimental data:

$$\varepsilon' = \frac{Cd_1}{0.2244A_1} \qquad \text{II-18}$$

$$\varepsilon'' = \varepsilon' G/\omega C \qquad \text{II-19}$$

where again d_1 and A_1 are in units of in. and in.^{2}
C is in picofarads, and G in picomhos (pico = 10^{-12}).

The effective area of the cell electrode plates, A_1, was found by measurement of the capacitance of the cell containing a standard quartz disk of diameter 2.0 inches and thickness 0.0538 in. supplied by Rutherford Research Products Co., Rutherford, New Jersey, U.S.A. and claimed to have a dielectric constant of 3.819.

THE Q-METER

Dielectric measurements on the polystyrene disk samples at frequencies in the range 25×10^3 to 15×10^6 s^{-1} were made using a Hewlett-Packard model 4342A Q-meter connected via a model 4342 adapter plate supplied by the aforementioned Rutherford Research Products Co. to a cell designed by Mr. B. K. Morgan of this laboratory. A diagram of this cell is shown in Fig. II-3. Basically, the cell consists of two capacitors sharing a common plate. One capacitor has the sample between the common plate and the case (ground), and the other has an air gap partially filled with a 1 in. diameter quartz disk between the common plate and the high electrode. The thickness of the air gap in the reference capacitor may be adjusted by screwing up or down a threaded shaft on which the quartz disk rests. The whole assembly is clamped together by a spring bellows bearing upon the low (ground) electrode of the sample capacitor. A switch arm mounted on the common central plate allows this plate to be connected either to the high or low side. When it is connected to the low plate of the sample capacitor, the common plate then becomes the low plate for the reference capacitor, and the sample capacitor is removed from the circuit. When the common plate is connected to the high plate of the reference capacitor, this capacitor is removed from the circuit, and the common plate becomes the high plate of the sample capacitor. In this manner the switch allows the Q-meter to examine either the sample capacitor or the reference capacitor.

Key to Figure II-3 on facing page

SB Spring bellows

L Low electrode in contact with case

CP Centre plate

H High electrode

I Insulating supports for high electrode (four)

G Locating guides for centre plate (three)

TC Thermocouple in well

H Handle for operation of switch

N Nitrogen gas inlet (outlet not shown)

S Switch assembly

BP Banana plug connectors for low (case) terminal

HC High electrode connection strip

Q Quartz spacer

SA Sample (2" dia. disk) location

E Electric heater coil

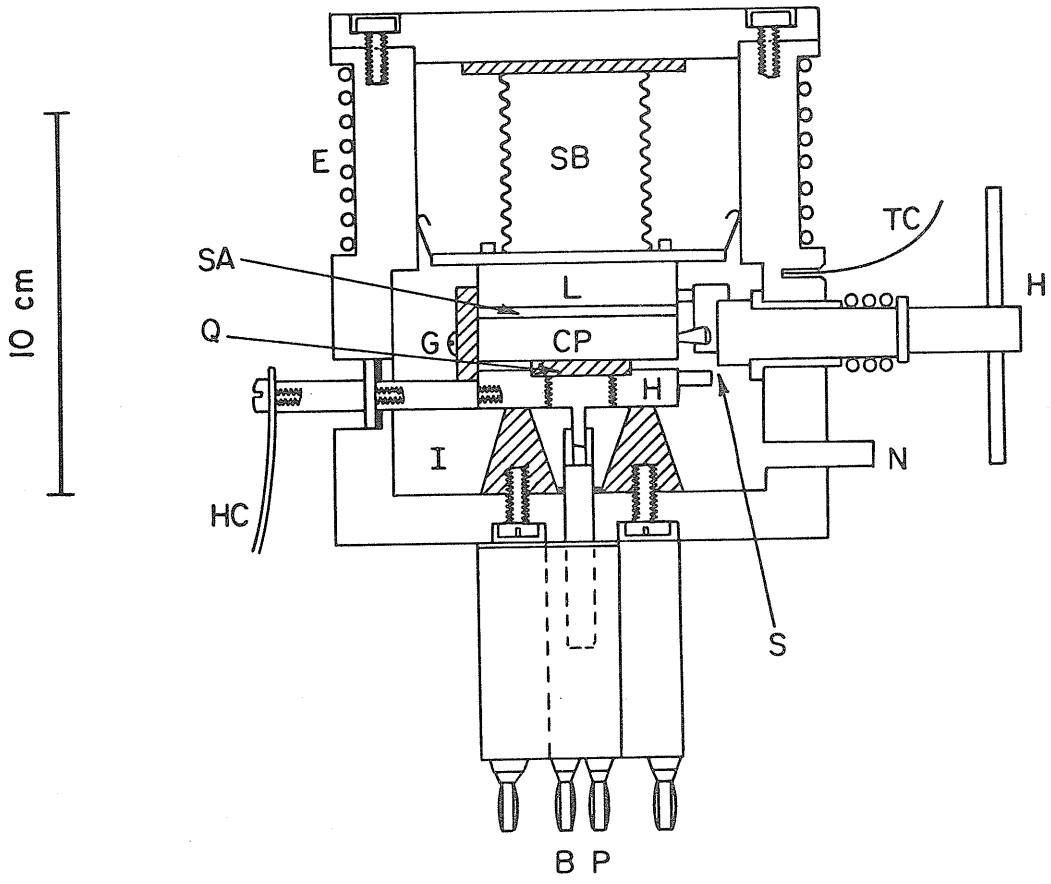

Figure II-3: The Morgan tri-electrode cell for Q-meter.
(key on facing page)

The cell case was similar to that of the cell used with the General Radio bridge, and temperature control of the cell and sample was accomplished in the same manner.

The experimenter places the sample in the appropriate location and adjusts the spacing of the reference capacitor plates so that the two capacitors have, as nearly as possible, the same capacitance value. This is judged by an ability to achieve resonance of the Q-meter circuits at the same settings of the capacitance controls of the meter for both capacitors. This adjustment is done only once at the beginning of a set of measurements on a sample, since the value of the capacitance is not important, as will be seen later. All that matters is that the two should be the same.

In principle the difference in capacitance between reference and sample capacitors may be related to the dielectric constant of the sample if this parameter is known for at least one frequency. However, attempts to use this information gave no consistent values for the dielectric constant of the sample, and therefore these data were not used.

For the present study, the important data were values of dielectric loss factor, ε'', as a function of frequency. If one assumes that the conductivity, G, of the measurement system consists of two additive components, one each for the sample and the measurement system

alone, then one obtains Eqn. II-20 after employing Eqns. II-15 and II-16 and bearing in mind the definition of Eqn. II-5 and the definition of Q.

$$(\tan \delta)_s = \frac{G_x - G_r}{\omega C}$$

$$= \frac{G_x}{\omega C} - \frac{G_r}{\omega C}$$

$$= \frac{1}{Q_x} - \frac{1}{Q_r}$$

$$= \frac{Q_r - Q_x}{Q_x} \times \frac{1}{Q_r}$$

$$= \frac{\Delta Q}{Q_x} \times \frac{\Delta C_r}{2C_r} \qquad \text{II-20}$$

where $(\tan \delta)_s$ = tan δ for the sample only ,

G is the total conductivity measured,

Q is the Q value for the capacitor being examined,

C_r is the capacitance of the reference capacitor,

ΔC_r is the width of the peak of Q versus C for the reference capacitor, measured at $Q_r/\sqrt{2}$,

ΔQ is the difference in Q readings for sample and reference, and subscripts x and r refer to measurements made when the switch is connected to allow examination of the sample and reference capacitors, respectively.

Now the value of C_r is not known. However, it was adjusted to be equal to the value of the sample capacitor, C_x. Application of Eqns. II-15 and II-17 and then Eqn. II-5 yields:

$$\varepsilon''_s = \frac{(\Delta Q)\ (\Delta C_r)\ (d_1)}{(Q_x)\quad (2)\ (0.2244A_1)} \qquad \text{II-21}$$

where ε''_s is the dielectric loss factor of the sample,

d_1 is the sample thickness in inches,

A_1 is the effective area of the cell electrodes in one of the capacitors,

and the remaining quantities are defined as in Eqn. II-20.

FAR-INFRARED INTERFEROMETRY

There are no strong sources of far-infrared radiation available presently which cover the whole range from 3 to 500 cm^{-1}. The most commonly used source is a mercury arc lamp which, as an approximation to a black body radiator, provides a spectral output containing a small proportion of far-infrared radiation, although the intensity is low. At the same time , there are few detectors available for this frequency range, all of which lack either sensitivity, wide frequency range response, or both. The most commonly used detector is the Golay detector which has quite wide frequency response but poor sensitivity. The combination of low signal intensity and low detector sensitivity means that the signal-to-noise ratio obtained with a conventional grating spectrophotometer is not adequate to differentiate the signal from random environmental noise in this frequency region.

The solution to this problem is to employ broad-band interferometry instead of grating spectrometers and then to extract the desired information of transmitted intensity versus frequency from the interferogram by Fourier transformation. In this technique, all of the source output in the frequency range of interest falls on the detector after passing through the sample so that the signal-to-noise ratio is vastly greater than would be the case if only a narrow band of frequencies selected by a diffraction grating were detected. The relevant mathematical equations have been shown by Strong and Vanasse[8] and Hurley[9] and

are summarized below.

If two monochromatic beams of radiation (frequency $\bar{\nu}$ cm^{-1}) of intensities a_1 and a_2 fall upon a detector after traversing paths with lengths differing by x cm., the intensity of the aggregate radiation, I(x), a function of x, is given by Eqn. II-22:

$$I(x) = a_1^2 + a_2^2 + 2a_1a_2 \cos(2\pi\bar{\nu}x) \qquad \text{II-22}$$

Provided that the amplitudes are equal, as they must be in an interferometer constructed for these purposes, we may write $a = a_1 = a_2$ and obtain Eqn. II-23 :

$$I(x) = 2a^2 (1 + \cos (2\pi\bar{\nu}x)) \qquad \text{II-23}$$

If we define a constant $I(\bar{\nu}) = 2a^2$, then

$$I(x) = I(\bar{\nu}) (1 + \cos (2\pi\bar{\nu}x)) \qquad \text{II-24}$$

If instead the radiation beams are polychromatic, integration of Eqn. II-24 yields Eqn. II-25:

$$I(x) = \int_{-\infty}^{+\infty} I(\bar{\nu})\, d\bar{\nu} + \int_{-\infty}^{+\infty} I(\bar{\nu}) \cos(2\pi\bar{\nu}x)\, d\bar{\nu} \qquad \text{II-25}$$

At x = 0, the intensity I(0) is given by Eqn. II-26.

$$I(0) = 2 \int_{-\infty}^{+\infty} I(\bar{\nu})\, d\bar{\nu} \qquad \text{II-26}$$

Therefore, we obtain Eqn. II-27:

$$I(x) = \tfrac{1}{2}I(0) + \int_{-\infty}^{+\infty} I(\bar{\nu}) \cos(2\pi\bar{\nu}x)\, d\bar{\nu} \qquad \text{II-27}$$

Defining the interferogram function, $F(x) = I(x) - \tfrac{1}{2}I(0)$, we obtain Eqn. II-28 :

$$F(x) = \int_{-\infty}^{+\infty} I(\bar{\nu}) \cos(2\pi\bar{\nu}x)\, d\bar{\nu} \qquad \text{II-28}$$

The intensity of the radiation of frequency $\bar{\nu}$ cm^{-1} reaching the detector is then obtained from the Fourier transform of Eqn. II-28, thus:

$$I(\bar{\nu}) = \int_{-\infty}^{+\infty} F(x) \cos(2\pi\bar{\nu}x)\, dx \qquad \text{II-29}$$

In practice, x may be varied within a finite range only. It is common to do this so that x is varied symmetrically about the x = 0 position between the limits x = +X and x = -X. Therefore, the integral of Eqn. II-29 is truncated. Further, F(x) is usually sampled at discrete equally-separated values of x, so that the integral may be approximated by a finite summation, as in Eqn. II-30 :

$$I(\bar{\nu}) = 2 \sum_{x=0}^{X} F(x) \cos(2\pi\bar{\nu}x)\, \Delta x \qquad \text{II-30}$$

If the maximum frequency to be sampled is $\bar{\nu}_{max.}$ cm^{-1}, then choosing a sampling interval for Δx of $1/\bar{\nu}_{max.}$ would provide contributions to the total signal from only the peaks of the interferogram due solely to radiation of frequency $\bar{\nu}_{max.}$. Therefore, to include both the maxima and minima of this monochromatic interferogram in the total polychromatic interferogram, one must employ a sampling interval given by Eqn. II-31 :

$$\Delta x = \frac{1}{2\bar{\nu}_{max.}} \qquad \text{II-31}$$

Similarly, in order to avoid contributions to the intensity $I(\bar{\nu})$ from harmonics of $\bar{\nu}$ above the limit $\bar{\nu}_{max.}$, one must eliminate these higher frequencies from the radiation beam reaching the detector. This may be accomplished by optical absorption filters such as the quartz window of the Golay detector (which is transparent only below 250 cm^{-1}), carbon-impregnated polyethylene ("black polyethylene", transparent only below 1000 cm^{-1}), and grooved polyethylene transmission gratings in which the high-frequency cutoff point is determined by the spacing of the ruled grooves.

Truncation of the integral of Eqn. II-29 has two effects on the transformed spectrum. The first is that the resolution, $\Delta\bar{\nu}$, is limited by Eqn. II-32 :

$$\Delta\bar{\nu} = 1/X \qquad \text{II-32}$$

The second effect is that the asymptotic value of the interferogram function, $F(x)$, as $x \to \infty$ is not available directly. However, it may be estimated from the observed data by application of an apodization function such as that of Eqn. II-33. Since the function $F(x)$ in Eqn. II-30 is now replaced by the function $G(x)$ from Eqn. II-33, the effect on the transformed interferogram is to degrade the theoretical resolution by about 50%, so that the actual resolution obtained is approximately 1.5 times that given by Eqn. II-32.

$$G(x) = F(x)\ (1 - |x/X|) \qquad \text{II-33}$$

Two far-infrared interferometers were used for the present study. The range 7 to 80 cm^{-1} was covered by a Beckmann/R.I.I.C. lamellar grating interferometer equipped with the model LR-100 lamellar grating drive, a Unicam SP50 Golay detector with quartz entrance window, model FS-200/7 electronics module and model FS-MC1 lamellar grating drive controller. The interferogram was displayed on a Hewlett-Packard model 680 analogue strip chart recorder and punched on paper tape by an Addo punch. A black polyethylene absorber and a grooved polyethylene grating transmission filter were placed in the optical path to limit the radiation reaching the detector to frequencies less than 80 cm^{-1}. The cell was the Beckmann/R.I.I.C. model FH-01 with high-density polyethylene windows mounted in the model VLT-1 cell holder. A double-stage rotary pump was used to evacuate the entire interferometer chamber to a pressure of less than 50 microns Hg (5×10^{-2} torr) to

remove from the spectrum absorptions due to atmospheric gases. The system was operated to yield a resolution of at least 5 cm^{-1}, the effect of apodization as outlined earlier being taken into account.

The second interferometer used was the Grubb-Parsons Modular Cube interferometer Mark II based on the design of the National Physical Laboratory. This instrument is a Michelson-type interferometer in which a Melinex beamsplitter of thickness approximately 12.5 microns was used to investigate the frequency region from 20 to 240 cm^{-1}. A black polyethylene filter and quartz entrance window of the Golay detector limited the radiation reaching the detector to frequencies below 250 cm^{-1}. The sample cell used was the Grubb-Parsons model G.L.C. 01 with high-density polyethylene windows. The interferogram was displayed on a Vitatron analogue strip chart recorder and punched on paper tape by an Addo punch. The machine was operated to yield a resolution of at least 7 cm^{-1}, and vacuum conditions within the interferometer were established as in the case of the lamellar grating interferometer.

Both of the far-infrared interferometers were single-beam instruments. Therefore, the interferograms for sample and background were recorded separately as close together in time as possible. For liquid solution samples, three different thicknesses of sample were used, the optical absorption coefficient, α, being calculated from Eqn. II-34, which is its definition.

$$\alpha = \frac{1}{t_2 - t_1} \log_e(I_1/I_2) \qquad \text{II-34}$$

where t_2 and t_1 are the thicknesses of two samples, and I_2 and I_1 are the transmitted intensity of these two.

The use of three thicknesses allowed three calculations of optical absorption coefficient from the three pairings of thicknesses. More importantly, the procedure avoids the possibility that measurement of the background intensity by the use of an empty cell might be erroneous owing to a difference in the reflection characteristics of the window/vacuum interface compared to that of the window/liquid sample interface.

A small thermocouple placed in contact with the sample cell showed that the temperature of the sample in the radiation beam was (302 ± 2) K. This was the temperature for recording all far-infrared absorption spectra reported in this thesis.

A slightly different procedure was used to record the spectra of polystyrene matrix solutions. Two sample disks were prepared from the same batch of matrix solution as outlined earlier in the "Polystyrene Matrix Sample Preparations" section of this chapter, the thicknesses of these two being different. The sample disks were

then cut with a sharp knife to produce pieces which would fit into the cell, and the edges were smoothed. The cell was assembled without the polyethylene windows to clamp one piece of matrix solution sample in the proper position. This procedure was carried out for two different thicknesses of matrix sample and Eqn. II-34 applied to the two transmitted intensity spectra so obtained. Repeat measurements on separately-prepared matrix samples showed that the absorption spectra obtained were reproducible to within the accuracy of the spectra which was about $\pm$ 10% or better.

Copies of the computer programs used throughout this work are available on request from the Chemistry Department, Lakehead University, Thunder Bay P, Ontario, Canada, P7B 5E1.

PURIFICATION OF MATERIALS

Chlorobenzene, benzonitrile and 1,1,1-trichloroethane were dried over anhydrous calcium chloride and fractionally distilled by the use of a Nester-Faust annular teflon spinning band still. The centre fractions were stored over an activated 4A molecular sieve to remove any small trace of water. Their purities were verified by gas chromatography and by correspondence of their refractive indices with reference values.

Fluorobenzene, bromobenzene, and iodobenzene were dried over anhydrous calcium chloride and stored over an activated molecular sieve. The benzene used for the dilute solutions studied in Chapter V was of spectrophotometric grade, stored over an activated molecular sieve to ensure dryness.

The various polar solutes used for the polystyrene matrix solution measurements of dielectric and far-infrared absorptions were used as supplied by the various manufacturers. It was not felt necessary to undertake lengthy purifications of these because the solute concentrations were typically less than 5% by weight. Thus, the absorptions which might have arisen owing to small traces of impurities would have been negligible in comparison to that of the solute itself. Structural diagrams of the molecules investigated are given in Appendix II.

REFERENCES

1. C. P. Smyth, "Dielectric Behaviour and Structure", McGraw-Hill Book Co., Inc., New York, New York, U. S. A., (1955), p. 218.

2. M. Sucher and J. Fox (eds.), "Handbook of Microwave Measurements", Vol. 1, Polytechnic Press of the Polytechnic Institute of Brooklyn, (1963), (distributed by Interscience Publishers, division of John Wiley and Sons, Inc., New York, New York, U. S. A.), p. 342.

3. S. K. Garg, H. Kilp and C. P. Smyth, J. Chem. Phys., 43, (1965), p. 2341.

4. E. H. Grant and S. E. Keefe, Rev. Sci. Instr., 39, (1968), p. 1800.

5. A. W. Cross, "Experimental Microwaves", W. H. Sanders (Electronics) Ltd., London, England, p. 140.

6. See p. 203 of reference 1.

7. F. E. Terman, "Radio Engineers' Handbook", (1st ed.), McGraw-Hill Publishing Co. Ltd., London, England, (1950), p. 112.

8. J. Strong and G. A. Vanasse, J. Opt. Soc. Amer., 49, (1959), p. 844.

9. W. J. Hurley, J. Chem. Ed., 43, (1966), p. 236.

CHAPTER III
Microwave Dielectric Studies

INTRODUCTION

In Chapter I it was shown that the high-frequency dispersion $\Delta\varepsilon' = \varepsilon_\infty - (n_{ir})^2$ associated with absorptions in the far-infrared frequency region are of particular interest because their origin is not understood fully. This chapter outlines some attempts made to measure this dispersion by means of established techniques of dielectric measurements.

As has been mentioned, the dispersions associated with the absorptions of the "normal" infrared region are quite small in comparison with the experimental errors of dielectrics, so that the refractive index of a liquid measured at the sodium D line in the visible region is an adequate approximation for n_{ir}.[1] Thus, much work in the literature has been centred on estimating the limiting high-frequency values of the dielectric constant in order to obtain $\Delta\varepsilon'$.

In 1957 van Eick and Poley[2] reported an interesting temperature dependence of $\Delta\varepsilon'$ over the range 253 to 333K for chloro- and bromobenzene. They reported a sharp decrease of $\Delta\varepsilon'$ within a relatively small (approximately 40 degrees) range of temperatures near room temperature. They concluded that the previously-suspected, high-frequency dispersion must, in fact, exist, and that its magnitude

must be strongly temperature-dependent.

Since that time the concurrent development of far-infrared interferometry and of high-speed computation facilities for Fourier transformation has made this frequency region directly accessible for absorption measurements. Several authors, including Pardoe[3] Kroon and van der Elsken[4], Jain and Walker[5], and this author[6,7] have shown that the far-infrared absorptions of pure liquids do change with temperature, but not in a sudden manner over a narrow temperature range. Now the Kramers-Kronig relationship[8], equation III-1, suggests that for $\Delta\varepsilon'$ to change markedly the far-infrared absorption band would have to show a similar sudden change:

$$\Delta\varepsilon' = \frac{2}{\pi} \int_{-\infty}^{+\infty} \varepsilon'' (\omega)\, d\,(\ell n\omega) \qquad \text{III-1}$$

Thus, recent experimental evidence was in disagreement with the van Eick and Poley results.

EXPERIMENTAL RESULTS

The parameter ε_∞ is estimated by extrapolation of a Cole-Cole plot which is a semicircle for simple dielectric relaxation systems. As with most extrapolations, this technique is sensitive to how close experimental points may be obtained to the extrapolated value. Poley's equipment allowed measurements at wavelengths down

to 0.8 cm. In this laboratory new microwave interferometers have been used to measure the real (ε') and imaginary (ε'') components of the complex dielectric permittivity of pure liquids at wavelengths of 0.4 and 0.2 cm. In addition, measurements have been made of these parameters at much longer wavelengths by use of the Grant cell, plus measurements of the refractive index at the sodium D line (n_D) and of the static dielectric constant (ε_o). The work was carried out over a suitable range of temperatures for four halobenzenes, 1,1,1-trichloroethane, and benzonitrile. These new experimental data are shown in Table I of Appendix I along with data drawn from Poley's work and from that of Mallikarjun and Hill[9]. These combined data were used to construct the Cole-Cole plots shown in Figs. III-1 through III-6. It may be noted that all have been drawn with the centre of the semicircle on the ε' axis (that is, assuming that the Cole-Cole distribution parameter, α, is zero). In the several cases, where many experimental points were available to define the curve, this procedure seems to be correct, and it is reasonable to assume that the same holds true for other temperatures. Further, in those graphs where only a few points were available it would not have been possible to discriminate between this situation (i.e., $\alpha = 0$) and the case of small positive values of $\alpha < 0.2$, which would place the centre of the semicircle below the ε' axis. The accuracy of the experimental measurements is not sufficient to justify such differentiation. In Fig. III-2(a), representing the

data for pure chlorobenzene at 244.5K, the points from Mallikarjun and Hill are noticeably below the curve drawn. To draw a semicircle through these points would require that its centre be considerably below the axis, and that α be correspondingly rather large and inconsistent with the rest of the results. It should be noted also that inspection of other graphs shows that their data is often in disagreement with the results of van Eick and Poley[2] and of this author.

It is felt that the addition of the two microwave interferometer measurements to the Cole-Cole plots has yielded more reliable estimates of ε_∞ than were available from Poley's work. These new values are shown in Table II of Appendix I along with earlier values from the literature for comparison. The errors in ε_∞ were estimated to be $\pm$ 0.05 for the halobenzenes and for 1,1,1-trichloroethane, and $\pm$ 0.10 for benzonitrile. The resulting new values of $\Delta\varepsilon'$ as a function of temperature have been graphed in Fig. III-7. It may be seen that, in all cases except that of 1,1,1-trichloroethane, the graph points may be fitted to a simple straight line the slope of which is small, unlike the results of van Eick and Poley. This aspect of the results is in agreement with expectations based on the known temperature dependence of far-infrared absorption spectra.

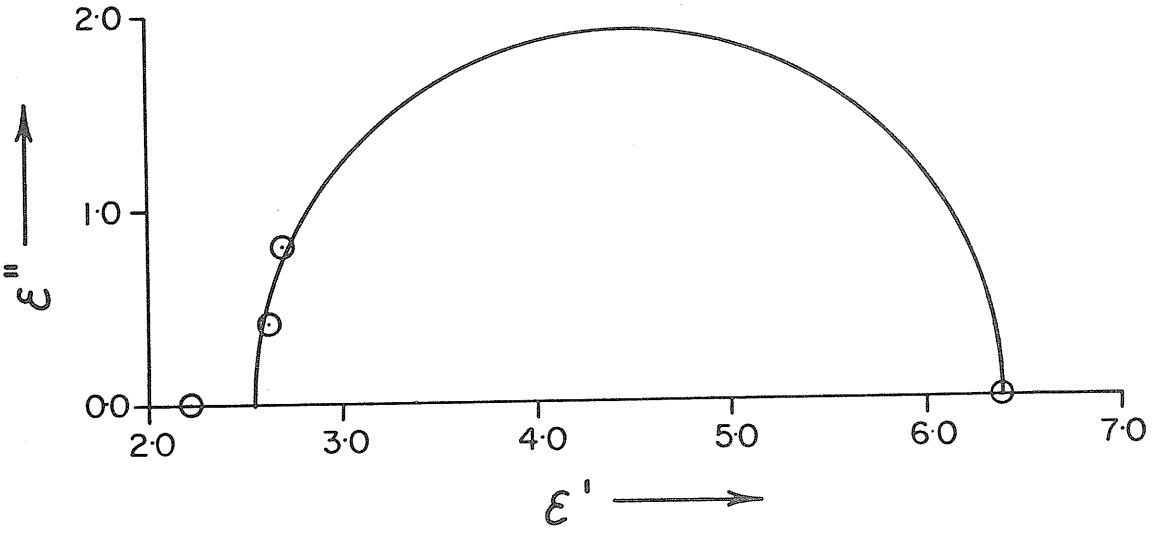

Figure III-1(a): Cole-Cole plot for pure fluorobenzene at 243.1K.

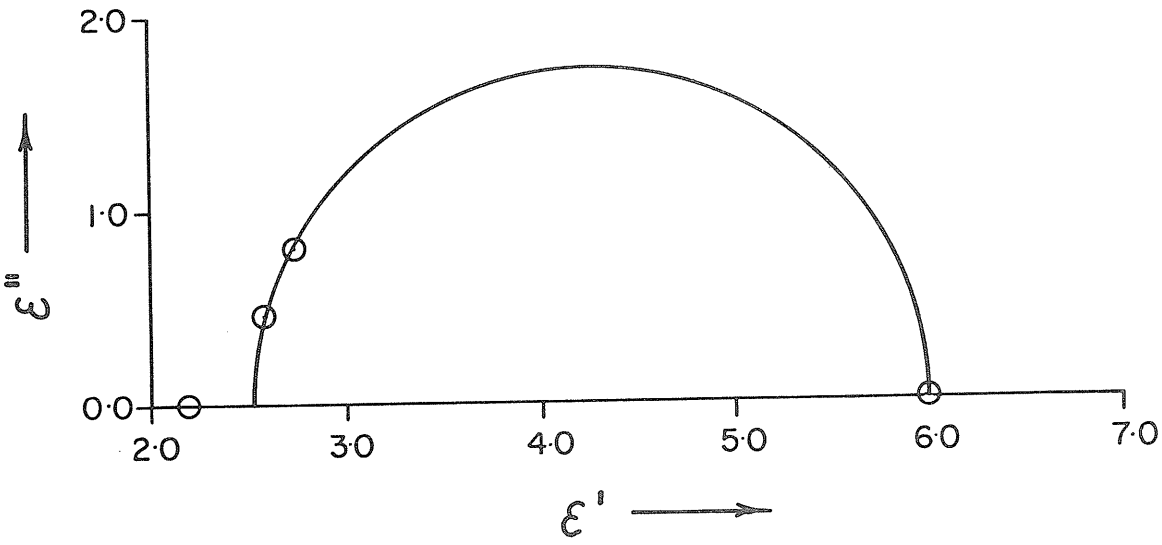

Figure III-1(b): Cole-Cole plot for pure fluorobenzene at 263.6K.

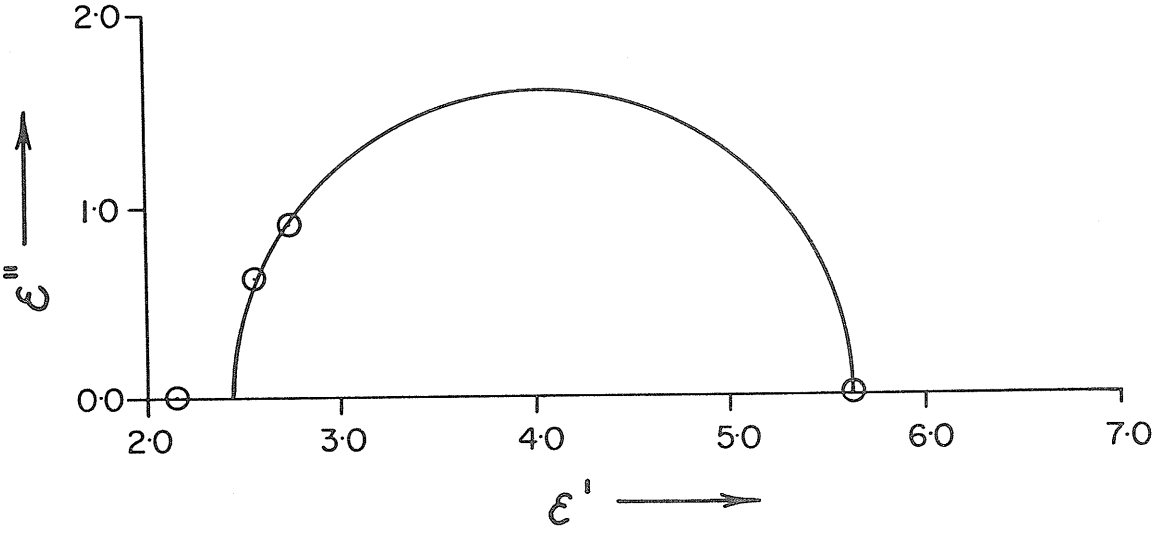

Figure III-1(c): Cole-Cole plot for pure fluorobenzene at 283.0K.

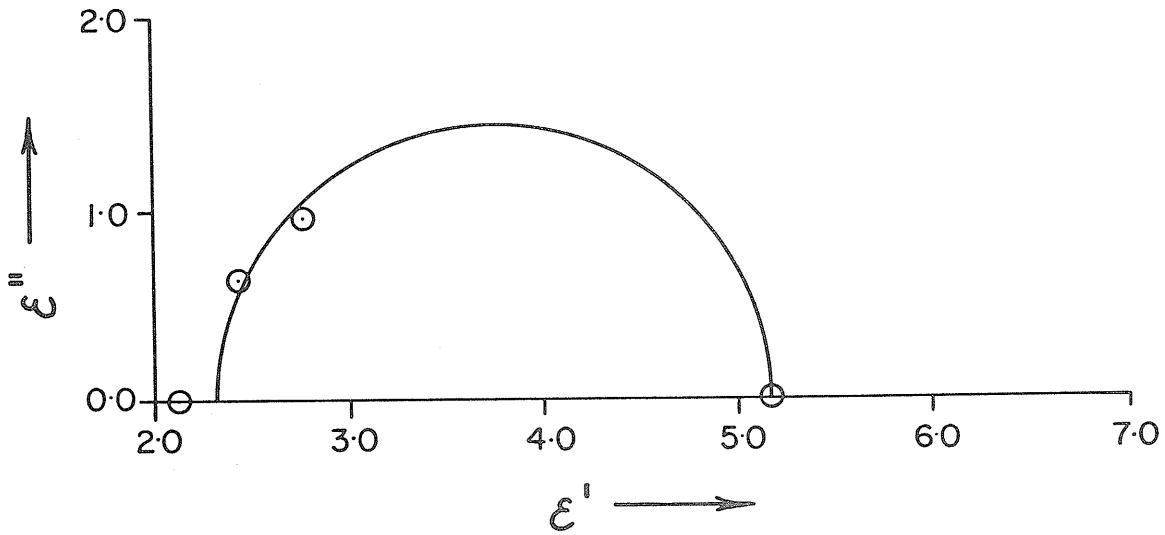

Figure III-1(d): Cole-Cole plot for pure fluorobenzene at 303.0K.

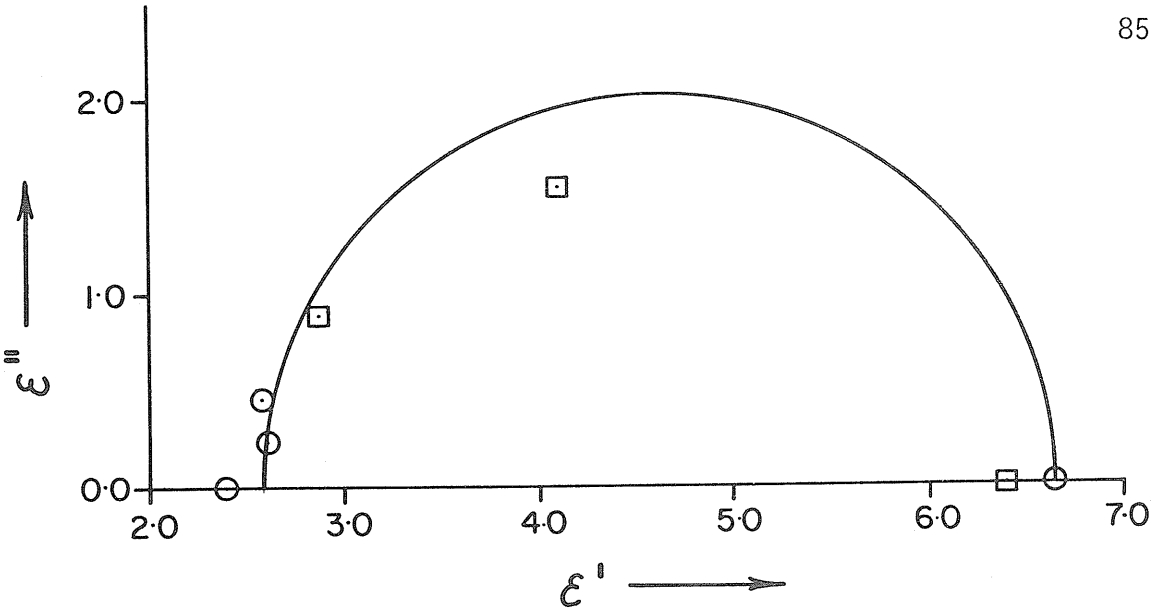

Figure III-2(a): Cole-Cole plot for pure chlorobenzene at 244.5K.
⊙, this work; ⊡, ref. 9.

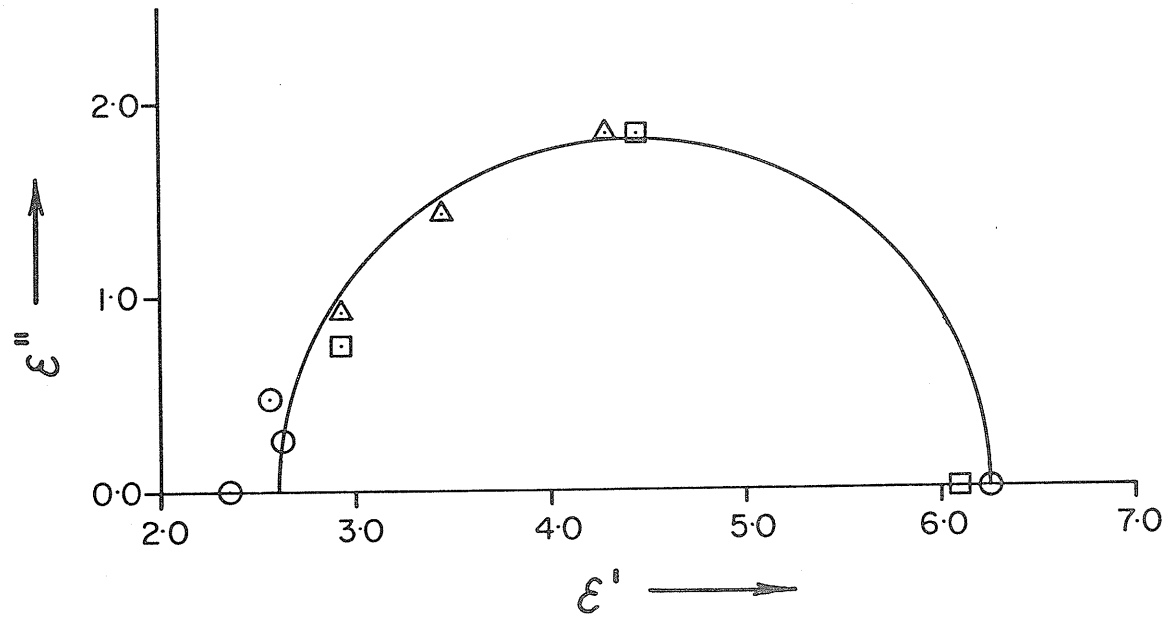

Figure III-2(b): Cole-Cole plot for pure chlorobenzene at 263.2K.
⊙, this work; △, ref. 2; ⊡, ref. 9.

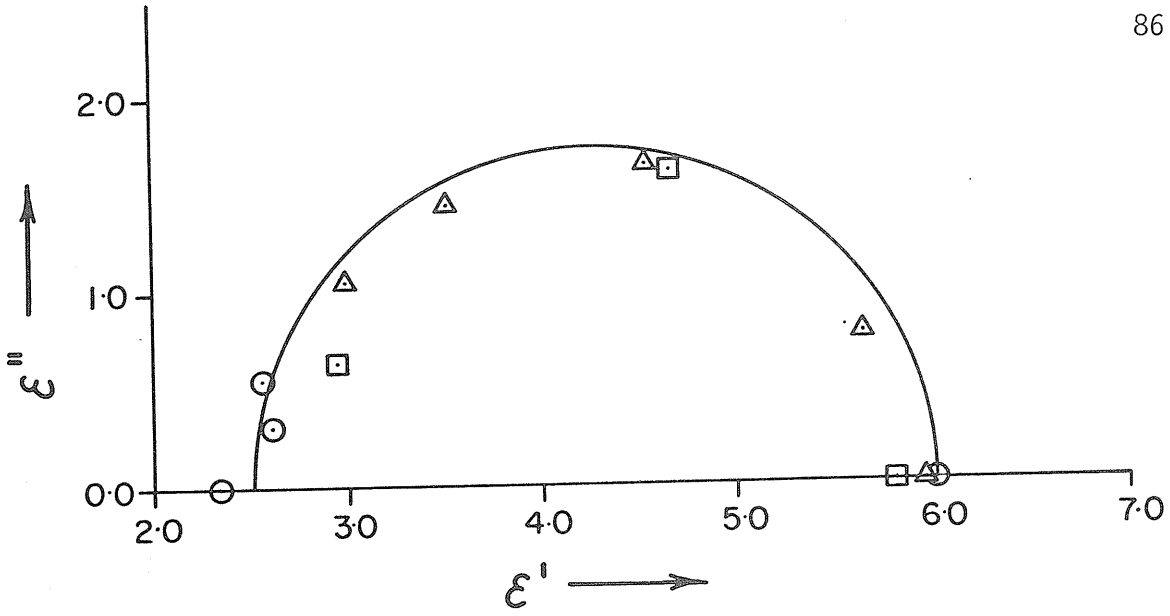

Figure III-2(c): Cole-Cole plot for pure chlorobenzene at 283.0K. ⊙, this work; △, ref. 2; ⊡, ref. 9.

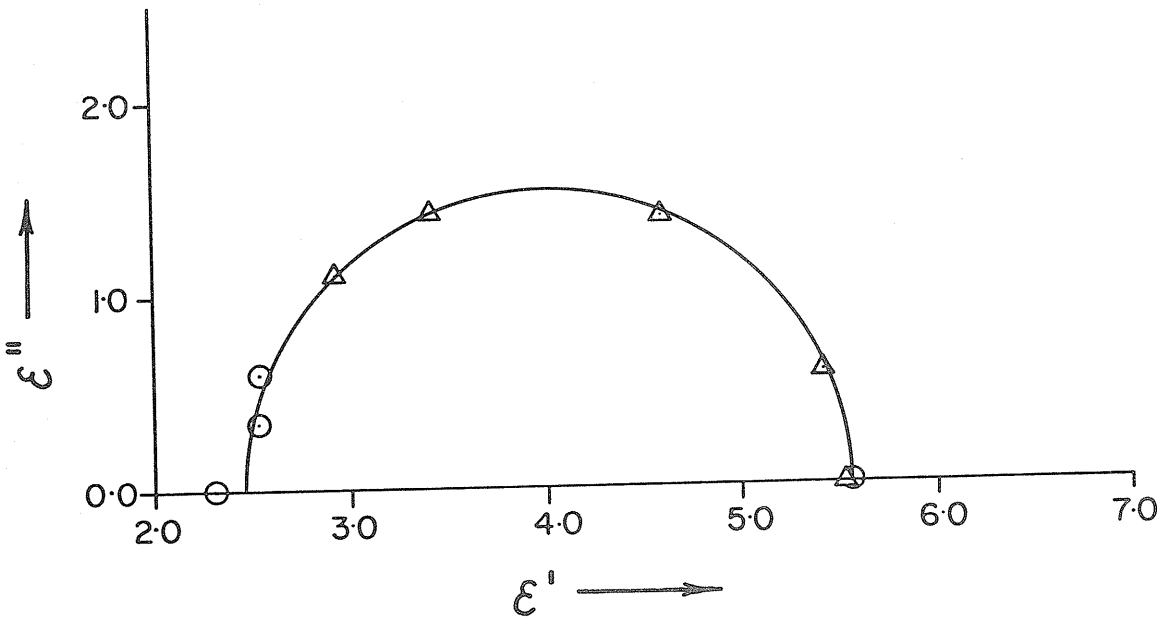

Figure III-2(d): Cole-Cole plot for pure chlorobenzene at 303.0K. ⊙, this work; △, ref. 2.

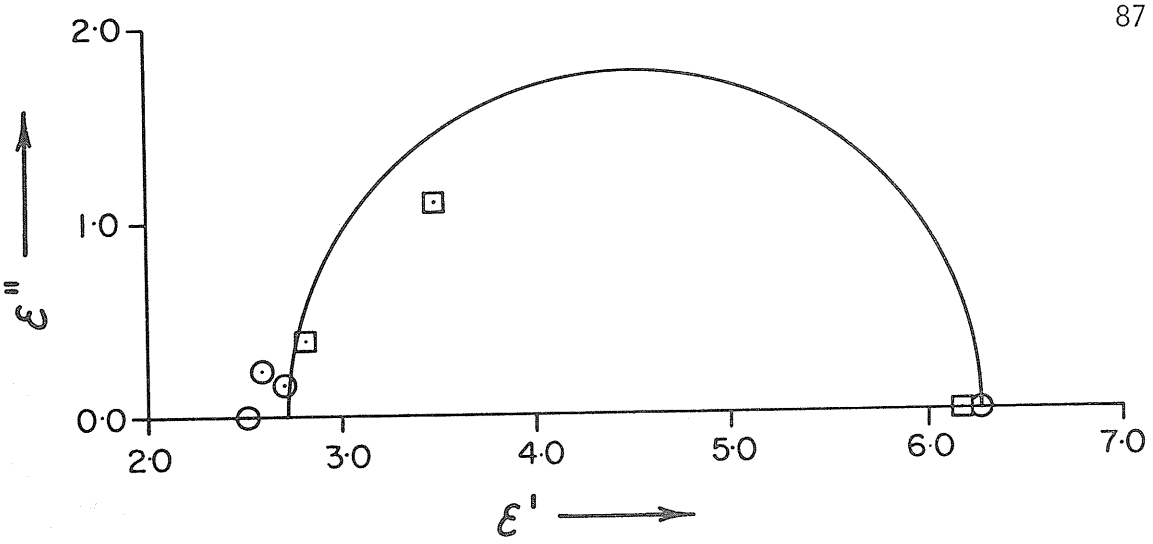

Figure III-3(a): Cole-Cole plot for pure bromobenzene at 244.0K.
⊙, this work; ⊡, ref. 9.

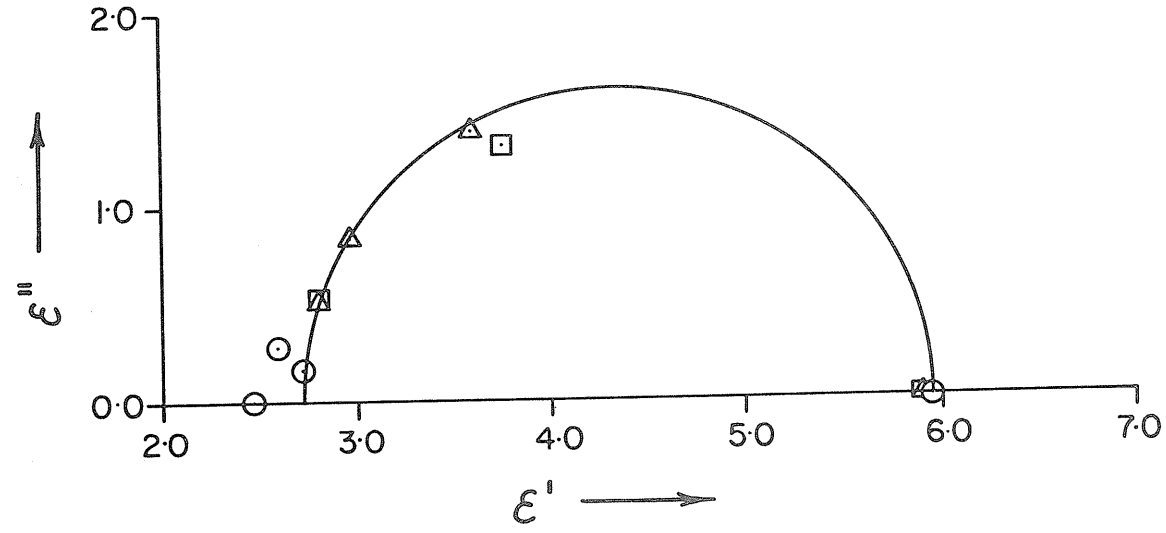

Figure III-3(b): Cole-Cole plot for pure bromobenzene at 264.0K.
⊙, this work; △, ref. 2; ⊡, ref. 9.

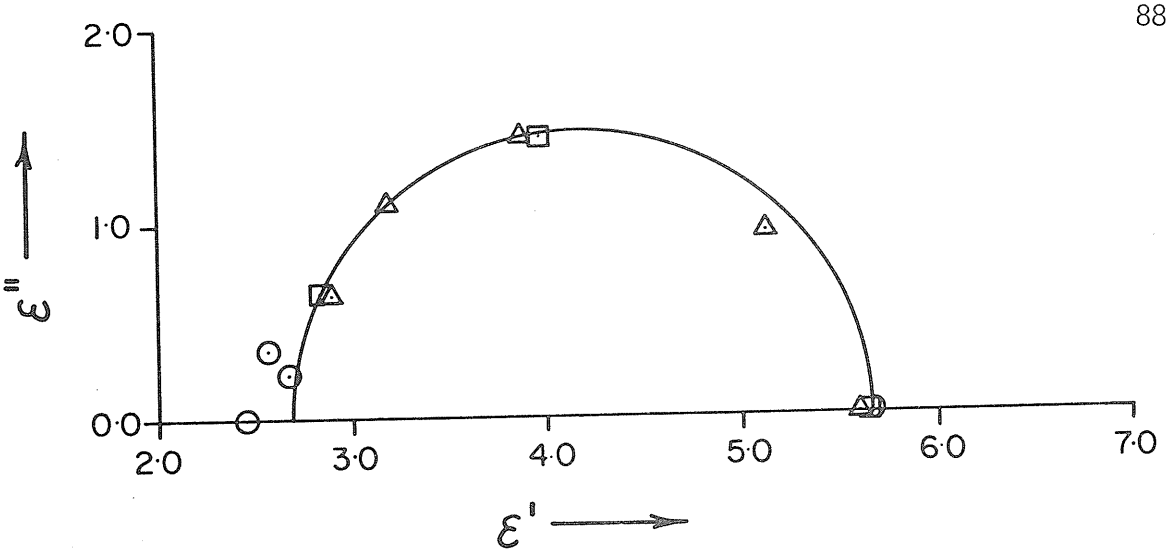

Figure III-3(c): Cole-Cole plot for pure bromobenzene at 283.0K.
⊙, this work; △, ref. 2; ⊡, ref. 9.

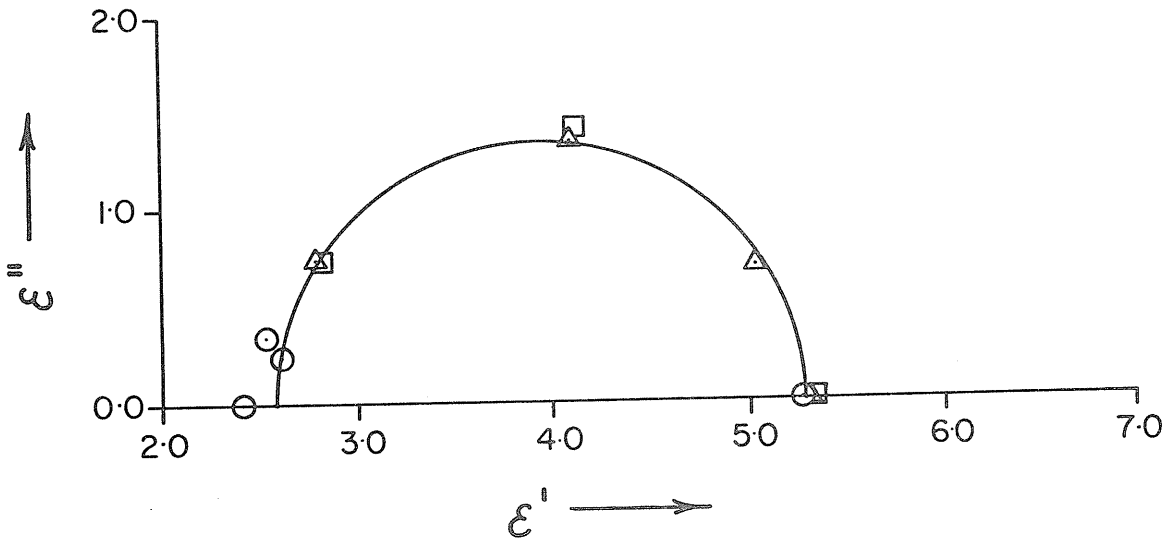

Figure III-3(d): Cole-Cole plot for pure bromobenzene at 303.0K.
⊙, this work; △, ref. 2; ⊡, ref. 9.

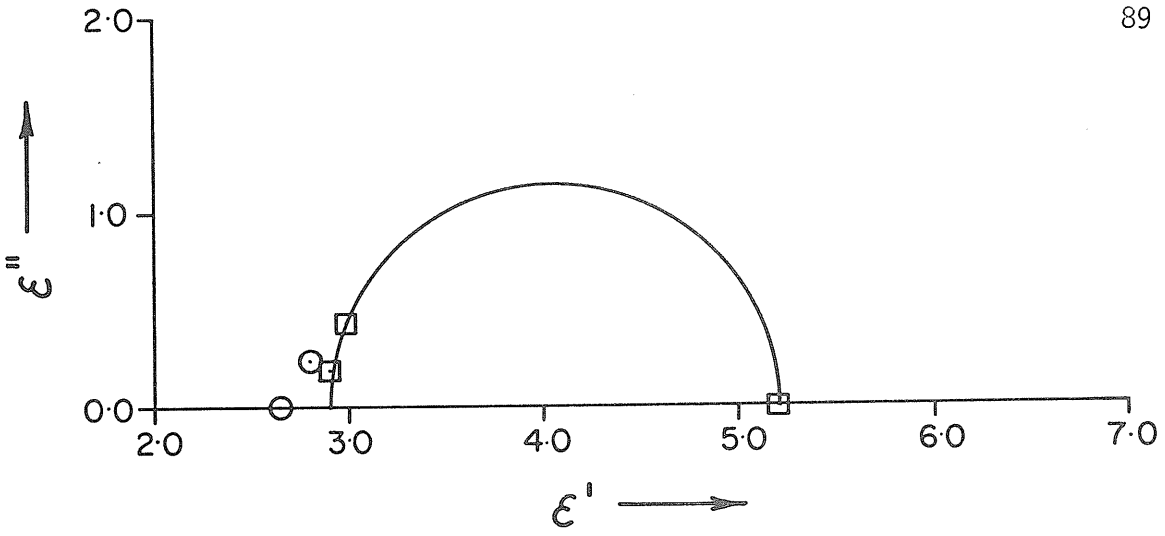

Figure III-4(a): Cole-Cole plot for pure iodobenzene at 243.7K.
⊙, this work; ⊡, ref. 9.

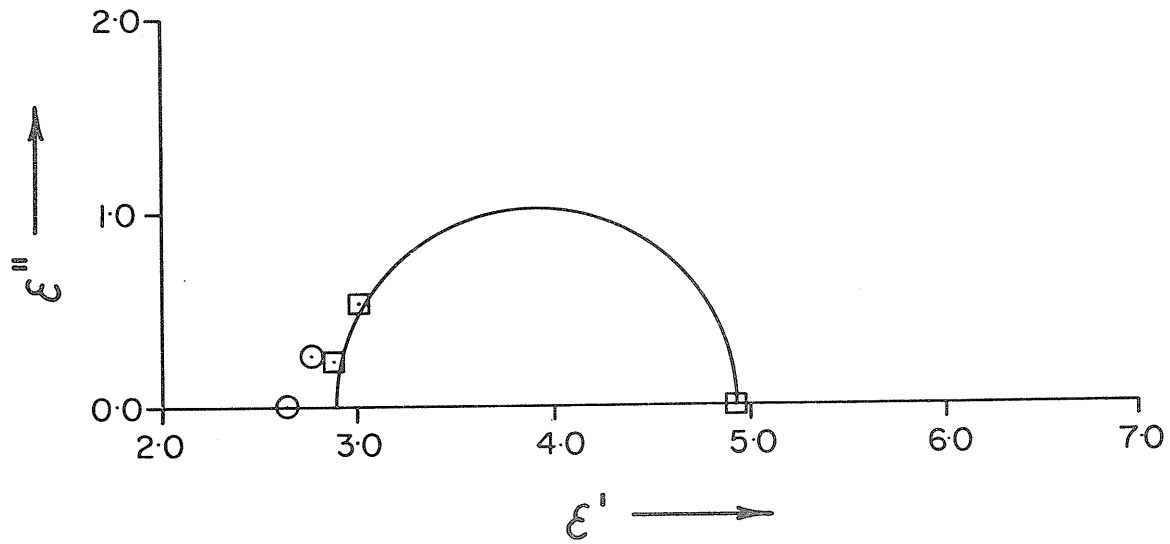

Figure III-4(b): Cole-Cole plot for pure iodobenzene at 263.3K.
⊙, this work; ⊡, ref. 9.

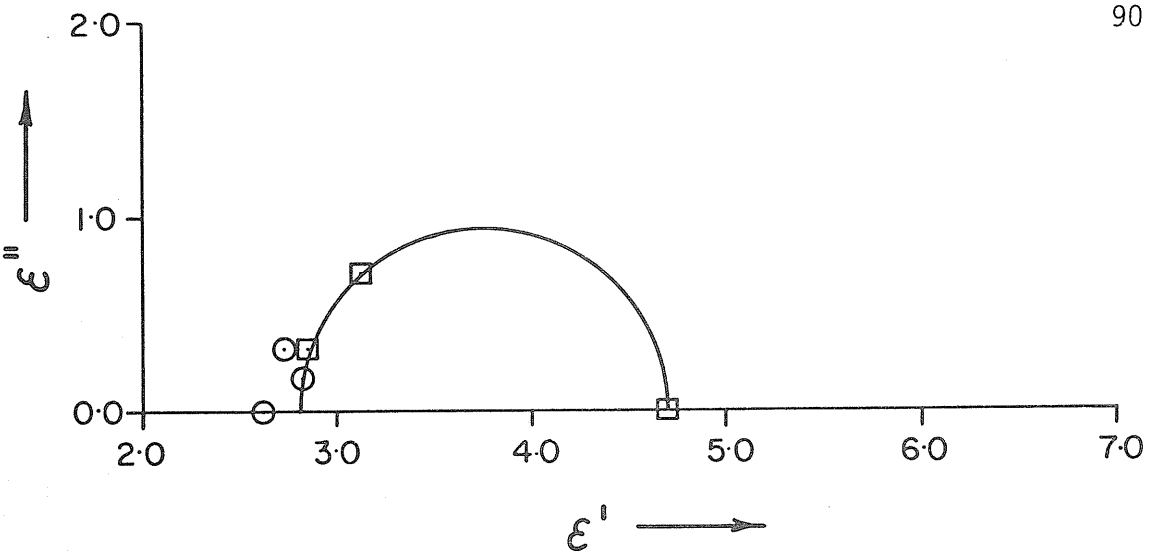

Figure III-4(c): Cole-Cole plot for pure iodobenzene at 283.0K. ⊙, this work; ⊡, ref. 9.

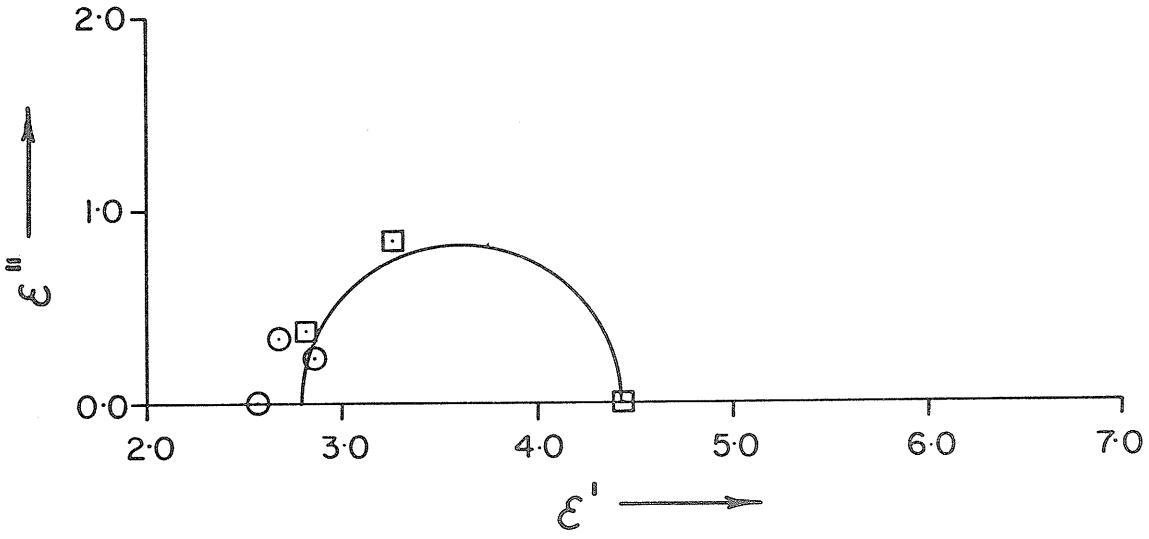

Figure III-4(d): Cole-Cole plot for pure iodobenzene at 303.0K. ⊙, this work; ⊡, ref. 9.

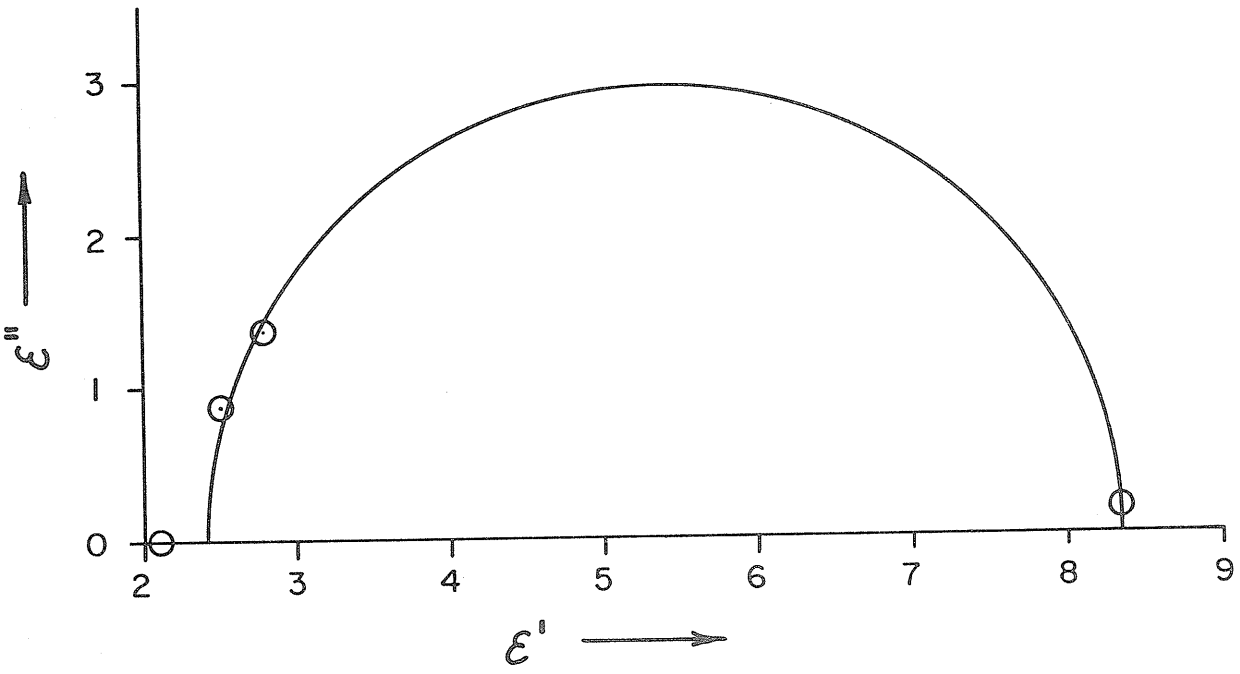

Figure III-5(a): Cole-Cole plot for pure 1,1,1-trichloroethane at 253.0K.

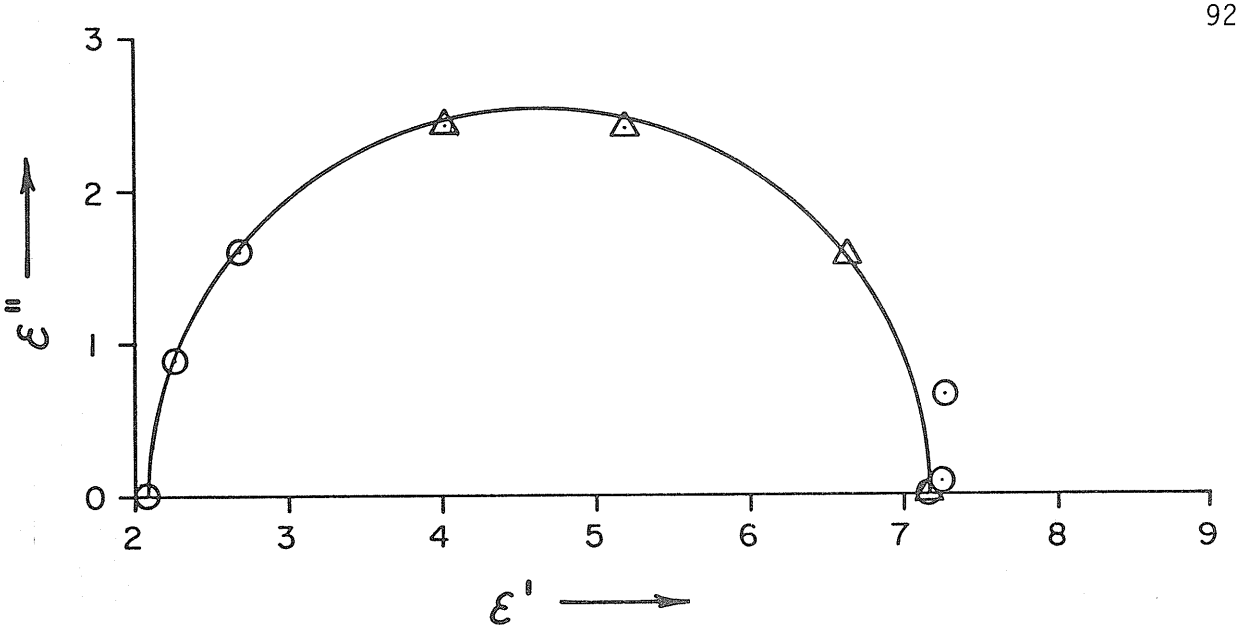

Figure III-5(b): Cole-Cole plot for pure 1,1,1-trichloroethane at 293.0K. ⊙, this work; △, ref. 2.

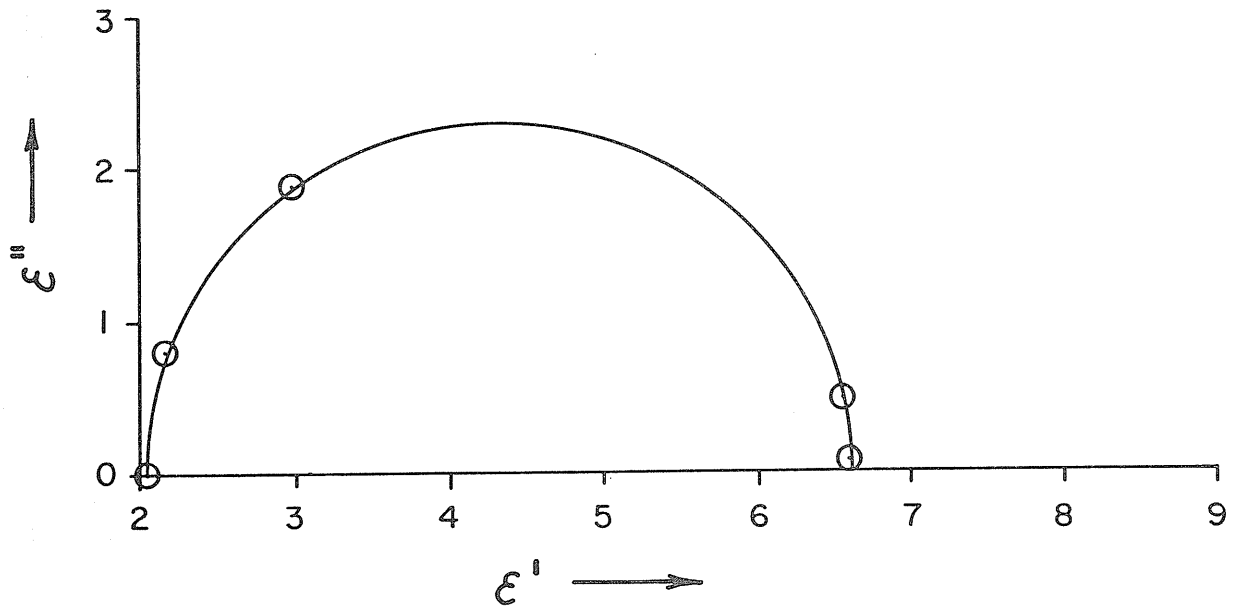

Figure III-5(c): Cole-Cole plot for pure 1,1,1-trichloroethane at 318.0K.

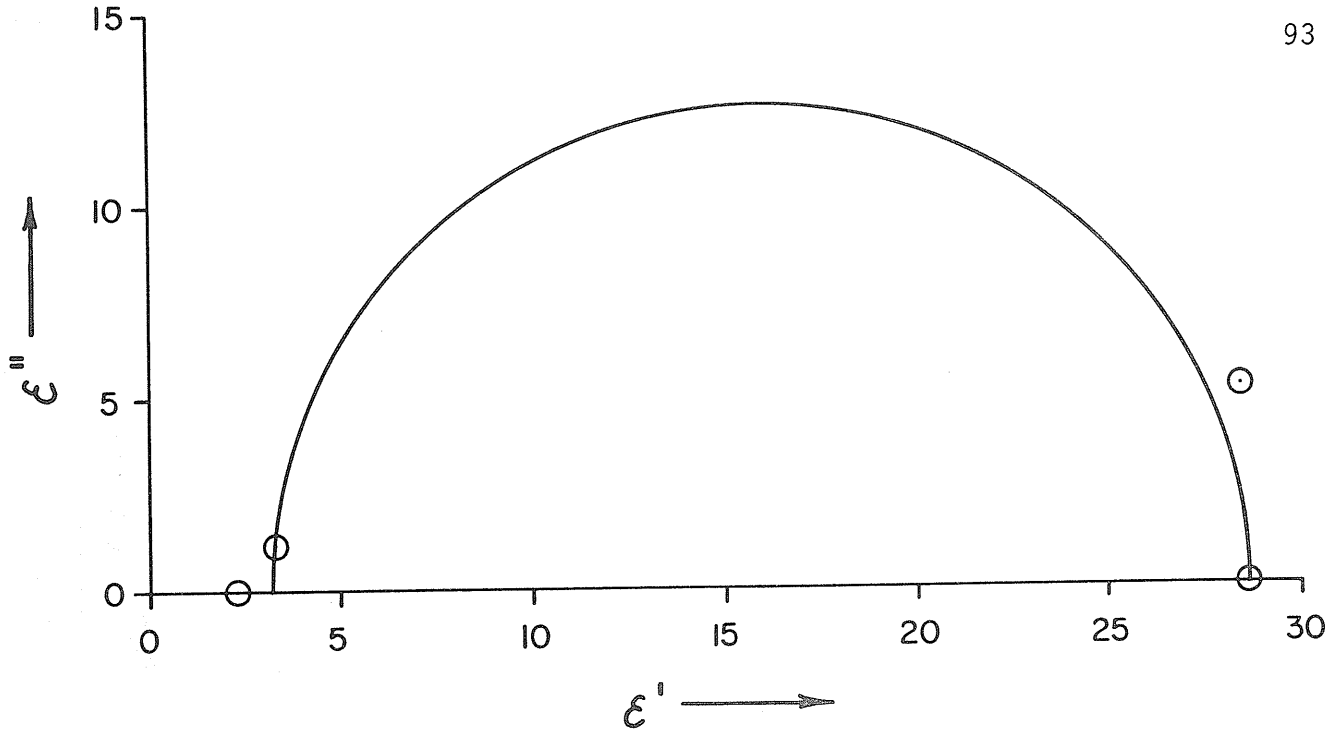

Figure III-6(a): Cole-Cole plot for pure benzonitrile at 263.0K.

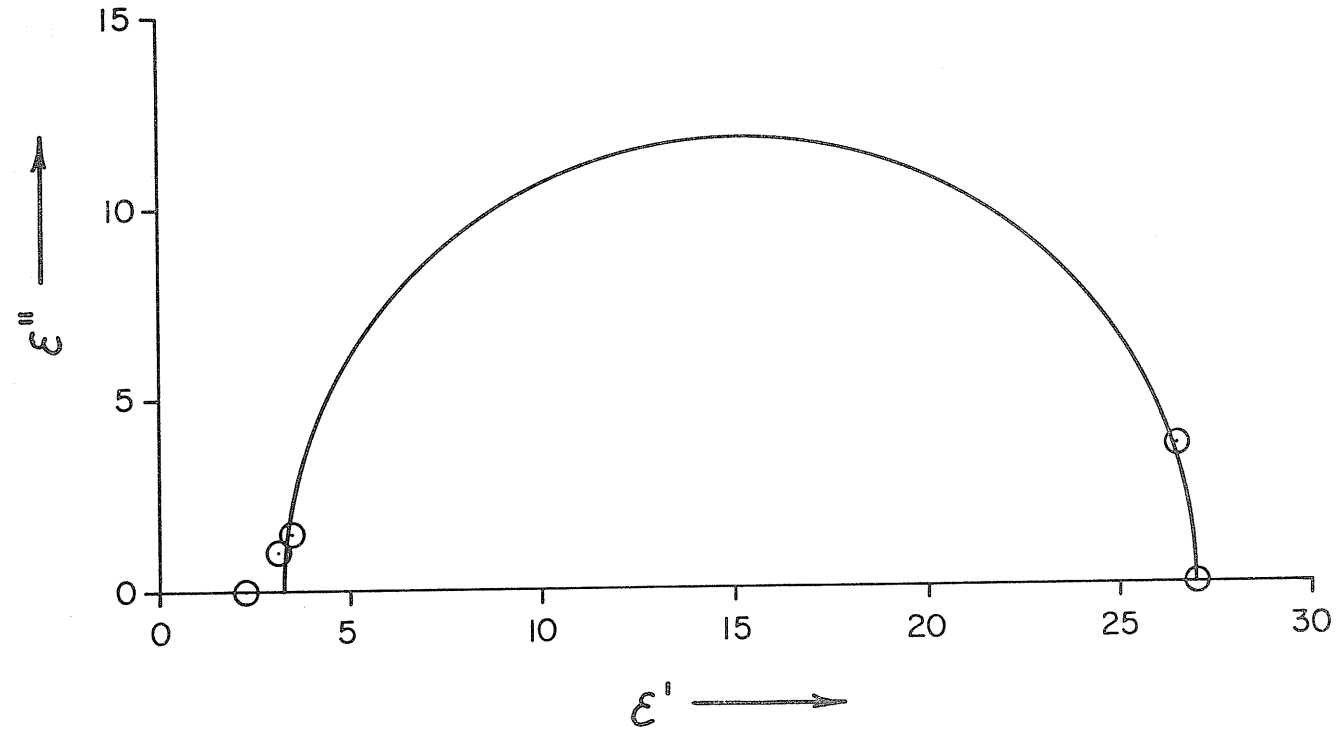

Figure III-6(b): Cole-Cole plot for pure benzonitrile at 278.0K.

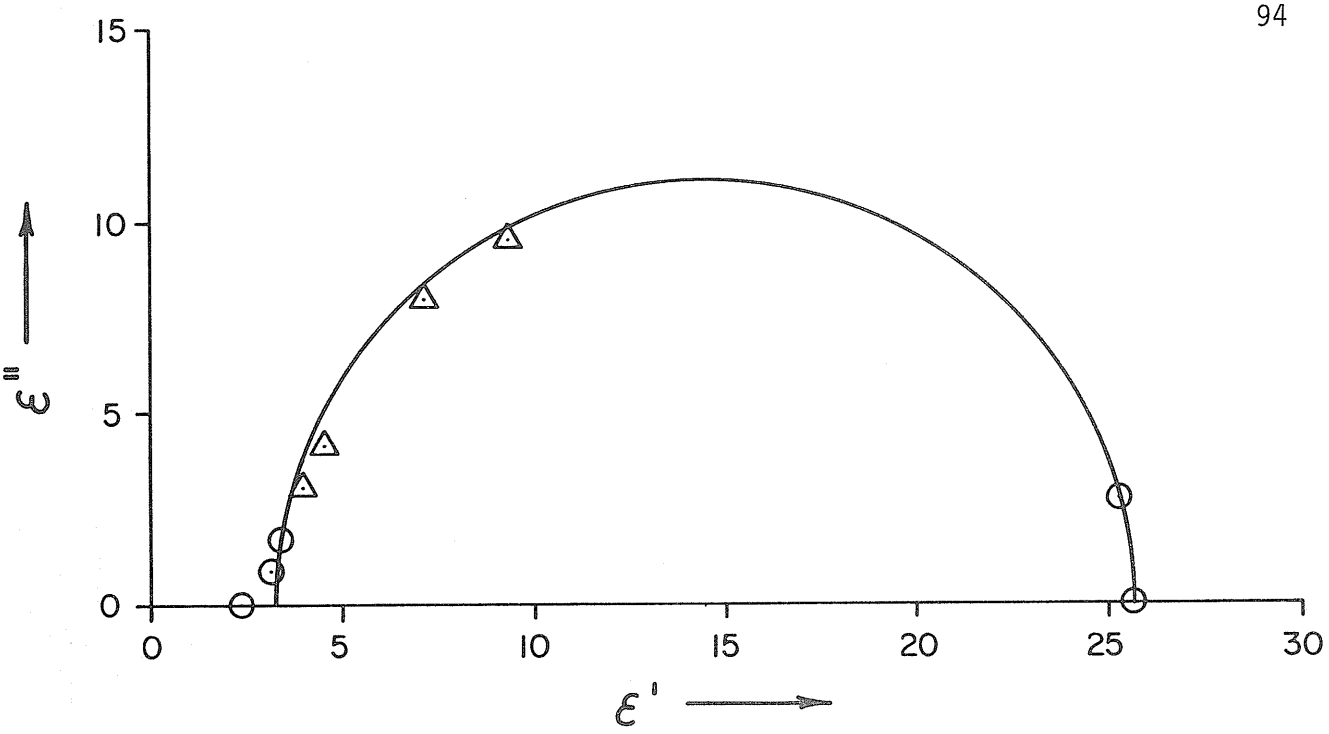

Figure III-6(c): Cole-Cole plot for pure benzonitrile at 294.0K. ⊙, this work; △, ref. 2.

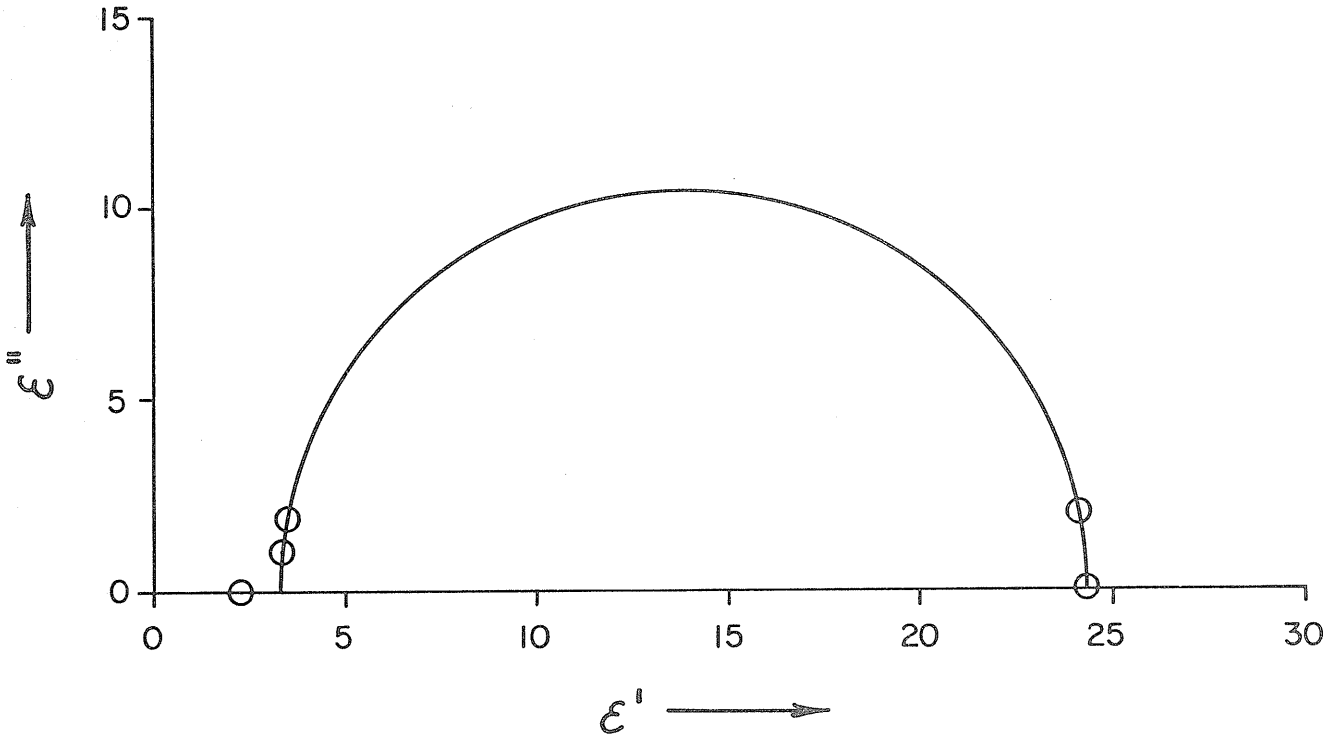

Figure III-6(d): Cole-Cole plot for pure benzonitrile at 308.0K.

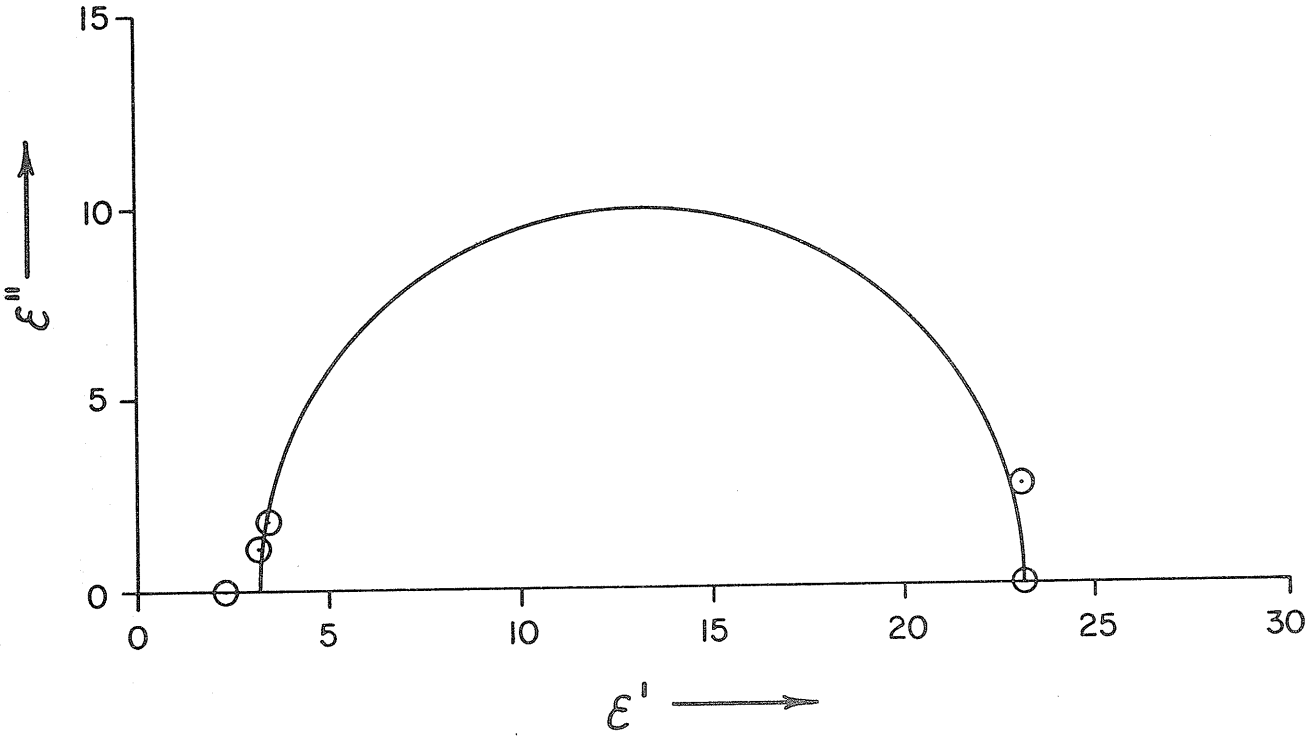

Figure III-6(e): Cole-Cole plot for pure benzonitrile at 323.0K.

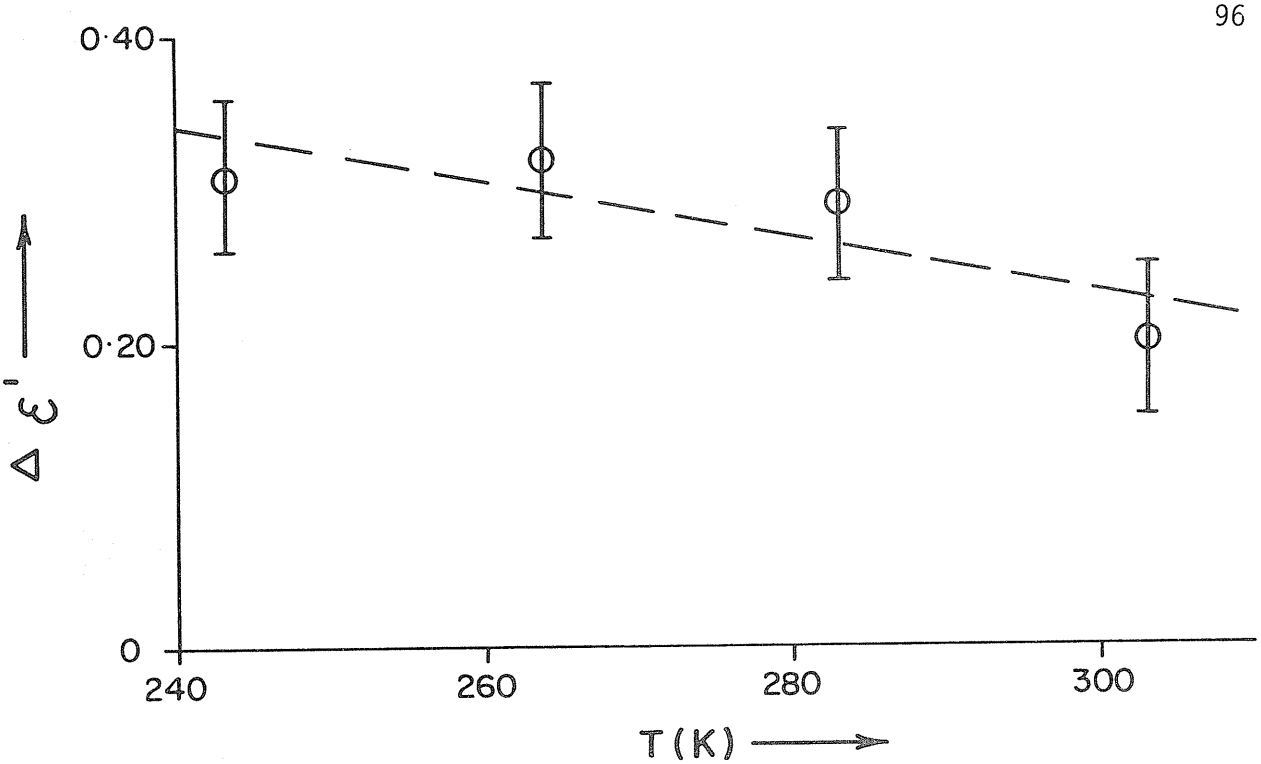

Figure III-7(a): $\Delta\varepsilon' = \varepsilon_\infty - (n_D)^2$ vs. T for pure fluorobenzene.

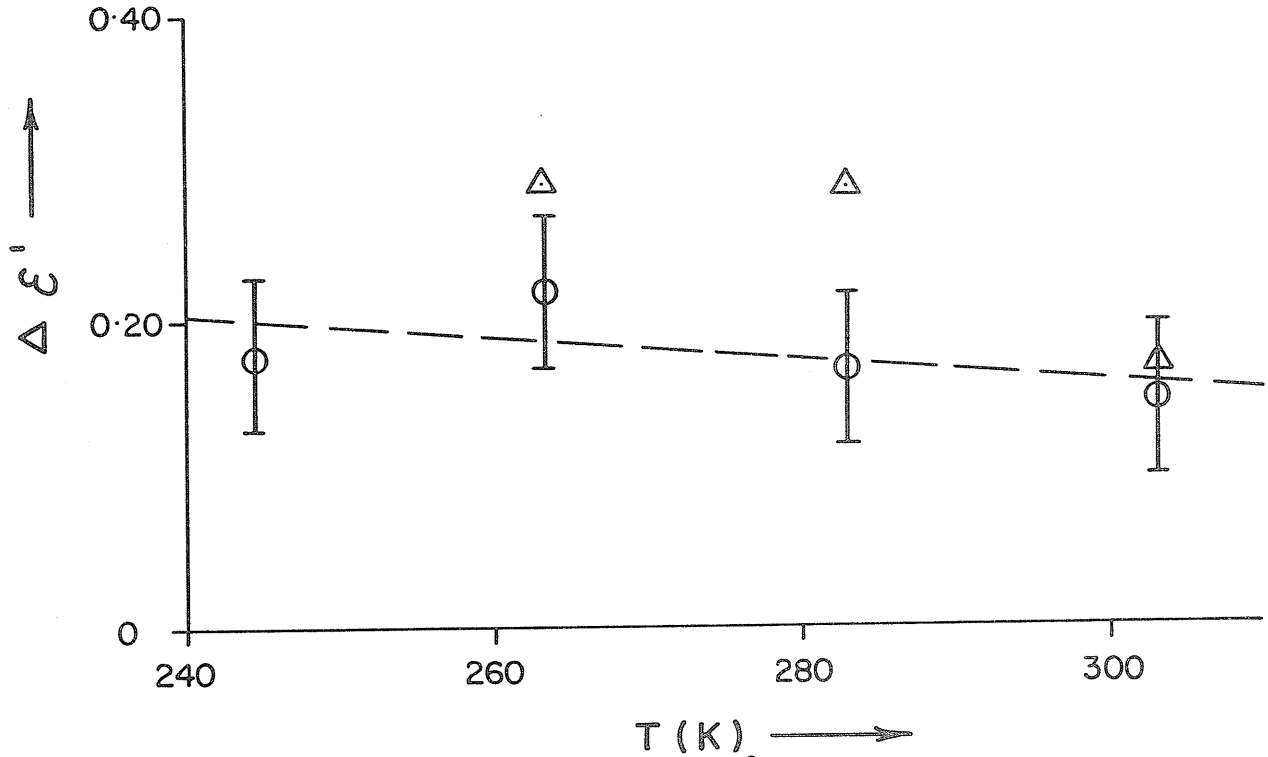

Figure III-7(b): $\Delta\varepsilon' = \varepsilon_\infty - (n_D)^2$ vs. T for pure chlorobenzene.

⊙, this work; △, ref. 2.

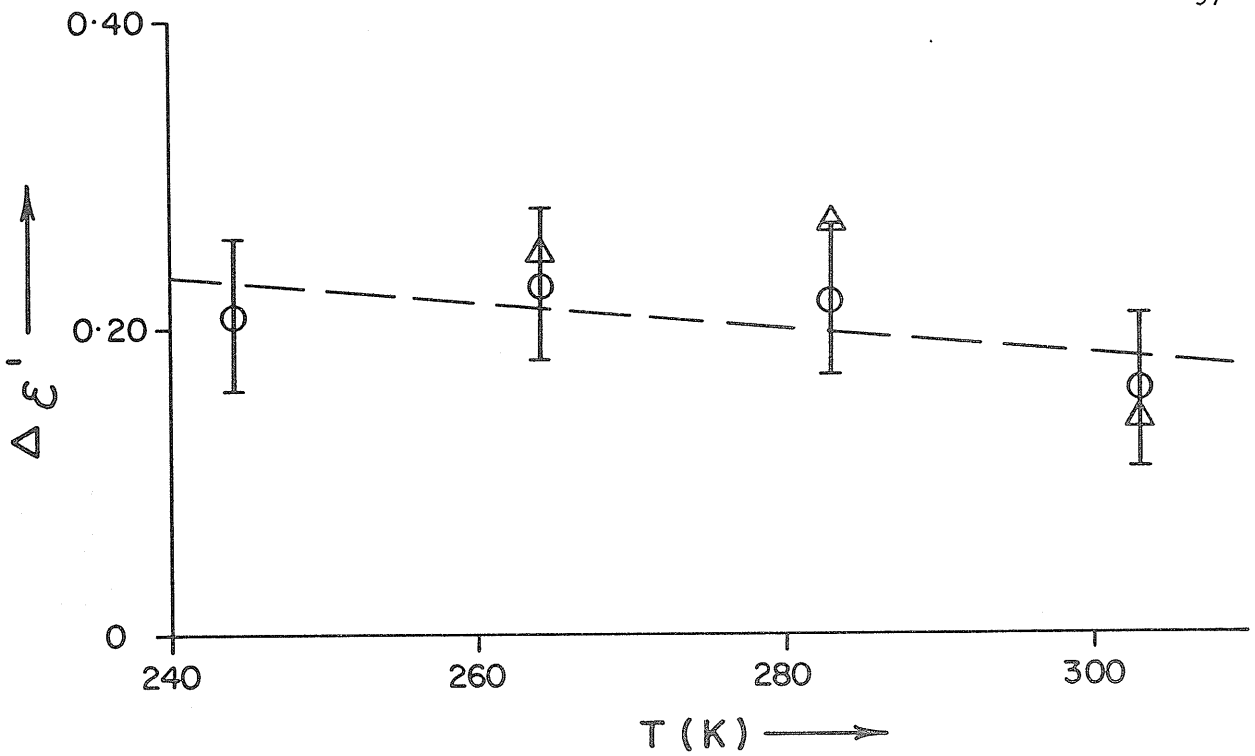

Figure III-7(c): $\Delta\varepsilon' = \varepsilon_\infty - (n_D)^2$ vs. T for pure bromobenzene. ⊙, this work; △, ref. 2.

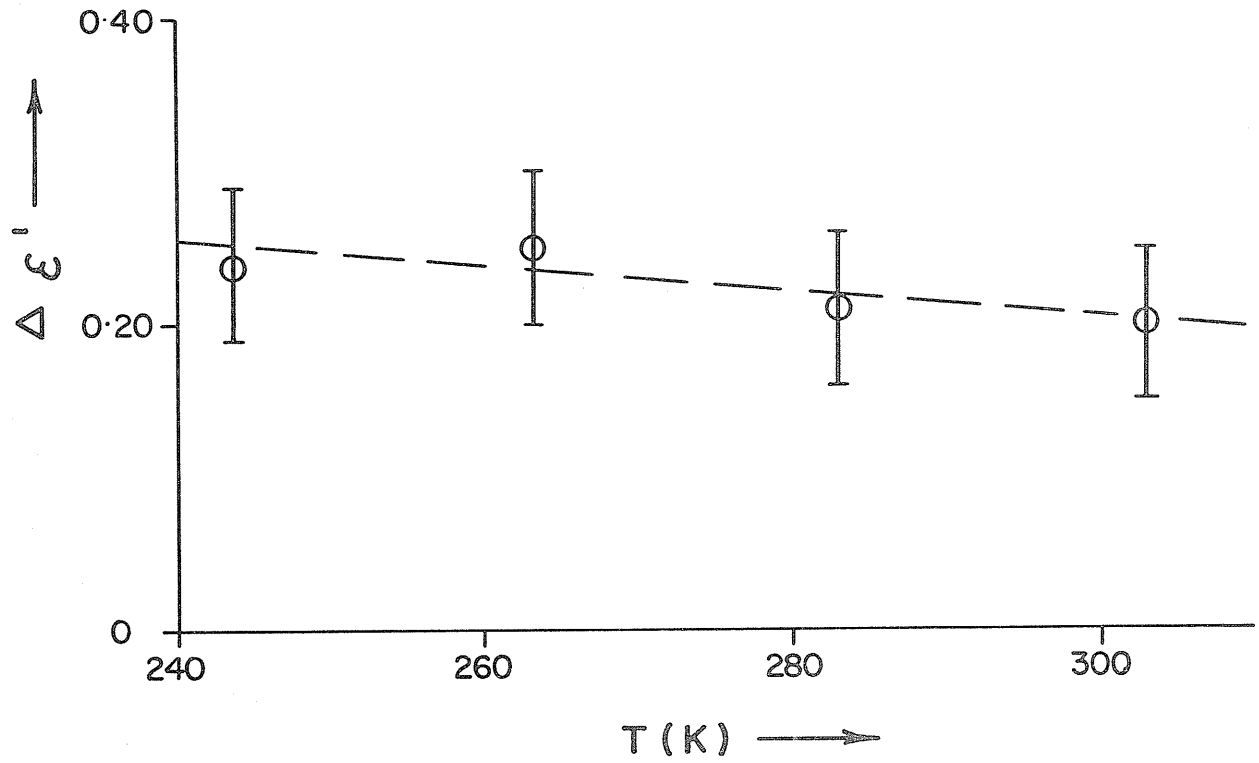

Figure III-7(d): $\Delta\varepsilon' = \varepsilon_\infty - (n_D)^2$ vs. T for pure iodobenzene

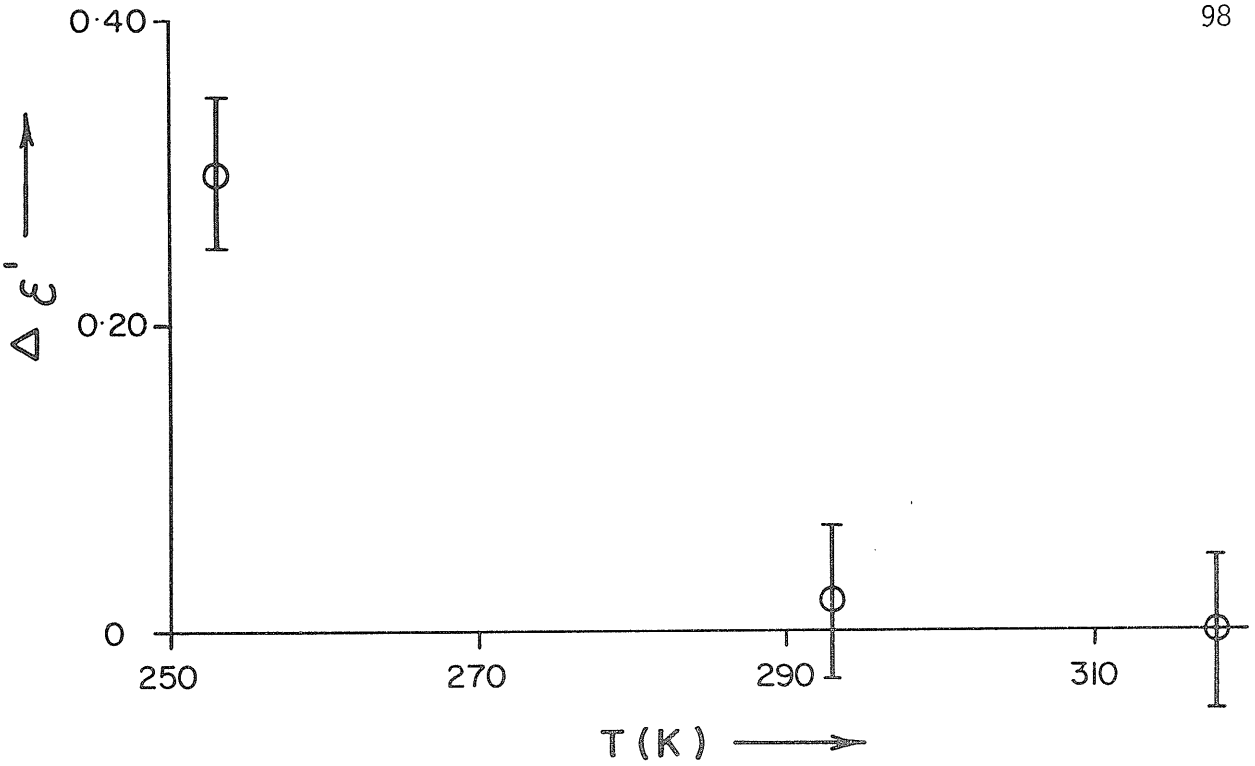

Figure III-7(e): $\Delta\varepsilon' = \varepsilon_\infty - (n_D)^2$ vs. T for pure 1,1,1-trichloroethane

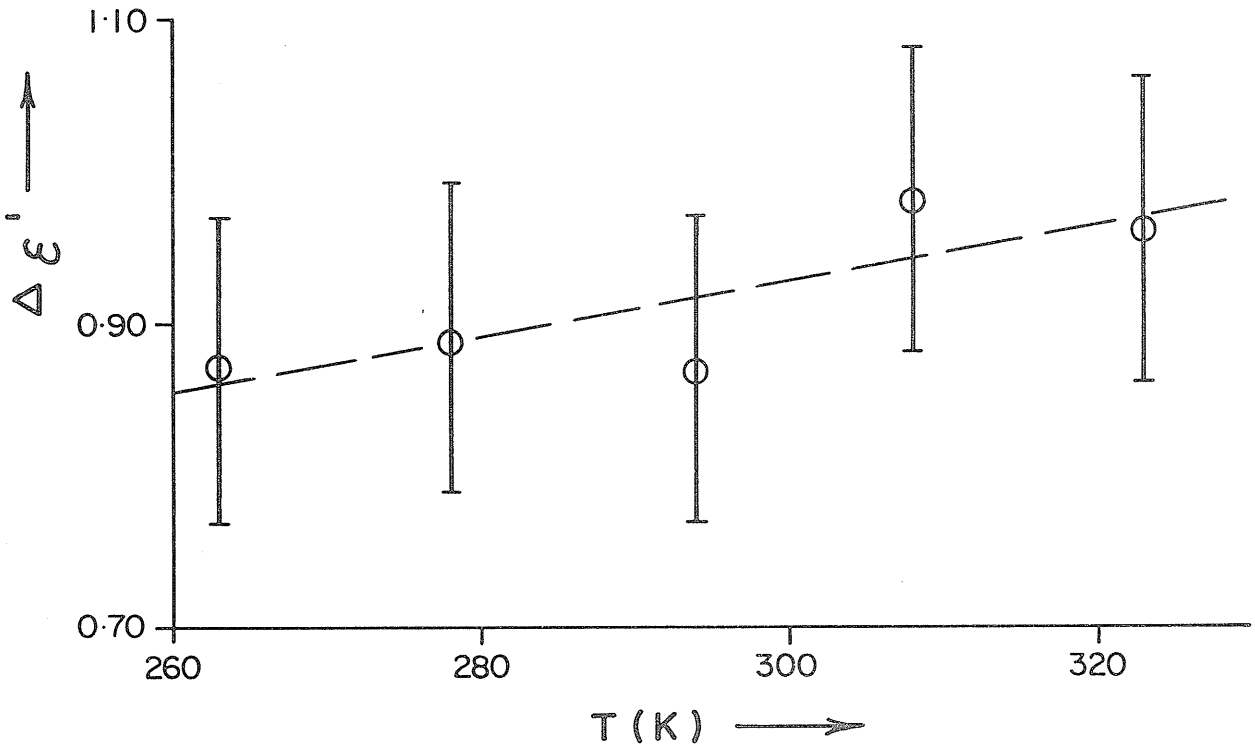

Figure III-7(f): $\Delta\varepsilon' = \varepsilon_\infty - (n_D)^2$ vs. T for pure benzonitrile

Discussion

The case of 1,1,1-trichloroethane provides some interesting information. Values of $\Delta\varepsilon'$ at both temperatures above 290K are indistinguishable from zero. If they really were zero, the Kramers-Kronig relationship predicts that there should be no absorption of far-infrared radiation, whereas this is not the case experimentally [6,7]. Davies et al.[10] and Poley[1] have obtained similar values of $\Delta\varepsilon'$ although the latter felt that his value might not be very accurate. Mallikarjun and Hill[9] obtained a very much larger value for this parameter, but this result was based on only two microwave measurements at wavelengths of approximately 3.3 and 0.8 cm., and the authors did not comment on its significance or its accuracy. It would seem, then, that the present values are in good agreement with reliable literature values.

Poley[1] noted another interesting fact with regard to the values of $\Delta\varepsilon'$. It appeared that its magnitude was proportional to the square of the permanent molecular dipole moment, μ. Jain and Walker[5] have reported that the maximum value of the optical absorption coefficient, α, measured for the broad band observed in the far-infrared region was

proportional to the quotient μ^2/I, where I is the mean moment of inertia for the rotational motion of the molecule. Now the dipole moments of 1,1,1-trichloroethane and of chlorobenzene are both approximately 1.6 Debye units[11] which suggests that their far-infrared absorption intensities, and hence the values of their high-frequency dispersions, should be comparable. Again we find that expectations based on other experimental evidence are not met by the experimental value for ε_∞ derived from a Cole-Cole plot analysis of microwave dielectric measurements. However, this value is in agreement with those of other workers. It appears that it might be appropriate to examine the validity of the Cole-Cole plot analysis procedure with respect to the determination of ε_∞.

Leroy et al.[12] have proposed a correlation function treatment of dielectric and far-infrared results. In their examination of a solution of 1,1,1-trichloroethane in n-hexane they found that the high-frequency (left-hand side) of the Cole-Cole plot deviated from a true semicircle. As frequency was increased and the decreasing values of the dielectric loss factor ε'' brought the graph line down towards the ε' axis, the line tended to bulge towards lower values of ε' and then to swing back towards higher values before the axis was reached. The value of

ε_∞ so obtained was larger than that which would have been obtained from a simple semicircular line fitting the lower-frequency experimental points from microwave measurements. They suggested that a Cole-Cole semicircle could not be relied upon to yield accurate values of ε_∞.

Another approach is to examine the graph of dielectric loss factor versus the natural logarithm of the angular frequency of the applied field. Such a graph is shown in Fig. III-8 for pure chlorobenzene at T=303K. The solid line represents the data generated using the Rocard and Powles[13] equation III-2 which includes a term to take into account the molecular moment of inertia.

$$\varepsilon'' = \frac{\varepsilon_0 - \varepsilon_\infty}{\left[1 - \left(\frac{I}{2kT\tau^2}\right)(\omega\tau)^2\right]^2 + (\omega\tau)^2} \qquad \text{III-2}$$

As usual, the symbol k represents the Boltzmann constant, and the values of the other parameters, derived from analysis of

experimental dielectric data, were:

$$\varepsilon_o = 5.56$$

$$\varepsilon_\infty = 2.46$$

$$\tau = 9.95 \times 10^{-12} \text{ s}$$

$$I = 6.16 \times 10^{-38} \text{ g-cm}^2$$

$$T = 303\text{K}$$

The dotted line represents the experimental values of ε'' obtained from measurement of pure chlorobenzene by means of Lamellar Grating and Grubb-Parsons modular cube far-infrared interferometers to cover the range of frequencies from 8 to 200 wavenumbers. For this purpose, ε'' was calculated from the far-infrared spectra by use of equation III-3 given by Hill *et al.*[14]

$$\varepsilon'' = \frac{n\alpha}{2\pi\bar{\nu}} \qquad \text{III-3}$$

Here ε'' is the dielectric loss factor, n is the refractive index, α is the optical absorption coefficient, and $\bar{\nu}$ is the frequency in wavenumbers.

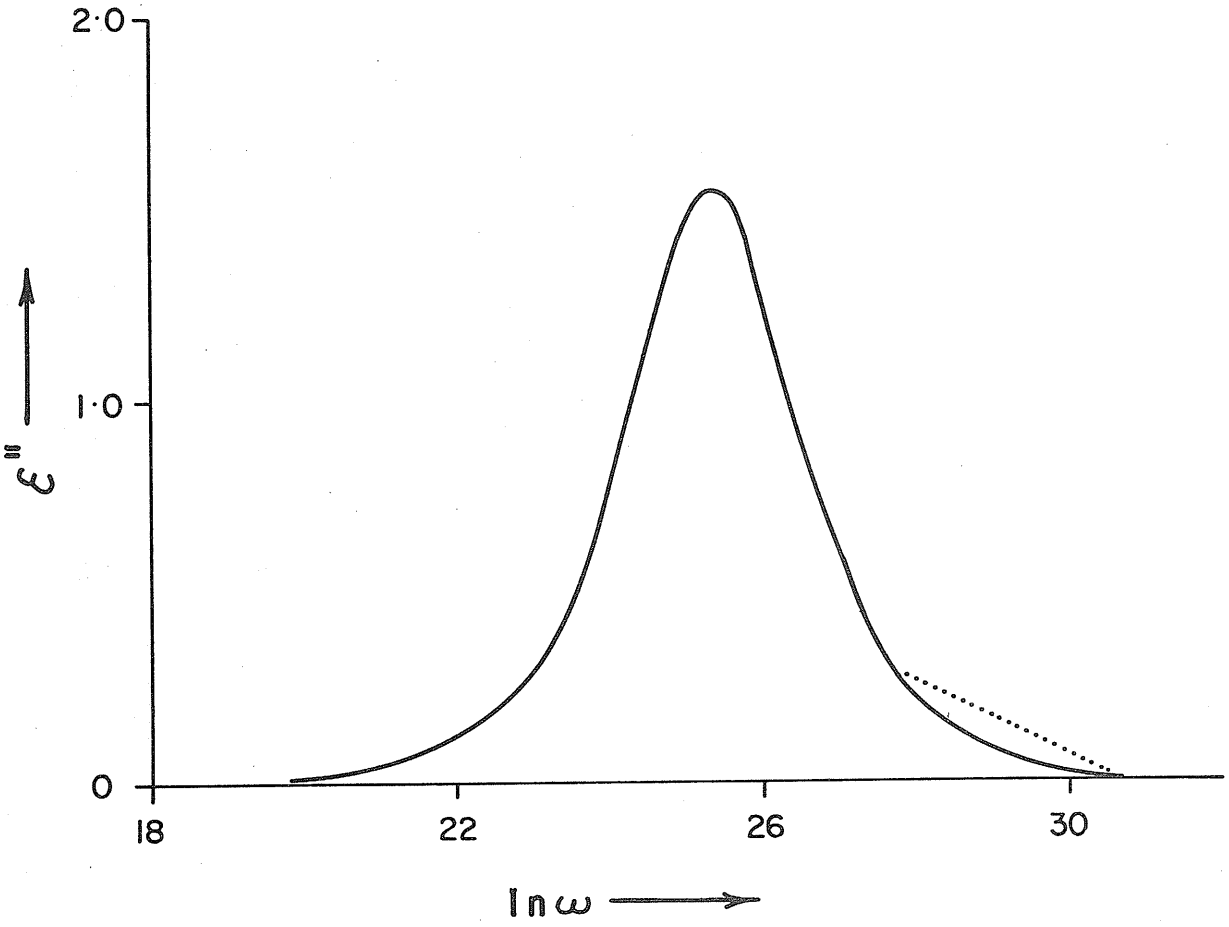

Figure III-8: Dielectric loss factor (ε") vs. natural logarithm of the angular frequency for pure chlorobenzene at T = 303K. The solid line represents data calculated from the Rocard and Powles equation. The dotted line represents the best smooth line through experimental data from Lamellar Grating and Michelson-type far-infrared interferometers.

Since the frequency appears in the denominator of this equation the important larger values of the dielectric loss factor are obtained in the lower frequency region of the far-infrared spectrum. Hence, the value used for the refractive index was not that found at the sodium D line but rather the square root of ε_∞ which should be a better estimate of the actual value of the refractive index at these frequencies.

It is clear that in the far-infrared region the experimental data exceed values given by the Rocard-Powles equation. More importantly, the far-infrared absorption overlaps the tail of the dielectric absorption. One can see then that the values of dielectric loss factor measured at the higher microwave frequencies (a wavelength of 0.2 cm corresponds to a frequency of 5 wavenumbers) may contain an appreciable contribution from the far-infrared absorptions. This would tend to push the left-hand side of a Cole-Cole semi-circle towards lower values of ε_∞ than should be obtained without this contribution from the far-infrared absorption. Such an effect would be enhanced by an increase in the magnitude of the far-infrared absorption and by its occurrence at lower frequencies.

Now we may examine how this overlap of absorptions

could affect the situations for chlorobenzene, 1,1,1-trichloroethane, and benzonitrile. In Table III-1 are summarized the results of some analyses of the dielectric data for these three. Note that, if $\omega_{max.}$ is defined as that frequency at which the dielectric loss factor reaches a maximum, then $\omega_{max.} = 1/\tau$.

TABLE III-1

Molecule	T(K)	$10^{12} \times \tau$ (s)	$\ln(\omega_{max.})$
Chlorobenzene	303.0	9.95	25.33
	263.2	14.9	24.92
1,1,1-trichloroethane	293.0	6.0	25.84
	253.0	7.8	25.58
Benzonitrile	294.0	32.0	24.17

One of the features which has emerged clearly in studies of the effects of temperature on the far-infrared absorption spectra of pure liquids is that, as temperature is decreased, both the maximum value of the optical absorption coefficient, α, and the frequency at which this occurs, $\bar{\nu}_{max.}$, increase. For chlorobenzene[5] at 295K, $\alpha_{max.} = 16\ cm^{-1}$ and $\bar{\nu}_{max.} =$

44 cm^{-1}, while at 248K, $\alpha_{max.}$ = 17 cm^{-1} and $\bar{\nu}_{max.}$ = 53 cm^{-1}.

For 1,1,1-trichloroethane[6] at 293K, $\alpha_{max.}$ = 36 cm^{-1} and

$\bar{\nu}_{max.}$ = 30 cm^{-1}, while at 242K $\alpha_{max.}$ = 33 cm^{-1} and

$\bar{\nu}_{max.}$ = 38 cm^{-1}. In other words, as temperature is decreased, the frequency of the maximum dielectric absorption decreases while the frequency for far-infrared absorption increases. This results in a greater separation of these two absorptions along the logarithmic frequency axis.

In comparing the data for chlorobenzene and 1,1,1-trichloroethane, one finds that the frequencies of the maximum dielectric absorptions are lower for chlorobenzene at both temperatures shown in Table III-1 and that the frequencies of far-infrared absorptions are higher for chlorobenzene. In fact, the far-infrared peak for 1,1,1-trichloroethane is found at a markedly lower frequency than those of most liquids reported in the literature. One may also note that the intensity of the far-infrared peak for 1,1,1-trichloroethane is about twice that of chlorobenzene. Therefore, it may be seen that the overlap of far-

infrared absorption with dielectric absorption is much greater in the case of 1,1,1-trichloroethane. This might be expected to produce correspondingly larger distortions of the Cole-Cole semicircle at high frequencies of dielectric measurements.

On the other hand, benzonitrile[5] at 295K shows $\alpha_{max.} = 94\ cm^{-1}$ and $\tilde{\nu}_{max.} = 53\ cm^{-1}$. At the same time its dielectric absorption is centred at a much lower frequency than those of the other two, resulting in a much larger separation of the two absorptions. One might expect that this would lead to less distortion of the Cole-Cole semicircle. Indeed the values of $\Delta\varepsilon' = \varepsilon_\infty - (n_D)^2$ derived from Fig. III-6 are all in agreement with one another within the estimated error of ± 0.1. It would seem from these considerations that any sudden change of $\Delta\varepsilon'$ with altered temperature is not a consequence of a strong temperature dependence of the far-infrared absorptions. Instead it is a direct result of the inadequacy of the Cole-Cole analysis technique at very high frequencies in the microwave region. It may be, as suggested by Leroy et al.[12], that this is due to a basic inadequacy in the Debye formulation. Alternatively it is possible that this formulation is reasonably correct but that the overlap of the higher-frequency processes observed in the far-infrared region causes the experi-

mental data to yield inaccurate values of ε_∞.

A different approach to estimating the magnitude of the high-frequency dispersion, $\Delta\varepsilon'$, has been attempted also. Let us assume for this purpose that the molecular motions giving rise to the dielectric and far-infrared absorptions are separate and distinct (that is, that these two absorptions are not the result of exactly the same motions). This is not to say that each of these two classes of motions contains only one motion, but merely that the several motions may be divided into two distinct classes. If one assumes further that the frequency dependence of the dielectric absorption may be described with reasonable accuracy by the Rocard and Powles equation III-2, then the contribution which is made by the dielectric processes at far-infrared frequencies may be calculated and subtracted from the total observed absorption. The residue should then be the absorption due solely to the far-infrared processes. Such a procedure is shown graphically for the far-infrared absorption of pure chlorobenzene at 303K in Fig. III-9. In this figure the solid line sweeping down from the top represents the values calculated from Eqn. III-2 with values for the appropriate parameters as specified earlier. The dashed line represents the best smooth line fit to the values of dielectric loss factor

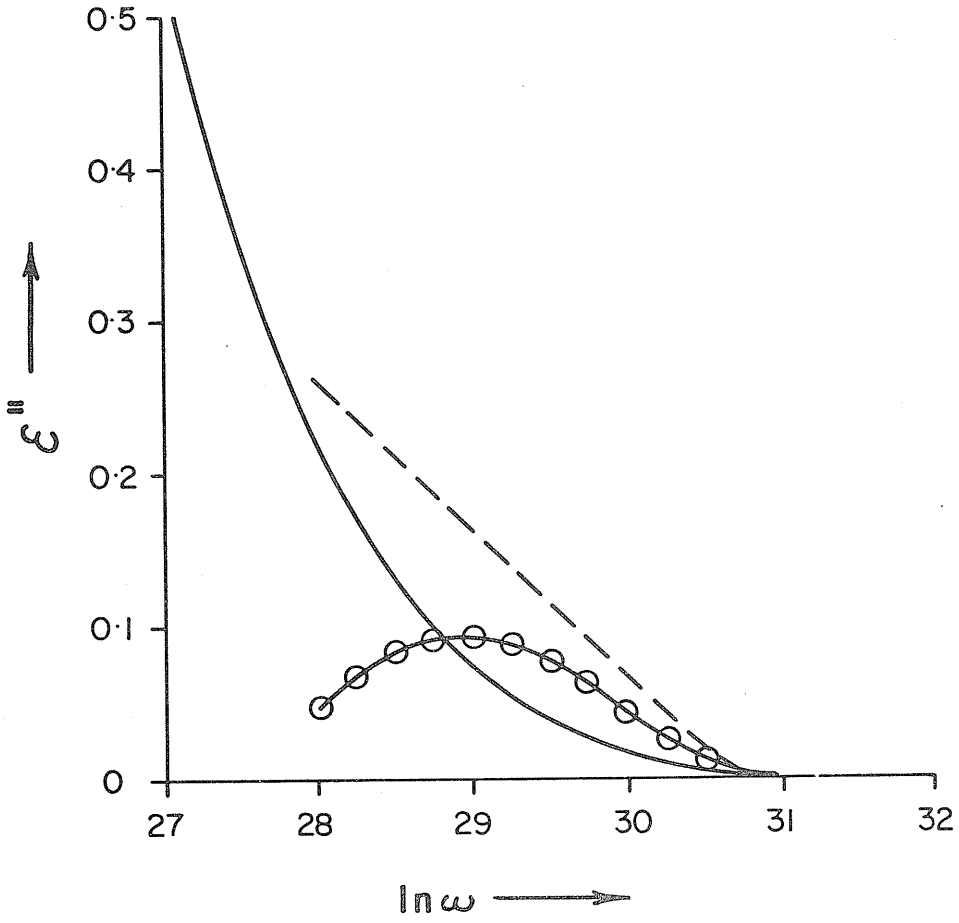

Figure III-9: Dielectric loss factor (ε'') vs. natural logarithm of the angular frequency for pure chlorobenzene at T = 303K. The upper solid line represents data calculated from the Rocard and Powles equation. The dashed line represents the best smooth curve through experimental data from Lamellar Grating and Michelson-type far-infared interferometers. The lower solid line through circled points represents the difference between these two.

calculated from the observed far-infrared absorption spectrum by means of Eqn. III-3 with the refractive index replaced by the square root of ε_∞ as mentioned previously. The humped curve joining the circled dots represents the difference between the first two lines. Now the Kramers-Kronig relationship, Eqn. III-1, may be applied to this residue. The lower-frequency tail of this residue is not fully defined, but the residue curve appears to be reasonably symmetrical about the maximum value which is located at $\ln \omega = 28.85$. Therefore, integration of only the right-hand side of this curve should yield one-half of its total area. The total area thus calculated is 0.207, resulting in a value for $\Delta\varepsilon' = 0.13$, in excellent agreement with the value of 0.15 ± 0.05 given in Table II of the appendix. The latter value was obtained through use of the Cole-Cole plot. It may be noted that in 1963 Hill[15] suggested an equation which led to the prediction that the far-infrared absorption of pure chlorobenzene should be centred at an angular frequency of 4.4×10^{12} s^{-1}, or 23.4 cm^{-1}. The residue peak calculated above is at 18 cm^{-1}.

One must now ask whether the procedure outlined above may be useful generally in view of the fact that it appeared to yield good results for chlorobenzene. A number of assumptions

was made in its development. Firstly, it was assumed that the Rocard and Powles equation correctly represented the dielectric absorption at high frequencies. Secondly, it was assumed that the value of the refractive index was approximately constant at low far-infrared frequencies and thirdly that this constant value was given by the square root of ε_∞. The value of this parameter must be estimated from the lower-frequency dielectric data via Cole-Cole analysis. In fact, this procedure of subtracting the Rocard and Powles tail of dielectric absorption would yield a new estimate of ε_∞, but these two estimates would not differ sufficiently to affect the results by very much, as is outlined below. A fourth assumption was that the residue curve was symmetrical about its peak value. Finally, the far-infrared and dielectric absorptions were assumed to appear from separate and distinct classes of molecular motion. That is a lengthy list of assumptions!

The Rocard and Powles equation has been used by Davies et al.[10] although they pointed out that, at frequencies above about 100 cm^{-1}, this expression yields values of optical absorption coefficient larger than experimentally observed values and is thus obviously in error at such frequencies. Hill[16] has considered its use and concluded that "it can be seen that

no advantage is to be gained by subtracting a Debye tail from the experimentally observed absorption". It would appear that the best that can be said of this formulation is that it is an improvement on the original simple Debye equations at higher frequencies but still inadequate to describe the real situation.

The use of a constant approximate value for the refractive index in Eqn. III-3 introduces only small errors. At worst, the actual value of refractive index may change from $\sqrt{2.46} = 1.57$ to 1.52, which is only three percent, a rather small error compared to those from other sources in this procedure.

The assumption of residue peak symmetry was based solely on the appearance of the peak on the graph and has no basis in theory, simply because there are no adequate theories to explain far-infrared absorptions. For the same reason the assumption of separable classes of molecular motion, and therefore of separable absorption peaks, may be questioned. Indeed, the lack of adequate theories was the stimulus for the present work which is aimed at obtaining experimental data from which such theories may be developed.

Conclusions

This investigation of dielectric and far-infrared experimental data for six pure liquids has shown that probably it is not possible to obtain accurate estimates of the limiting high-frequency value of the dielectric constant and hence of the magnitude of the dispersion associated with the far-infrared absorption bands. A major difficulty in any such attempt is that the absorptions due to the dielectric and far-infrared processes overlap considerably. There appears to be no accurate mathematical formulation to describe either one or the other to facilitate separate accurate measurements of the associated dispersions. If, on the other hand, the far-infrared absorptions are not due to some class of molecular motion distinct and separate from those of dielectric relaxations, then the value of ε_∞ should not be estimated from the Debye theory at all. Rather, it should be obtained from the square of the refractive index of the sample at a frequency above that of the far-infrared broad band absorption but below that of low-frequency fundamental vibrations of the molecule.

It seems, then, that investigations centred on measurement of these dispersions, and particularly of ε_∞, are an

inappropriate technique for the acquisition of information about the nature of the far-infrared absorption processes. A more fruitful approach seems to be to investigate the effects of experimental parameters on the observed absorptions in order to provide information on their possible origins. With this in mind, the investigations reported in the remainder of this work have been centred on the effects resulting from a considerable decrease of the translational and large-angle rotational motions of dipolar molecules.

REFERENCES

1. J. Ph. Poley, J. Appl. Sci. Res., B4, (1955), p. 337.

2. A. J. van Eick and J. Ph. Poley, J. Appl. Res., B6, (1957), p. 359.

3. G. W. F. Pardoe, Trans. Faraday Soc., 66, (1970), p. 2699.

4. S. G. Kroon and J. van der Elsken, Chem. Phys. Lett., 1, (1967), p. 285.

5. S. R. Jain and S. Walker, J. Phys. Chem., 75, (1971), p. 2942.

6. C. K. McLellan, M. Sc. Thesis, Lakehead University, Thunder Bay, "P", Ontario, Canada, P7B 5E1, (1971).

7. C. K. McLellan and S. Walker, J. Phys. Chem., 75, (1971), p. 2942.

8. K. D. Möller and W. G. Rothschild, "Far-Infrared Spectroscopy", Wiley-Interscience (John Wiley and Sons, Inc.), New York, New York, U. S. A., (1971), p. 419.

9. S. Mallikarjun and N. E. Hill, Trans. Faraday Soc., 61, (1965), p. 1389.

10. M. Davies, G. W. F. Pardoe, J. E. Chamberlain, and H. A. Gebbie, Trans. Faraday Soc., 64, (1968), p. 847.

11. A. L. McClellan, "Tables of Experimental Dipole Moments", W. H. Freeman and Company, San Francisco, Calif., U. S. A., (1963).

12. Y. Leroy, E. Constant, C. Abbar, and P. Desplanques, Adv. Mol. Relaxation Processes, 1, (1967), p. 273.

13. J. G. Powles, Trans. Faraday Soc., 44, (1948), p. 802.

14. N. E. Hill, W. E. Vaughan, A. H. Price, and M. Davies, "Dielectric Properties and Molecular Behaviour", Van Nostrand Reinhold Company Ltd., London, England, (1969).

15. N. E. Hill, Proc. Phys. Soc., 82, (1963), p. 723.

16. N. E. Hill, J. Phys., C4, (1971), p. 2322.

CHAPTER IV

Dielectric Studies in Polystyrene Matrices

INTRODUCTION

As has been outlined in Chapter I, several concepts have been suggested in the literature to explain the broad band absorptions observed in the far-infrared region. The consensus seems to be that the absorption processes involve some combination of rotational and translational motion of the molecules, a popular model being that the test molecule is trapped temporarily in a cage of short lifetime composed of neighbouring molecules. In this model the potential energy barriers to small-angle rotations may vary as the cage is distorted by collisions from other outside molecules.

Among other things, any attempt to understand the far-infrared broad band absorptions will necessitate an examination of the various experimental parameters which influence the observed spectra. In previous work by this author[1,2] it became clear that, in order for the typical broad band to be observed, the polar molecules must have some rotational freedom. It seemed worthwhile determining whether the broad band absorption was modified if molecular rotation of a rigid molecule was suppressed and the frequency of collisions reduced considerably. Moreover, the results would be interesting if a flexible molecule were examined under these same conditions where molecular rotation was restricted but where

substituent group rotation was still rapid. One technique which would reduce the rate of rotation of a molecule, or perhaps even suppress it, appeared to be to dissolve the molecule in a solid polymer matrix and to examine it at low temperatures. Even if molecular rotation were not totally eliminated, it would be considerably slowed. Further, the frequency of (polymer) solvent-solute molecular collisions would be drastically reduced from that of the liquid state. Thus, in all probability translational motion of the solute would be diminished considerably.

A study of the far-infrared absorption spectra of rigid and flexible polar molecules dissolved in a polymer matrix would necessitate first an investigation of the molecular and the substituent group rotational motions in such systems. A convenient technique for this work is to examine the dielectric absorptions of such systems at a variety of temperatures. Such a procedure provides information as to the nature of the species in motion, the rate of its relaxational motion (often rotations), and the energy barriers to such relaxations.

The energy barrier to rotation of an acetyl group substituent to an aromatic ring has received some attention: far-infrared study[3] of acetophenone in the gas phase gave a value of 13.0 kJ mol^{-1}; ab initio calculations[4] yielded 18.4 kJ mol^{-1}; Fong and Smyth studied

2-acetylnaphthalene and 4-acetyl-o-terphenyl[5], 4-phenylacetophenone, and 1,4-diacetylbenzene[6] in benzene solution and obtained values of 4.2 to 6.3 kJ mol^{-1} for the activation enthalpy barrier (ΔH_{E2} from Eyring rate theory) encountered by the acetyl group as it rotates; liquid phase N.M.R. studies[7] yielded an estimated free energy barrier to rotation of 26 kJ mol^{-1}. The energy barriers estimated by these several procedures differ considerably. Clearly, they merit further investigation.

An interesting approach seemed to be to examine acetophenone and related molecules dissolved in a solid matrix of polystyrene. Equation IV-1 has been derived from considerations of the effect of the medium on the relaxation behaviour of a dipolar molecule [8]:

$$\tau' = \frac{4\pi\eta a^3}{kT} \qquad \text{IV-1}$$

where τ' is the relaxation time of the molecule, η is the viscosity of the medium, a is the radius of the spherical molecule, k is the Boltzmann constant, and T is the absolute temperature (K).

While equation IV-1 is known to be inadequate, it is found experimentally that the molecular relaxation time is approximately proportional to the volume of the rotating species and to the viscosity of the medium. Now ordinary atactic polystyrene is an amorphous polymer with no rigidly-defined crystalline lattice structure. Dielectric measurements have indicated that dipolar molecules dissolved in a polystyrene matrix behave somewhat as if they were in a medium of very high viscosity.[9,10] The frequency at which the maximum value of dielectric loss factor is found is then considerably lower than that for the case of a liquid solution. Further, this effect of viscosity on relaxation time is expected to be more pronounced for molecular rotation, which involves the motion of a species of large volume, than for the rotation of smaller substituent groups within the molecule. Thus, studies of the dielectric absorptions of acetophenone and like molecules in a polystyrene matrix appeared to be more straightforward than similar studies in dilute liquid-phase solutions. In the latter type of work, relaxations of the molecules and of their substituent groups overlap, necessitating the use of a Budó analysis to find the relaxation times of the groups, which is now known to be unsatisfactory in a number of cases.[11] Since such measurements must be carried out at several temperatures to obtain the activation energy barrier to group relaxation, the errors in this parameter derived from liquid solution measurements may be very large.

EXPERIMENTAL RESULTS

Measurements of the real and imaginary parts of the complex dielectric permittivity $\varepsilon^* = \varepsilon' - i\varepsilon''$ have been made for dilute solutions of several acetophenone-type molecules in a polystyrene matrix over suitable ranges of temperatures and frequencies by means of the General Radio bridge and the Hewlett-Packard Q-meter, as outlined in Chapter II.

The dielectric loss factor of pure polystyrene, obtained through similar measurements, was subtracted from that observed for the matrix solutions to yield a "corrected" $\Delta\varepsilon'' = \varepsilon''$ (matrix) - ε'' (polystyrene). The polystyrene used, supplied by Monomer-Polymer Laboratories, had a nominal molecular weight $M_w = 230{,}000$. A sample of 50 g of this material placed in a vacuum oven at 475K for 18 hours lost 0.201 g, or about 0.4% by weight, suggesting that it contained very little volatile monomer.

For each measurement temperature, the data of dielectric loss factor as a function of frequency were subjected to analysis by the Fuoss-Kirkwood equation,[12] Eqn. IV-2, used by Davies.[9,10]

$$\cosh^{-1}\left[\frac{\Delta\varepsilon''_{max.}}{\Delta\varepsilon''}\right] = \beta \ln\left[\frac{f_{max.}}{f}\right] \qquad \text{(IV-2)}$$

This analysis was done by a computer program written in the APL language. By iteration the program finds that value of $\Delta\varepsilon''_{max.}$ which provides the best straight line fit to the plot of $\cosh^{-1}(\Delta\varepsilon''_{max.}/\Delta\varepsilon'')$ versus ln(f). The value of the distribution parameter, β, is obtained from the slope of this line, and the frequency of maximum dielectric loss, $f_{max.}$, from this slope and the intercept of the line on the $\cosh^{-1}$ axis. Sample graphs of $\Delta\varepsilon''$ versus log(f) for solutions of approximately 3% (wt.) acetophenone in polystyrene are shown in Figs. IV-1 and IV-2. The Fuoss-Kirkwood straight line plot for the data of Fig. IV-1 from measurements obtained by means of the General Radio bridge is shown in Fig. IV-3, and that for the data of Fig. IV-2 from Q-meter measurements is shown in Fig. IV-4.

Visual inspection of such graphs yields an estimate of $\pm$ 0.1 or less for the error in $\log(f_{max.})$. However, standard statistical techniques[13] provide another means of estimating errors in fitting a straight line to a set of graph points. To minimize the mean square deviation of N experimental points (x_i, y_i) from the best-fit line of the form $y = ax + b$, the slope and intercept of the calculated line are given by Eqns. IV-3 and IV-4.

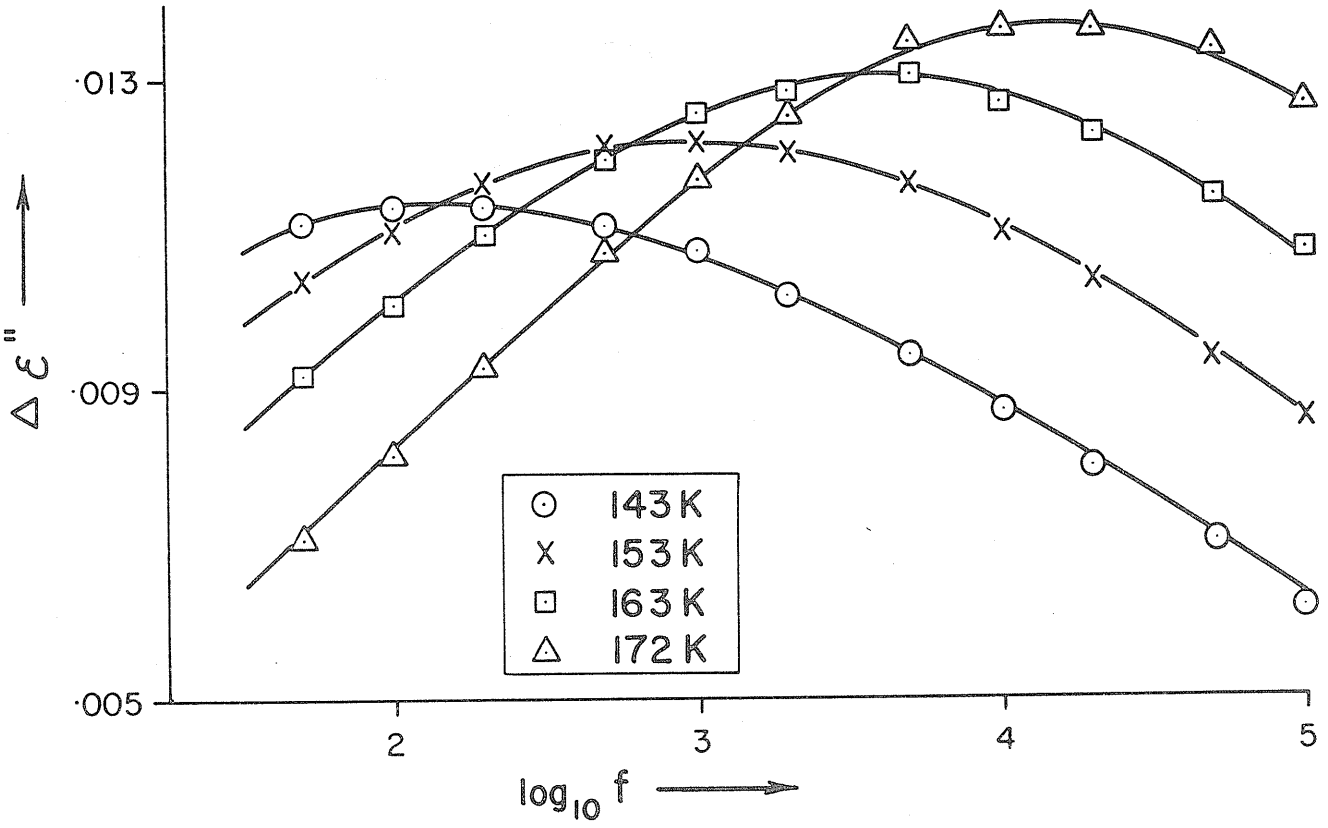

Figure IV-1: Dielectric loss factor $\Delta\varepsilon'' = \varepsilon''(\text{matrix}) - \varepsilon''(\text{polystyrene})$ vs. $\log_{10} f$ for 0.2649M acetophenone in a polystyrene matrix at temperatures as indicated (data from General Radio Bridge).

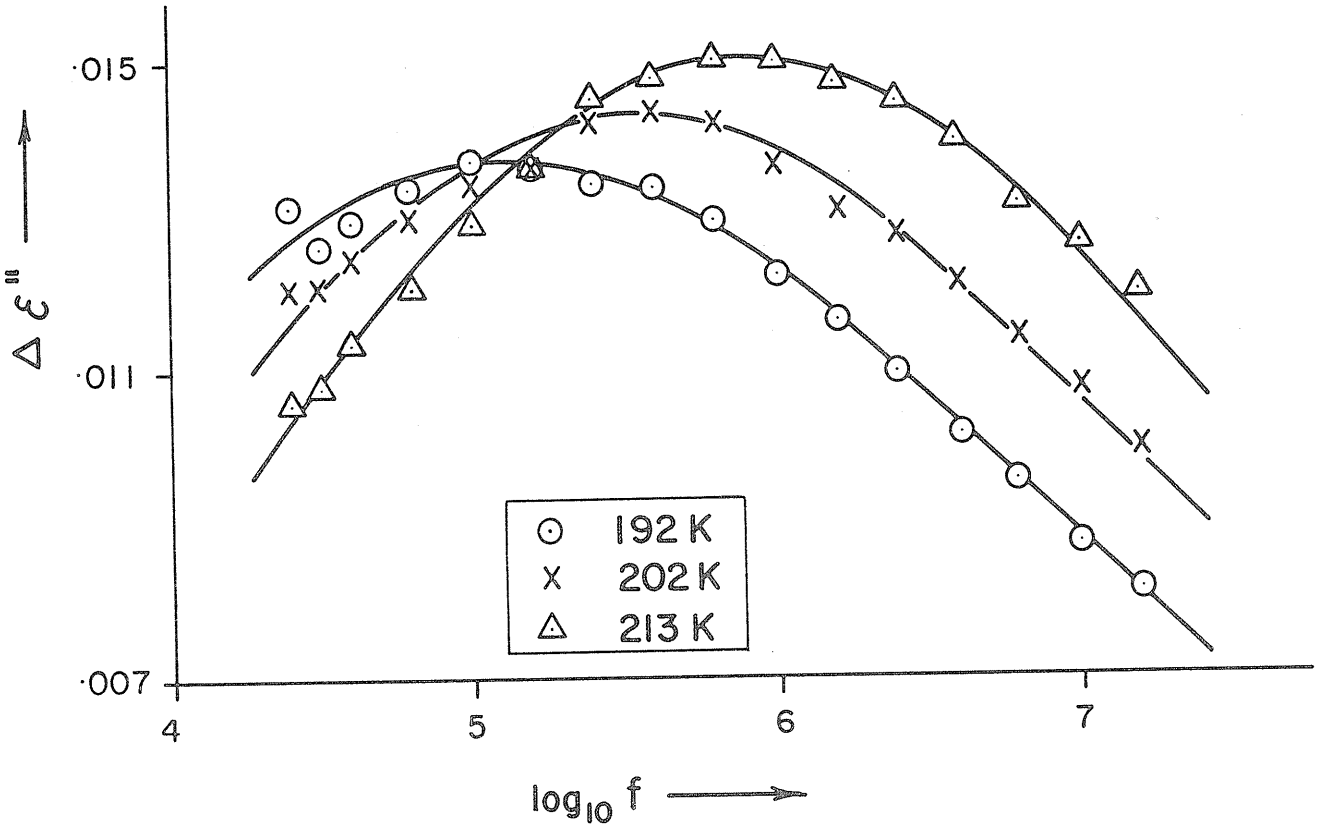

Figure IV-2 : Dielectric loss factor $\Delta\varepsilon'' = \varepsilon''(\text{matrix}) - \varepsilon''(\text{polystyrene})$ vs. $\log_{10} f$ for 0.2649M acetophenone in a polystyrene matrix at temperatures as indicated (data from Hewlett-Packard Q-meter).

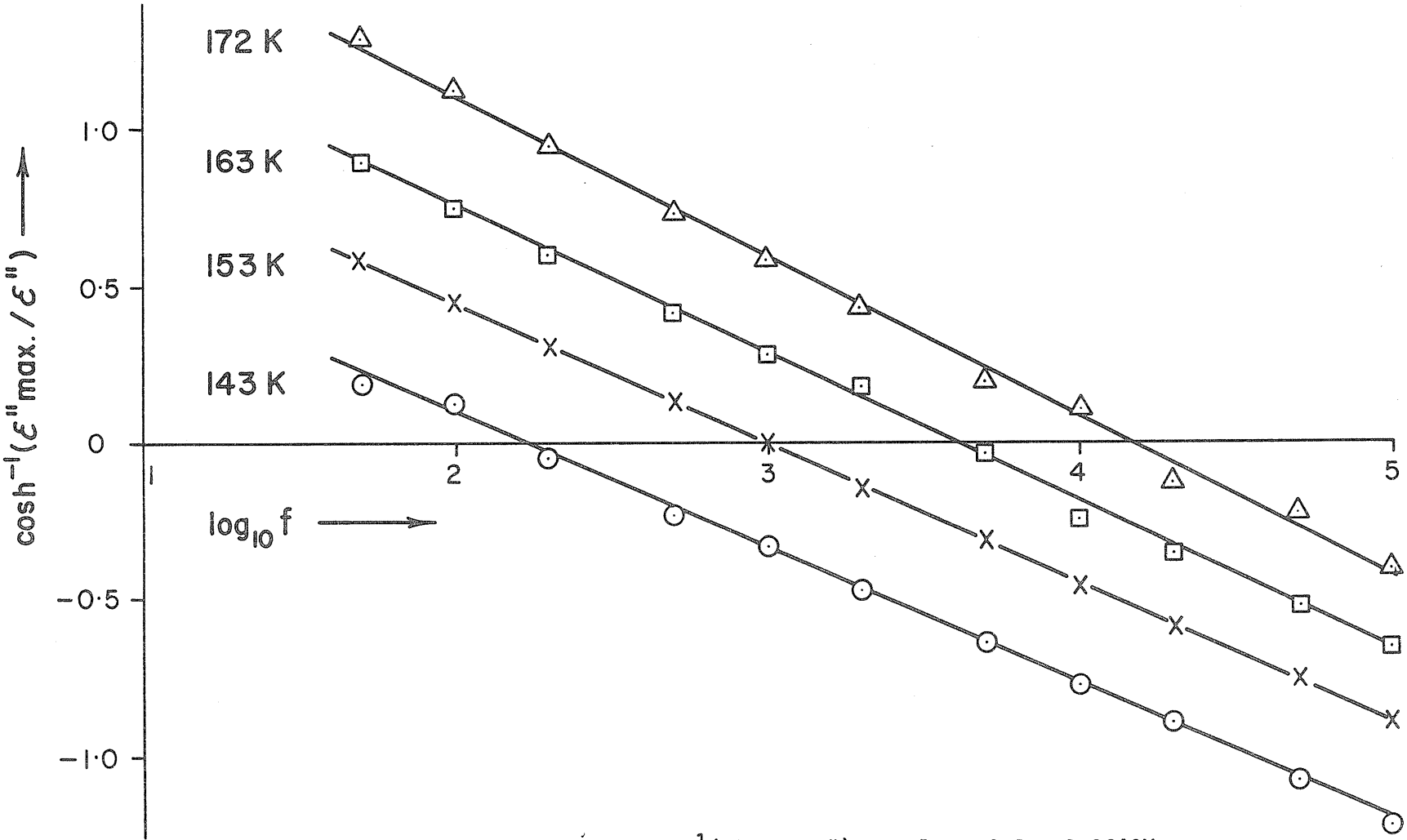

Figure IV-3: Fuoss-Kirkwood plot of $\cosh^{-1}(\varepsilon''_{max.}/\varepsilon'')$ vs. $\log_{10} f$ for 0.2649M acetophenone in a polystyrene matrix at temperatures as indicated (data from General Radio Bridge). Note that, for $f > f_{max.}$, the ordinate is $-\cosh^{-1}(\varepsilon''_{max.}/\varepsilon'')$.

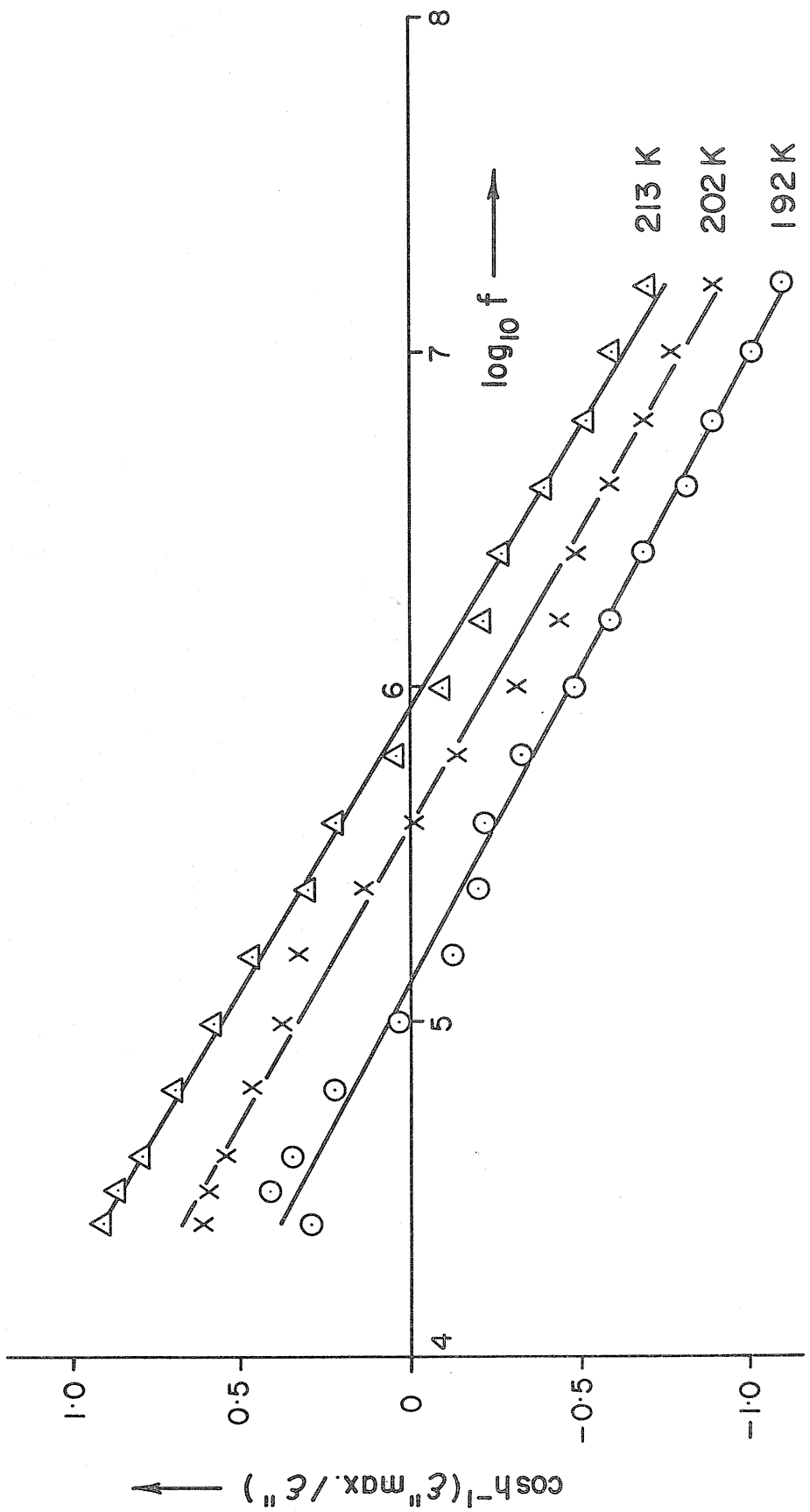

Figure IV-4: Fuoss-Kirkwood plot of $\cosh^{-1}(\varepsilon''_{max.}/\varepsilon'')$ vs. $\log_{10} f$ for 0.2649M acetophenone in a polystyrene matrix at temperatures as indicated (data from Hewlett-Packard Q-meter). Note that, for $f > f_{max.}$, the ordinate is $-\cosh^{-1}(\varepsilon''_{max.}/\varepsilon'')$.

$$a = \frac{\sum_{i=1}^{N} (x_i - \bar{x})\,(y_i - \bar{y})}{\sum_{i=1}^{N} (x_i - \bar{x})^2} \qquad \text{(IV-3)}$$

$$b = \bar{y} - a\bar{x} \qquad \text{(IV-4)}$$

where $\bar{x}$ and $\bar{y}$ are the mean values of x and y, respectively.

The statistical variances S_a^2 and S_b^2 of the slope and intercept, respectively, are given by Eqns. IV-5 and IV-6.

$$S_a^2 = \frac{S_E^2}{\sum_{i=1}^{N} (x_i - \bar{x})^2} \qquad \text{(IV-5)}$$

$$S_b^2 = S_E^2 \left[\frac{1}{N} + \frac{\bar{x}^2}{\sum_{i=1}^{N} (x_i - \bar{x})^2} \right] \qquad \text{(IV-6)}$$

where $S_E^2 = \dfrac{\sum_{i=1}^{N} (y_{i(obs)} - y_{i(calc)})^2}{N - 2}$

and $y_{i(calc)} = ax_i + b$

From these variances one may calculate confidence intervals for each of the slope and intercept as $\pm t\sqrt{S_a^2}$ and $\pm t\sqrt{S_b^2}$, respectively, where t is the value obtained from a student t-table for the desired level of confidence and (N-2) degrees of freedom. (Since two points define a straight line, there are (N-2) degrees of freedom in fitting a line to N experimental points.)

By these procedures the program FUOSSK calculated intervals of 90%, 95%, 98%, and 99% confidence for both the Fuoss-Kirkwood distribution parameter, β, and $\log(f_{max.})$. The 95% confidence interval was chosen as a good representation of experimental error. That is, there is a probability of 95% that the true value of a parameter is within this interval centred about the calculated value of the parameter and a 5% chance that the true value lies outside this range. The magnitudes of these confidence intervals were typically $\pm$ 0.05 to $\pm$ 0.10 for $\log(f_{max.})$.

The Fuoss-Kirkwood formulation, Eqn. IV-2, does not deal with the real part of the complex dielectric permittivity, nor with its limiting values at low and high frequencies, ε_o and ε_∞, respectively. However, the total dispersion for each dielectric absorption process is given by Eqn. IV-7:

$$\Delta\varepsilon' = \varepsilon_o - \varepsilon_\infty = \frac{2\varepsilon''_{max.}}{\beta} \qquad \text{(IV-7)}$$

Another equation commonly used to describe the frequency dependence of dielectric permittivity in a system involving a distribution of relaxation times is Eqn. IV-8 proposed by Cole and Cole.[14]

$$\varepsilon^* = \varepsilon' - i\varepsilon'' = \varepsilon_\infty + \frac{\varepsilon_0 - \varepsilon_\infty}{1 + (i\omega\tau_0)^{(1-\alpha)}} \qquad \text{(IV-8)}$$

In this equation, τ_0 is the mean relaxation time for the whole system, and the distribution parameter, α, may take values from zero to one. Separation into real and imaginary parts leads to Eqns. IV-9 and IV-10.

$$\frac{\varepsilon' - \varepsilon_\infty}{\varepsilon_0 - \varepsilon_\infty} = \frac{1 + (\omega\tau_0)^{(1-\alpha)} \sin(\alpha\pi/2)}{1 + 2(\omega\tau_0)^{(1-\alpha)} \sin(\alpha\pi/2) + (\omega\tau_0)^{2(1-\alpha)}} \qquad \text{(IV-9)}$$

$$\frac{\varepsilon''}{\varepsilon_0 - \varepsilon_\infty} = \frac{(\omega\tau_0)^{(1-\alpha)} \cos(\alpha\pi/2)}{1 + 2(\omega\tau_0)^{(1-\alpha)} \sin(\alpha\pi/2) + (\omega\tau_0)^{2(1-\alpha)}} \qquad \text{(IV-10)}$$

The Cole-Cole distribution parameter, α, may be obtained from the Fuoss-Kirkwood distribution parameter, β, by Eqn. IV-11 given by Hill et al.[12]

$$\beta = \frac{1 - \alpha}{\sqrt{2}\cos\left[\frac{\pi(1-\alpha)}{4}\right]} \qquad \text{(IV-11)}$$

Thus, in order to obtain ε_∞ we must supplement the Fuoss-Kirkwood analysis with the Cole-Cole equations. Eqns. IV-9 and IV-11 may be used in conjunction with experimental values of ε' as a function of frequency to obtain several estimates of ε_∞. A computer program performed this work and calculated the average of these estimates, along with a value for ε' at the frequency of maximum dielectric loss, $\omega_{max.} = 1/\tau_o = 2\pi f_{max.}$

The value of the effective dipole moment involved in the dielectric relaxation process may now be calculated from either the Debye[15] equation IV-12 or the Onsager[16] equation IV-13.

$$\mu^2 = \frac{27000\ kT\ (\varepsilon_o - \varepsilon_\infty)}{4\pi\ Nc\ (\varepsilon' + 2)^2} \qquad \text{(IV-12)}$$

$$\mu^2 = \frac{9000\ kT\ (2\varepsilon_o + \varepsilon_\infty)\ (\varepsilon_o - \varepsilon_\infty)}{4\pi\ Nc\ \varepsilon_o\ (\varepsilon_\infty + 2)^2} \qquad \text{(IV-13)}$$

where $(\varepsilon_o - \varepsilon_\infty) = 2\Delta\varepsilon''_{max.}/\beta$ (Fuoss-Kirkwood Eqn. IV-7),

ε' is the value of ε' at $\omega_{max.} = 1/\tau_o$,

ε_o is the static dielectric constant derived from

ε_∞ and Eqn. IV-7,

N is Avogadro's number, 6.02257×10^{23} molecules mol^{-1},(17)

c is the solute concentration in moles per litre,

k is the Boltzman constant, 1.38054×10^{-16} erg K^{-1},(17)

and T is the temperature in K.

These two equations yield μ in units of e.s.u. -cm. It is more common to express this parameter in Debye units where $1D = 1 \times 10^{-18}$ e.s.u. -cm.

The Fuoss-Kirkwood analysis and calculations of ε_∞ and μ were carried out at each temperature. (Values of ε' from Q-meter data were unreliable, so ε_∞ and μ could not be calculated here.) Further processing of the results of these analyses from the several temperatures employed for a particular sample was then carried out. To begin, attempts were made to estimate the values of dipole moment at temperatures above those of measurement. The simplest

technique is that employed by Davies and Swain[10] of assuming that the dipole moment is a linear function of temperature. This appeared to give reasonable results in their work although there is little theoretical basis for such a procedure. However, it is well established that in many cases the variation of ε_0 and ε_∞ with temperature may be described by an equation of the form $\log(\varepsilon) = aT + b$.[18] Extrapolated values of ε_0 and ε_∞ derived in this manner have been used in conjunction with Eqn. IV-12 to calculate dipole moments at warmer temperatures. The linear extrapolation technique of Davis and Swain outlined above was also used.

The energy barrier opposing the dielectric relaxation process was obtained by use of the Eyring rate equation IV-14, a procedure commonly adopted in dielectrics work:[9,10,19]

$$\tau = \frac{1}{\text{rate}} = \frac{h}{kT} \exp(\Delta G/RT) \qquad \text{(IV-14)}$$

$$\ln(T\tau) = \frac{\Delta H}{RT} - \left[\frac{\Delta S}{R} - \ln(h/k)\right]$$

Plots of $\log(T\tau)$ versus $(1/T)$ yielded good straight lines, and values of the enthalpy of activation, ΔH_E, and the entropy of activation, ΔS_E, were obtained from the slope and intercept, respectively of such graphs by a computer program based on Eqns. IV-3 and IV-4. The 95% confidence intervals calculated

for $\log(f_{max.})$ by the program FUOSSK were then compared to the differences between observed and calculated values of $\log(T\tau)$ from the EYRING program. Any experimental point which deviated from the calculated line by more than its allowed confidence interval was deleted from a repeat run of the EYRING program.

If the visual-inspection estimates of the error in $\log(f_{max.})$ were used (i.e., ±0.1), the error estimate for ΔH_E would be about ± 10%. This assumes the worst case of the maximum error in the two most widely separated points on the Eyring linear graph. However, it then becomes very difficult to estimate the error in the intercept and hence of ΔS_E. The technique adopted instead was to calculate the 95% confidence intervals for both ΔH_E and ΔS_E by means of Eqns. IV-5 and IV-6. It is to be noted that, since N appears in the denominator of both of these equations, a smaller error is to be expected from the use of a larger number of points on the Eyring plot. In addition, the square of the mean value of the x variable (in this case, 1/T) appears in the numerator of the second term of Eqn. IV-6 to give the variance on the intercept. Thus, smaller confidence intervals on ΔS_E are obtained if (1/T) can be brought closer to zero. The combined effect of these two considerations was illustrated clearly in repeat measurements on solutions of approximately 3% (wt.) solutions of acetophenone in polystyrene. An early result based on measurements with the General Radio bridge for seven temperatures in the range 141K to 168K yielded

ΔH_E = 28.9 ± 2.3 kJ mol^{-1} and ΔS_E = 27.5 ± 15.0 J K^{-1} mol^{-1}. Later measurements on a new sample containing the same concentration of solute obtained by both the General Radio bridge and the Q-meter at twelve temperatures over the wider range of 143K to 213K yielded ΔH_E = 29.6 ± 0.6 kJ mol^{-1} and ΔS_E = 26.3 ± 3.3 J K^{-1} mol^{-1}. The reduction in confidence interval magnitudes is striking, particularly in the case of ΔS_E. The linear Eyring graph for these later data is shown in Fig. IV-5. It is noteworthy that separate determinations on different samples prepared and analysed in the same manner have yielded values in excellent agreement, well within the 95% confidence intervals chosen. The net result of these considerations of errors has led to the conclusion that the error in ΔH_E is at worst ± 10%, while that of ΔS_E may be as high as ± 50% in cases where fewer than six temperatures were employed for the acquisition of dielectric data. The results of Eyring analyses have been quoted in this work to two digits for comparative purposes only. It should not be inferred that the errors in the values are limited to ± 1 in the second digit.

Meakins[20] has employed Eqn. IV-15 to obtain the energy difference, V, between the two sides of the activation energy barrier from plots of $\ln(\varepsilon''_{max.} T)$ versus (1/T).

$$\varepsilon''_{max.} = \frac{B}{kT} \exp(-V/RT) \qquad \text{(IV-15)}$$

where B is a simple proportionality constant.

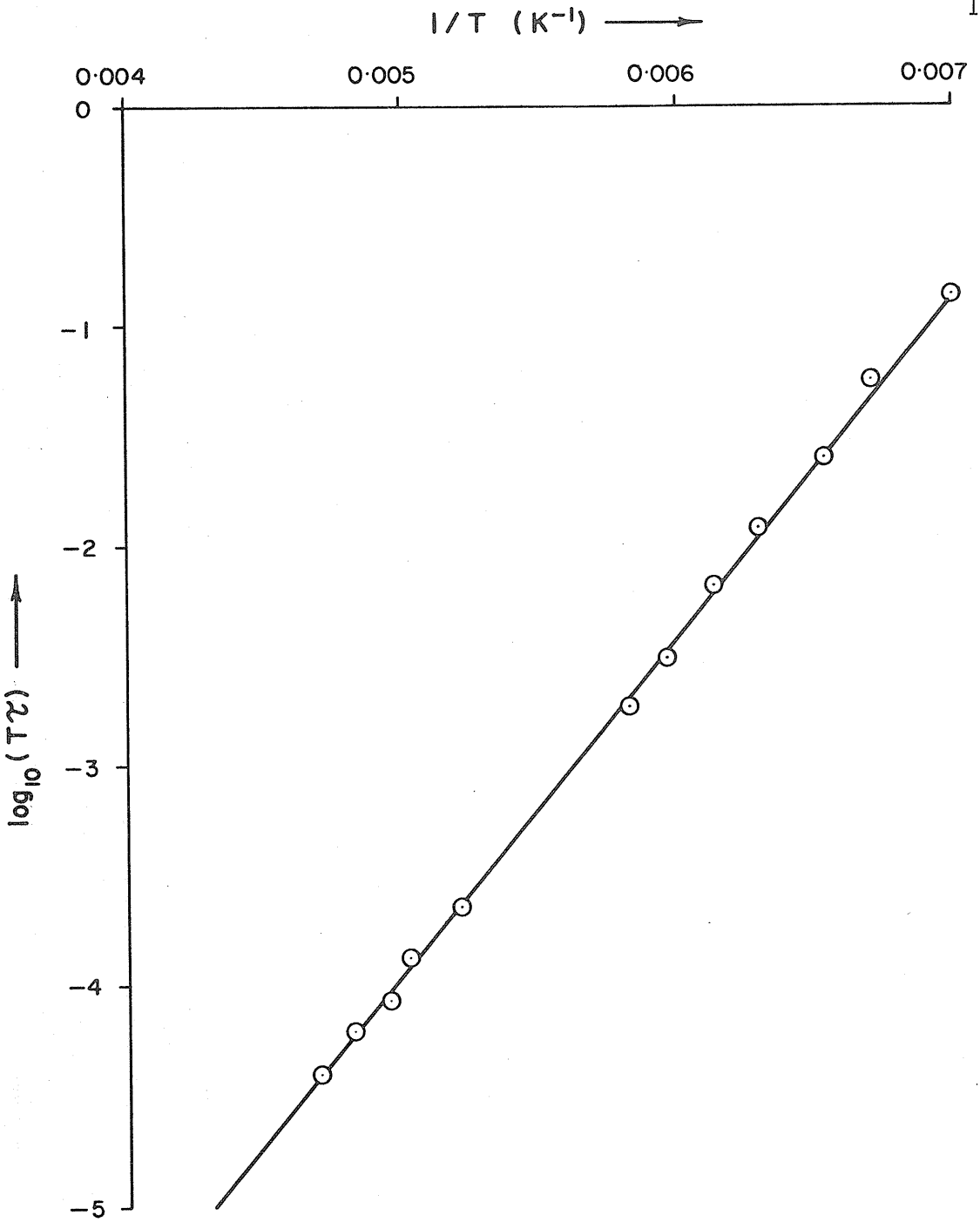

Figure IV-5: Eyring plot of $\log_{10}(T\tau)$ vs. 1/T for 0.2649M acetophenone in a polystyrene matrix.

These analyses of the present data have been performed by a computer program and in all cases the values were less than the mean thermal energy and therefore, according to Meakins, should not be considered to be different from zero.

The results of the analyses of dielectric data to obtain the Fuoss-Kirkwood parameters $\log(f_{max.})$, $\Delta\varepsilon''_{max.}$, and β, the limiting high-frequency dielectric constants, ε_∞, and the effective dipole moments, μ, are given in Table III of Appendix I for several molecules related to acetophenone and for several rigid molecules of similar sizes and shapes. The results of the Eyring analyses of these data are given in Table IV of that appendix.

The last three entries in Table IV give the results from analyses of the data from polystyrene matrices containing solutes for which the activation parameters for rotation of a substituent group have been reported in the literature. For 2-furanaldehyde, the present work yielded ΔH_E = 38.0 ±1.9 kJ mol^{-1} and ΔS_E = -17 ±7 JK^{-1} mol^{-1} (95% confidence intervals). Pethrick and Wyn-Jones[21] have combined their ultrasonic measurements with literature values from n.m.r. experiments to yield ΔH_E = 39.7 ±0.3 kJ mol^{-1}. (Their error estimation procedure was not specified. However, the error of ±0.3 kJ mol^{-1} may

be a misprint, as the data from which this value was derived indicated that the correct error estimate is ±2.5 kJ mol^{-1}.)

The present result for the energy barrier to ring inversion in bromocyclohexane was ΔH_E = 47.3 ±2.2 kJ mol^{-1} and ΔS_E = 13±8 JK^{-1} mol^{-1}. This may be compared to an n.m.r. result of ΔG = 45 kJ mol^{-1} at 218K, for which the authors suspected a rather large error estimate.[22] At 218K, the present work yields ΔG = 44.5 kJ mol^{-1}. Heijboer[23] found the activation energy for bromocyclohexane ring inversion to be 48 kJ mol^{-1} by mechanical relaxation measurements in polymeric systems.

Formyl group rotation in 4-methoxybenzaldehyde has been studied by Klinck and Stothers[24] who used an n.m.r. method. They obtained ΔH_E = 38.1 ±0.8 kJ mol^{-1} and ΔS_E = 5 ±4 JK^{-1} mol^{-1} with ΔG = 36.8 ±1.7 kJ mol^{-1} at 298K (error estimates here are standard deviation values). This work obtained ΔH_E = 37.6 ±1.9 kJ mol^{-1} and ΔS_E = 15 ±9 JK^{-1} mol^{-1} with ΔG_{298} = 33.1 ±4.6 kJ mol^{-1}, where the error estimates are 95% confidence intervals which are approximately 2.4 times the standard deviation values.

From this information it would appear that the present technique of investigating the dielectric absorptions of solutes in

a polystyrene matrix agrees quite well with studies in the liquid phase by n.m.r. and ultrasonic relaxation techniques and with mechanical relaxation work in polymeric media.

For convenience, structural diagrams of the molecules investigated are given in Appendix II located at the end of this thesis.

DISCUSSION

The enthalpies of activation, ΔH_E, obtained by this work for four aromatic molecules containing the acetyl substituent group and dissolved in a polystyrene matrix were: acetophenone, 30 kJ mol^{-1} 1,4-diacetylbenzene, 29 kJ mol^{-1}, 4-acetylbiphenyl, 30 kJ mol^{-1}, and 2-acetylfluorene, 32 kJ mol^{-1}. Thus, all four of these exhibited dielectric absorptions in similar ranges of temperature and frequency, yielding ΔH_E values in very good agreement, well within the estimated experimental error.

According to the work of Davies *et al.*,[9,10] the two possible sources of these dielectric absorptions are molecular or group relaxation. For several flexible molecules examined by those authors, only intramolecular relaxation was observed; indeed, they felt that "molecular relaxation is at such low frequency that it does not appear at all." It is to be noted that the four aromatic molecules above differ appreciably in size, whereas one expects the enthalpy of activation for molecular relaxation to tend to increase with size. Certainly Debye's Eqn. IV-1 suggests that the relaxation times of molecular rotations should increase with size, although the relaxation times calculated from the Eyring analyses may be seen in Table IV of Appendix I to be to be 980, 200, 400, and 2300 picoseconds, respectively, for these four molecules at T=300K. These relaxation times are not consistent

with the assignment of their sources to molecular rotation.

In order to show that the relationship between molecular size and activation enthalpy does follow expectations, several rigid molecules, the sizes and shapes of which are similar to those of the four ketones, have been investigated by the author and by several co-workers (see footnote to Table IV in Appendix I). Their activation enthalpies, in units of kJ mol^{-1}, were: iodobenzene, 16; 4-bromotoluene, 30; 4-bromobiphenyl, 60; and 4-nitrobiphenyl, 86. Since these rigid molecules are all at least as large as the corresponding ketones, the values of the rigid molecules may be regarded as lower limits for the values expected if the motions of the ketones were molecular relaxation. Particularly in the cases of the 4-substituted biphenyls and of 2-acetylfluorene the activation enthalpy of the ketone is much too small to be due to molecular motion. In addition the relaxation times calculated at 300K for the 4-bromo- and 4-nitrobiphenyls are greater than those of 4-acetylbiphenyl by a factor of about 10^6. Further, it may be noted in Table IV that a second region of dielectric absorption above room temperature was found for 4-acetylbiphenyl and for 2-acetyl-fluorene in polystyrene. The Eyring activation parameters and dielectric relaxation times for this process correspond well to those derived from molecular relaxation of the two rigid biphenyls.

In a pure crystalline solid sample one may expect that

the lattice structure would preclude rotation of a molecule, although rotation of a substituent group within the molecule might occur without disturbing the lattice greatly. Measurements on pure crystalline 1,4-diacetylbenzene, 4-acetylbiphenyl and 2-acetylfluorene have yielded values of ΔH_E (kJ mol^{-1}) of 27, 33 and 32, respectively, in good agreement with those obtained in dilute polystyrene matrix solutions near 150K.

In the case of 1,4-diacetylbenzene the components of the dipole moments of the two substituent groups along the long axis of the molecule cancel each other, resulting in a net expected permanent molecular dipole of zero along that axis. Another way for this molecule to have a non-zero permanent molecular dipole moment capable of responding to the applied electric field would be for something like a rigid cis arrangement of the two acetyl substituents. This would imply a very high energy barrier to group rotation, much higher than that obtained by any of the methods to which reference has been made in the introduction to this chapter. That being the case, it appears that by far the most likely source of the observed dielectric relaxation in 1,4-diacetylbenzene is relaxation of the acetyl substituent groups.

Thus, consideration of the enthalpies of activation and relaxation times of these four ketones,

of the corresponding values for similarly-sized rigid molecules, of the information obtained from measurements of the pure crystalline solid forms of three of these ketones, and of possible sources of the dielectric absorption observed for 1,4-diacetylbenzene all lead to the conclusion that the process which occurs must be relaxation of the acetyl substituent groups in the respective molecules at temperatures near 150K.

The possibility must be considered that the present matrix values do not correspond to those of a molecule isolated from others of its own type. Borisova and Chirkov[25] found that the energy barrier for molecular relaxation of small molecules in a polystyrene matrix increased with concentrations of solute above about 5 to 7 mole percent. Hains and Williams[26] have reported a similar result, concluding that this effect is linked to the fact that, as solute concentration is increased, the surroundings of a given solute molecule are altered from simple polymer segments to some mixture of polymer segments and other solute molecules. However, the present results for all the ketones were obtained from samples with concentrations much lower than this. Further, one might expect that group relaxation would be less sensitive to environment than molecular relaxation.

The possibility of steric hindrance to rotation of the acetyl group by two methyl groups in ortho positions make 2,4,6-trimethylace-

tophenone an interesting case. To ensure precise results, the polystyrene matrix containing this solute was examined over a very wide temperature range by means of both the General Radio Bridge and the Q-meter. This yielded ΔH_E = 23.3 ±0.5 kJ mol^{-1} and ΔS_E = -12 ±3 JK^{-1} mol^{-1} (95% confidence intervals). The enthalpy of activation is markedly lower than those for the four unhindered ketones and is also considerably lower than that for the slightly smaller rigid molecule, 4-bromotoluene. Further, the relaxation times for 2,4,6-trimethylacetophenone are shorter than those for 4-bromotoluene. Thus, it would appear that the process in 2,4,6-trimethylacetophenone is not molecular relaxation but is relaxation of the acetyl substituent group through less than a 180° angle. That is, the acetyl group moves between two limiting positions on either side of a plane perpendicular to the aromatic ring but rarely if ever becomes coplanar with the ring because of the presence of methyl groups at the 2 and 6 positions.

4-methyl- and 4-nitroacetophenone yielded values for ΔH_E of 37 and 39 kJ mol^{-1} respectively, both larger than values for the first three ketones. Whether the relaxation processes in these molecules is group or molecular is not clear from these data alone. However, if one examines the values of the activation entropies for the first four ketones, they all fall in the range 31 ±5 JK^{-1} mol^{-1}. Values of ΔS_E for 4-methyl- and 4-nitroacetophenone were 32 and 0.9 JK^{-1} mol^{-1} respectively, indicating that the former is in agreement with the

earlier ketones while the latter is not in agreement for this parameter. In addition, the relaxation time of 4-methylacetophenone at 300K is larger than those of the other ketones by a factor of 10 whereas the relaxation time for 4-nitroacetophenone is larger than these by a factor of 1000. It is interesting to note that a recent measurement by a co-worker [27] on the similarly-sized molecule 4-iodotoluene yielded ΔH_E = 33 kJ mol^{-1}, the relaxation times being 165 μs at 200K and 0.14 μs at 300K. The entropy value of -3 JK^{-1} mol^{-1} for this molecule is in much better agreement with that of the 4-nitroacetophenone than with that of 4-methylacetophenone. Likewise, the relaxation times agree well with those of the slightly larger 4-nitroacetophenone whereas they exceed those of 4-methylacetophenone considerably. In making relaxation time comparisons between 4-iodotoluene and 4-methylacetophenone one should bear in mind that the latter is expected to have the larger relaxation time. For example, Buckley and Maryott[28] have quoted relaxation times measured in pure liquid phase at 293K of 27 picoseconds for iodobenzene and 39 picoseconds for acetophenone. Another point is that pure solid 4-nitroacetophenone exhibited no dielectric relaxation process, unlike solid 1,4-diacetylbenzene and 4-acetylbiphenyl. These considerations suggest that group relaxation was responsible for the dielectric absorptions observed in 4-methylacetophenone, but that molecular relaxation was responsible in the case of 4-nitroacetophenone. However, the evidence cannot by any means be considered conclusive at this point.

The next molecule for which data are given in Tables III and IV of Appendix I is 1-acetylcyclohexene which is not aromatic but does have the possibility of conjugation of π electrons between the carbonyl group of the acetyl substituent and the C $=$ C bond of the ring. For this molecule, ΔH_E = 25 kJ mol^{-1} which is about 15% less than the value obtained for acetophenone. Again, the possible sources of this dielectric absorption are relaxation of the acetyl group about the C_{acetyl}—C_{ring} bond and relaxation of the entire molecule. If the source is group relaxation, the lower value of the activation enthalpy could be due to lower π electron density along the group-ring bond linked to the loss of aromaticity in the ring on passing from acetophenone to 1-acetylcyclohexene. It is also possible that the relaxation is that of the whole molecule, although the relaxation time of this molecule of 880 picoseconds at T=300K is in very good agreement with those of the first four ketones in which the absorptions have already been assigned to relaxation of the acetyl group. Thus, the relaxation observed in 1-acetylcyclohexene appears to be group motion, but the evidence here is inconclusive.

The results for N-acetylindole were ΔH_E=48kJ mol^{-1} and ΔS_E=70JK^{-1} $mol.^{-1}$. The size of this molecule is similar to that of 1-halonaphthalenes. For these latter rigid molecules, Tay and Walker (29) have reported enthalpies of activation around 20 kJ mol^{-1} and entropies of activation close to zero. From this it would appear unlikely that the dielectric absorption observed in N-acetylindole was due to molecular relaxation. For relaxation of the acetyl group one must consider the effect of the lone pair of electrons

on the nitrogen atom. It is probable that this factor would increase the barrier to group rotation. Indeed the present experimental results suggest that this has been observed. Dahlqvist and Forsén [30] obtained $\Delta H = 50 \pm 2$ kJ mol^{-1} for acetyl group rotation in N-acetylpyrrole by n.m.r., in good agreement with the present result for N-acetylindole. They commented that this value was markedly larger than those found for non-aromatic amides and that "the interaction between the lone pair on the nitrogen and the carbonyl group is believed to be the main contributor to restricted > N - C ≤ rotation in amides."

CONCLUSIONS

Altogether, the experimental data favour the assignment of the observed dielectric absorptions to acetyl group relaxation in the four ketones acetophenone, 1,4-diacetylbenzene, 4-acetylbiphenyl, and 2-acetylfluorene. The present value of ΔH_E = 30 kJ mol^{-1} agrees well with the n.m.r. value[7] of 26 kJ mol^{-1} for the free energy barrier to group rotation in acetophenone. In fact, this estimate made by Grindley *et al.*[7] was based on data reported by Klinck, Marr, and Stothers[31] for two para-substituted acetophenones. These latter workers were unable to measure the temperature dependence of the free energy barrier to group rotation. Thus they could deduce only approximate values at the coalescence temperatures of the n.m.r. peaks for the two ring protons ortho to the acetyl group. These values then provide only an approximate estimate for the value to be found in acetophenone, and therefore it is conceivable that the small discrepancy between the N.M.R. value and that of the present work should not be considered significant. The agreement with the ab initio calculations[4] is perhaps all that can be expected when the differences in phase and the complexity of such calculations are borne in mind.

There is serious disagreement between the present results and those obtained from (a) far-infrared data in the gas phase, and

(b) the dielectric absorption of aromatic ketones in dilute benzene solutions. In the latter case the enthalpy of activation for acetyl group relaxation was about a factor of five less than the present work. It was pointed out earlier that recent work suggests that the analysis techniques used for dielectric measurements on dilute liquid solutions may be subject to error. With regard to the results from far-infrared data, Grindley, Katritzky and Topsom [32] have pointed out that this indirect method involves certain assumptions concerning the shape of the potential function giving rise to the energy barrier and have stated "the assumptions commonly made are reasonable when applied to the gas phase but probably less so in the case of the liquid phase." They concluded that "the results of the direct and indirect techniques cannot be compared directly." Certainly such comments regarding comparisons of results from far-infrared gas phase studies with those from n.m.r. studies in pure liquids are equally valid for comparisons of the former techniques with the present work performed on dilute solutions in polystyrene matrices.

It appears that further work is necessary to compare the energy barriers to group rotation estimated by different techniques applied to different phases. In particular, it would be interesting to compare results from the direct techniques of dielectric absorption, ultrasonics, and n.m.r., and to examine further whether energy barriers

estimated from dielectric absorption measurements employing the polymer matrix technique correspond to those from n.m.r. data in the liquid phase. If accurate values of these barriers can be established, then these ought to be of considerable interest in relating their magnitudes to conjugative, inductive, and steric effects in small aromatic molecules. Such effects were indicated in 2,4,6-trimethylacetophenone and in N-acetylindole in the present study.

The work reported in this chapter has shown that the relaxation time of an acetyl group substituent to a small aromatic molecule dissolved in a polystyrene matrix is longer than that expected in dilute liquid solution. It may be recalled that in Chapter III the relaxation time at 303K for the rigid molecule chlorobenzene in the pure liquid state was approximately ten picoseconds. The polystyrene matrix technique, on the other hand, has given acetyl group relaxation times of about 800 picoseconds at 300K. However, the effect of the polystyrene matrix is much greater on the relaxation times of molecular motion, as is evident from the fact that 4-bromo- and 4-nitrobiphenyl yielded relaxation times at 300K longer than that of the acetyl group by a factor of 10^6 which factor far exceeds the differences in sizes.

Some patterns in the relaxational behaviour of several molecules and of the acetyl substituent group having been established, it is now possible to return to consideration of the effects of some experimental parameters on absorptions in the far-infrared frequency region. In particular, it would appear worthwhile to examine the effects on such

spectra produced by a considerable reduction in the rate of re-orientation of molecules and of flexible substituent groups within these molecules.

REFERENCES

1. C. K. McLellan, M. Sc. Thesis, Lakehead University, Thunder Bay, "P", Ontario, Canada, P7B 5E1, (1971).

2. C. K. McLellan and S. Walker, J. Chem. Phys. 61, (1974), p. 2412.

3. F. A. Miller, W. G. Fateley, and R. E. Witkowski, Spectrochimica Acta, 23A, (1967), p. 891.

4. W. J. Hehre, L. Radom, and J. A. Pople, J. Am. Chem. Soc., 94, (1972), p. 1496.

5. F. K. Fong and C. P. Smyth, J. Am. Chem. Soc., 85, (1963), p. 548.

6. F. K. Fong and C. P. Smyth, J. Am. Chem. Soc., 85, (1963), p. 1565.

7. T. P. Grindley, A. R. Katritzky, and R. D. Topsom, Tetrahedron Letters, No. 26, (1972), p. 2643.

8. N. E. Hill, W. E. Vaughan, A. H. Price, and M. Davies, "Dielectric Properties and Molecular Structure", Van Nostrand Reinhold Co., London, England (1969), p. 90.

9. M. Davies and A. Edwards, Trans. Faraday Soc., 63, (1967), p. 3163.

10. M. Davies and J. Swain, Trans. Faraday Soc., 67, (1971), p. 1637.

11. J. Crossley, S. P. Tay, and S. Walker, Adv. in Molecular Relax. Processes, 6, (1974), p. 79.

12. See p. 292 of reference 8.

13. B. Ostle, "Statistics in Research", (2nd ed.), Iowa State University Press, Ames, Iowa, U. S. A., (1963).

14. C. P. Smyth, "Dielectric Behaviour and Structure", McGraw-Hill Book Co., Inc., New York, New York, U. S. A., (1955), p. 68.

15. See p. 235 of reference 8.

16. C. J. F. Bottcher, "Theory of Electric Polarisation", Elsevier Publishing Co., Amsterdam, the Netherlands, (1952), p. 323.

17. R. C. Weast (ed.), "Handbook of Chemistry and Physics", (49th ed.), The Chemical Rubber Co., Cleveland, Ohio, U. S. A., (1968).

18. A. A. Maryott and E. R. Smith, "Table of Dielectric Constants of Pure Liquids", National Bureau of Standards Circular No. 514, U. S. Government Printing Office, Washington 25, D. C., U. S. A., (1951).

19. See p. 69-71 of reference 8.

20. R. J. Meakins, Trans. Faraday Soc., 51, (1955), p. 371.

21. R. A. Pethrick and E. Wyn-Jones, J. Chem. Soc., A (1969), p. 713.

22. L. W. Reeves and K. O. Strømme, Can. J. Chem., 38, (1960), p. 1241.

23. I. J. Heijboer, Koll. Z., 171, (1960), p. 7.

24. R. E. Klinck and J. B. Stothers, Can. J. Chem., 54, (1976), p. 3267.

25. T. I. Borisova and V. N. Chirkov, Russian J. Phys. Chem., 47, (1973), p. 949.

26. P. J. Hains and G. Williams, Polymer, 16, (1975), p. 725.

27. A. Lakshmi, unpublished data.

28. F. Buckley and A. A. Maryott, "Tables of Dielectric Dispersion Data for Pure Liquids and Dilute Solutions", National Bureau of Standards Circular No. 589, U. S. Government Printing Office, Washington 25, D. C., U. S. A., (1958).

29. S. P. Tay and S. Walker, J. Chem. Phys. 63, (1975), p. 1634.

30. K. I. Dahlqvist and S. Forsén, J. Phys. Chem. 73, (1969), p. 4124.

31. R. E. Klinck, D. H. Marr, and J. B. Stothers, Chem. Comm., (1967), p. 409.

32. T. B. Grindley, A. R. Katritzky, and R. D. Topsom, J. Chem. Soc. Perkin Trans. II, (1974), p. 289.

CHAPTER V

Far-Infrared Studies

INTRODUCTION

Work aimed at measuring the high-frequency limiting value of the dielectric constant, ε_∞, in order to determine the magnitude of the "residual dispersion" associated with absorptions observed in the far-infrared region was reported in Chapter III of this thesis. It appeared that such efforts based on dielectric measurements in the microwave frequency range cannot be expected to yield reliable results. Consideration of a second approach involving subtraction of a predicted contribution due to dielectric absorption from the total absorption led similarly to the conclusion that this technique also could not be relied upon. It was suggested that attempts to measure the far-infrared dispersion were not appropriate to investigations aimed at understanding the fundamental processes which produce these dispersions and the associated absorptions.

The basic questions pertaining to the broad band absorptions found in the far-infrared region are: what process(es) are responsible for their existence; and how may such a process or processes best

be described in a mathematical model so that precise predictions may be made and tested against observations?

The first thing to be considered in far-infrared spectra is the problem of whether or not the absorptions are due to some type of molecular motion different from what is already reasonably well understood for the lower-frequency dielectric absorptions. There has been some debate on this point.[1] For example, Zwanzig[2] has suggested that, by extending his theoretical approach to the inclusion of several more terms than he originally employed, one should obtain contributions to the total observed absorption from bands located at successively higher frequencies. More often, however, some model akin to that of Hill[3] is considered. In these models a central test molecule is temporarily trapped in a cage composed of its neighbours. The cage provides potential energy wells within which the test molecule may execute a limited rotation at a frequency determined by the cage size with the possibility that the oscillations may be damped by the non-rigidity of the cage boundaries. Rotational movement from one potential energy well to another within the cage, possibly over several intervening wells, is the process associated with what is commonly called dielectric relaxation. The dimensions of the cage, and therefore the depth and shape of the potential energy wells, are altered by distortions of the cage either through collisions from external

molecules or through inelastic collisions of the test molecule with the walls of its well. Thus, one expects in this model that the absorptions will be affected by both small- and large-angle molecular rotations and by molecular translational motions .

In this author's earlier work on the far-infrared absorption spectra of various liquid and solid phases[4,5] it became clear that molecular rotational freedom was a necessary prerequisite to the observation of broad absorption bands in the far-infrared region. Further, the absorptions in solid samples which allow molecular rotation were similar to those of the liquid phase. This suggested that molecular translational motions were less important than rotations. Similar results have been reported by Haffmans and Larkin[6]. Therefore, it appeared interesting to examine the far-infrared absorption spectra of polar solute molecules in a polystyrene matrix solution in which both translational and large-angle rotational motions of the polar solute molecules are expected to be much slower than in liquid phase. The fact that the large-angle molecular rotations were very much slower would mean that the dielectric absorptions associated with such motions would be at a very much lower frequency than the far-infrared absorption

bands. Hence the information gained could shed some light on the question of whether or not the far-infrared absorptions are merely an extension of dielectric absorption. The studies reported in Chapter IV of this thesis have provided sufficient background information to make an investigation of this type in the far-infrared region feasible.

EXPERIMENTAL

Two far-infrared interferometers were used in this study. The frequency region from 8 to 70 cm^{-1} was covered by a Lamellar Grating type interferometer, the Beckman/RIIC model LR-100 with FS-200/7 electronics module, manufactured by Research and Industrial Instruments Company. The sample cell was the RIIC FH-01 mounted in the VLT-2 holder to allow temperature control via an RIIC model TEM-1 indicating proportional controller. The frequency range from 20 to 200 cm^{-1} was covered by a Michelson interferometer manufactured by Sir Howard Grubb Parsons and Company Limited. The cell was the Grubb Parsons model G.L.C. 01 which allows measurements at ambient temperature only.* This

*Late in the experimental program a low-temperature cell was developed. It is described briefly in the "RESULTS" section of this chapter.

temperature was 302 ± 2 K when the cell was in the radiation beam under vacuum conditions. Unfortunately a malfunction of the Lamellar Grating interferometer prevented an investigation of the effects of decreased temperature on spectra observed with this instrument.

Measurements on liquid solutions were accomplished by assembling the cell with two windows of high density polyethylene, one on each side of a teflon spacer. Three different spacer thicknesses were used for each solution, the thicknesses being measured soon after recordings on an interferogram had been completed. This allowed three separate calculations of the absorption spectrum. (The details of this calculation procedure were outlined in Chapter II.)

For measurements on polystyrene matrix solutions it was not necessary to use the polyethylene windows. The solid sheet of matrix material cut from a disk prepared exactly as for earlier dielectric studies was simply clamped between the end plates of the cell assembly. Since failure to use a sample to record the background spectra might have given rise to spurious results from uncompensated surface reflections in the sample spectrum, spectra were recorded for two different thicknesses of matrix material from the same single batch of solute/polystyrene solution.

The solvent chosen for liquid solution studies was dried spectroscopic grade benzene. The absorption spectra of benzene and polystyrene were recorded and are shown in Figs. V -1 and V -2, respectively. To obtain the absorption spectrum of a solute, the spectrum of the solution was plotted and then the spectrum of the solvent (corrected for its concentration in the solution) was plotted on the same graph. Thereafter, a point-by-point subtraction of solvent from solution absorption yielded the portion of the total absorption due to the solute molecules alone.

The optical absorption coefficient, α, in units of cm^{-1}, is defined by equation V -1:

$$\alpha = \frac{1}{d} \times \ln (I_o/I) \qquad \text{V -1}$$

where d = sample path length difference in cm,

I_o = transmitted intensity for background measurement,

and I = transmitted intensity for sample measurement.

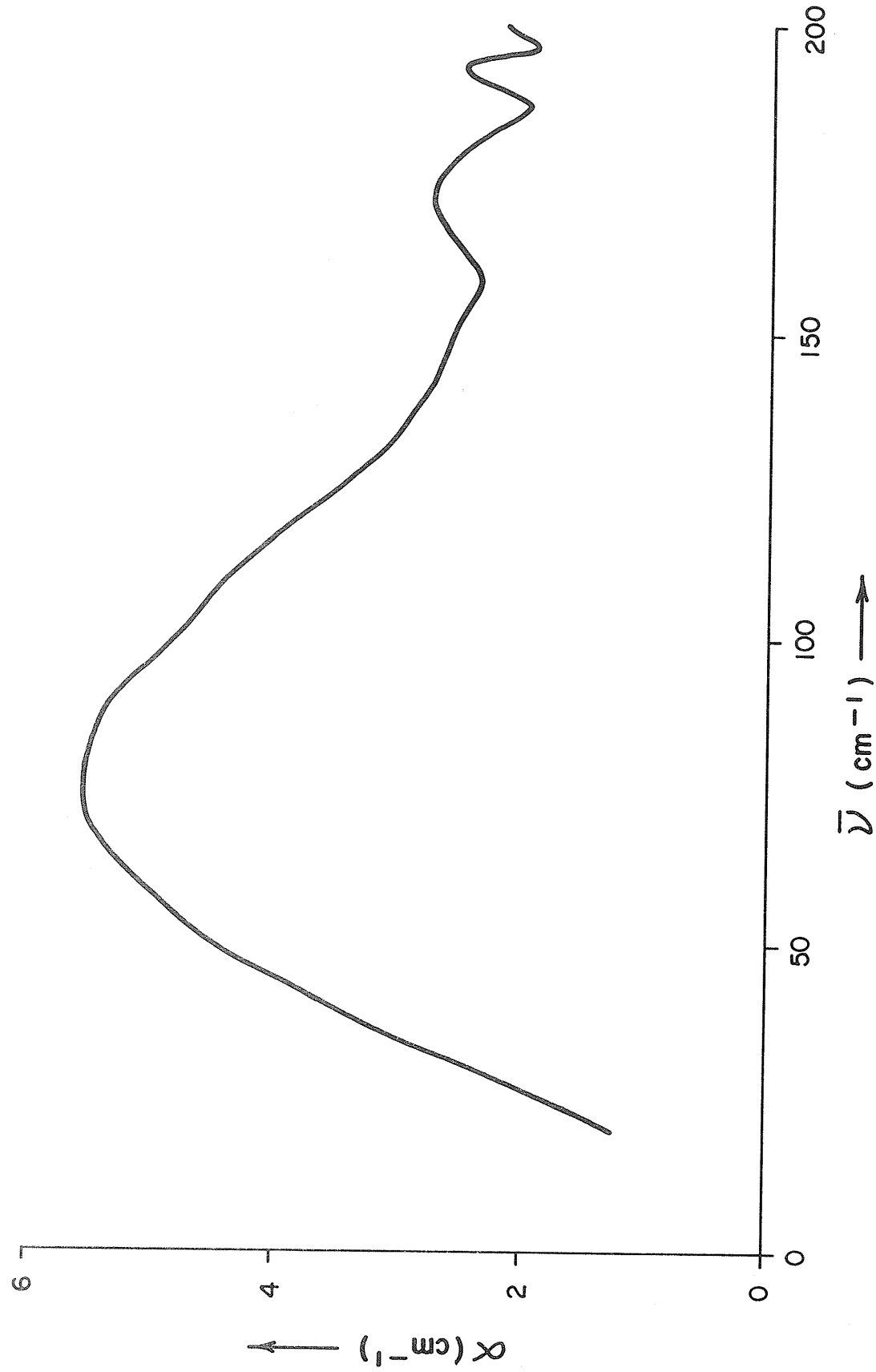

Figure V -1: Far-infrared absorption of pure (11.119M) benzene at 302K.

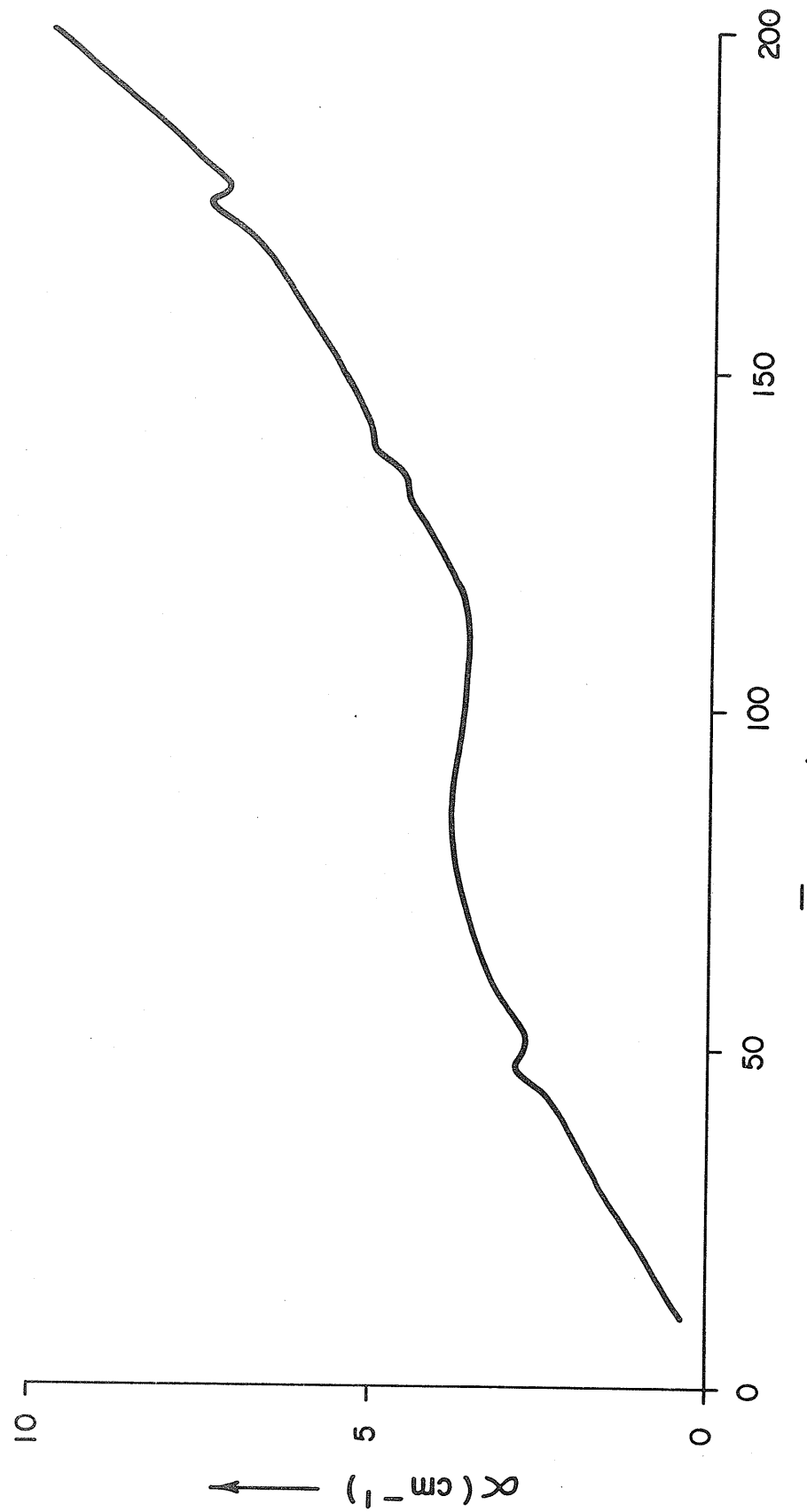

Figure V -2: Far-infrared absorption of pure (10.034M) atactic polystyrene (M_w = 230,000) at 302K.

This quantity is, of course, dependent on the concentration of the absorbing species. Therefore, it is more convenient to express the absorption intensity as an absorption cross-section, σ, in units of $cm^2\ mol^{-1}$, defined by equation V -2:

$$\sigma_{max.} = \frac{\alpha_{max.}}{c} \times 1000 \qquad V\text{ -}2$$

where $\sigma_{max.}$ is the absorption cross-section at maximum absorption,

$\alpha_{max.}$ is the maximum value of the optical absorption coefficient,

and c is the absorbing species' concentration in moles/l.

The magnitude of the estimated errors in the parameters obtained from the solute absorption curves depended to a large extent on the concentration of the solution. A small difference between solution and solvent absorption curves means that a relatively large error must be associated with the difference.

The error in the frequency of maximum absorption, $\bar{\nu}_{max.}$, ranges from $\pm$ 2 cm^{-1} for sharp high-frequency bands to $\pm$ 10 cm^{-1} for very broad weak bands in the lower frequency region, a typical value being $\pm$ 4 cm^{-1} for the broad band absorption. The error estimate for the band width at half height, $\Delta\bar{\nu}_{\frac{1}{2}}$, is about $\pm$ 10 cm^{-1} in most cases. For the maximum value of the absorption coefficient

of the solute the error is ±15% or less normally, but may be up to ±30% when this absorption is small. The error in the solute concentration was usually very much smaller than that in $\alpha_{max.}$ so that the error in the maximum value of the optical absorption cross-section, $\sigma_{max.}$, is essentially that of $\alpha_{max.}$

RESULTS

The far-infrared absorption spectra are presented as graphs of α (cm^{-1}) versus $\bar{\nu}$ (cm^{-1}), with three curves representing solution, solvent, and difference spectra on each. In the cases of pure acetophenone and acetophenone in cyclohexane only one curve is shown, since in the former case there is no solvent correction, and in the latter the solvent absorption is negligibly small in comparison with that of the solute.(7) Parameters derived from these spectra are summarized in Table V -1.

As Table IV of Appendix I shows, the relaxation times for acetyl group relaxation in the molecules investigated by the far-infrared technique at 300K were: acetophenone, 9.8×10^{-10} s; 1,4-diacetylbenzene, 2.0×10^{-10} s; and 4-acetylbiphenyl, 4.0×10^{-10} s. At 300K, the molecular relaxation time of 4-nitrobiphenyl was 3.7×10^{-4} s, and that of 4-acetylbiphenyl was 2.2×10^{-3} s. This means that the frequency of maximum dielectric absorption due to acetyl group relaxation was lower than 2.6×10^{-2} cm^{-1}, and that dielectric absorption due to molecular relaxation of the two larger molecules was at frequencies lower than this by a factor of about 10^6. By contrast, broad band absorption in the far-infrared spectra was observed at frequencies above 50 cm^{-1}. Thus there is a separation in the polystyrene matrix solutions of dielectric absorption from far-infrared absorption by a factor of 2×10^3 for group relaxation and about 10^9 for relaxation of the biphenyl molecules. These separations are considerably greater than those which may be achieved in

TABLE V -1: Far-infrared absorption spectra parameters for pure solvents and for residual (solution - solvent) absorptions.

Solute	Solvent	Conc. (mol l^{-1})	$\bar{\nu}_{max.}$ (cm^{-1})	$\Delta\bar{\nu}_{1/2}$ (cm^{-1})	$\alpha_{max.}$ (cm^{-1})	$\alpha_{max.}/c$ (cm^2 mol^{-1})
	Benzene	11.119	78	109	5.55	0.50×10^3
	Polystyrene	10.034	(only a rising tail up to $\bar{\nu}$ = 200 cm^{-1})			
Acetophenone	(pure)	8.515	58	103	47.6	5.6×10^3
			159	11	11.5	1.4×10^3
	Cyclohexane	0.880	67	88	12.4	14×10^3
	Benzene	0.440	75	88	7.15	16×10^3
	Polystyrene	0.880	77	80	8.6	10×10^3
1,4-diacetyl-benzene	Benzene (302K)	0.123	85	70	2.7	22×10^3
			160	23	2.0	16×10^3
	Polystyrene (302K)	0.652	90	70	17.6	27×10^3
			160	40	12	18×10^3
	Polystyrene (124K)	0.652	93	66	20	30×10^3
			160	36	13	19×10^3
4-acetylbiphenyl	Benzene	0.214	80	74	2.7	13×10^3
			166	13	0.9	4.2×10^3
	Polystyrene	0.533	82	80	7.55	14×10^3
			170	34	4.90	9.2×10^3

TABLE V -1: continued.

Solute	Solvent	Conc. (mol l^{-1})	$\bar{\nu}_{max.}$ (cm^{-1})	$\Delta\bar{\nu}_{\frac{1}{2}}$ (cm^{-1})	$\alpha_{max.}$ (cm^{-1})	$\alpha_{max.}/c$ (cm^2 mol^{-1})
4-nitrobiphenyl	Benzene	0.127	55	81	1.82	14×10^3
			179	14	1.10	8.6×10^3
	Polystyrene	0.539	81	99	3.85	7.1×10^3
			185	11	5.0	9.3×10^3
n-propylbenzene (m.p. 173K)	(pure)	7.17	~67	(shoulder)	3.5	0.49×10^3
	(300K)		125	~95	5.3	0.74×10^3
	(203K)		87	72	5.6	
			125		7.0	
			153	(shoulder)		
	(178K)		83	72	7.7	
			129	120	8.6	
	(168K)		85	90	7.6	
			130		8.7	
			155	(shoulder)		
	(142K)		85	82	6.9	
			130	84	8.4	

TABLE V -1: continued.

Solute	Solvent	Conc. (mol l^{-1})	$\bar{\nu}_{max.}$ (cm^{-1})	$\Delta\bar{\nu}_{1/2}$ (cm^{-1})	$\alpha_{max.}$ (cm^{-1})	$\alpha_{max.}/c$ (cm^2 mol^{-1})
n-propylbenzene	(pure) (123K)		73	30	11.3	
			97		10.8	
			127		13.3	
			135		12.9	
			160	(shoulder)	9.9	

liquid phase solutions.

Figure V -3 shows the far-infrared absorption spectra of acetophenone in four states: (a) pure liquid; (b) 10% solution in cyclohexane; (c) 5% solution in benzene; and, (d) 10% solution in polystyrene. It is apparent from these figures that the spectrum exhibits a peak at similar frequencies and of similar shape in all four states. The numerical data in Table V -1 show that the peak frequencies and half-height widths are virtually the same in benzene and polystyrene solutions, with some reduction of maximum absorption cross-section in the polystyrene matrix solution. Solutions of 1,4-diacetylbenzene in benzene (Fig. V -4(a)) and polystyrene (Fig. V -4 (b)) showed the same agreement of peak frequency and width, and also agreement of absorption cross-section, for the lower-frequency broad band. There was even similar agreement for the higher-frequency band around 160 cm^{-1}. This higher-frequency peak is not part of the characteristic broad band absorption of the far-infrared region. It has been attributed to out-of-plane bending of the acetyl group.[8]

Figure V -5 shows the spectra of solutions of 4-acetyl-biphenyl in (a) benzene and (b) polystyrene. Again, Table V -1 shows that there was very good agreement between the two spectra for the peak frequency, width and maximum absorption cross-section of the low-frequency broad band. The 165 cm^{-1} band appeared to have a greater intensity in polystyrene than in benzene. However,

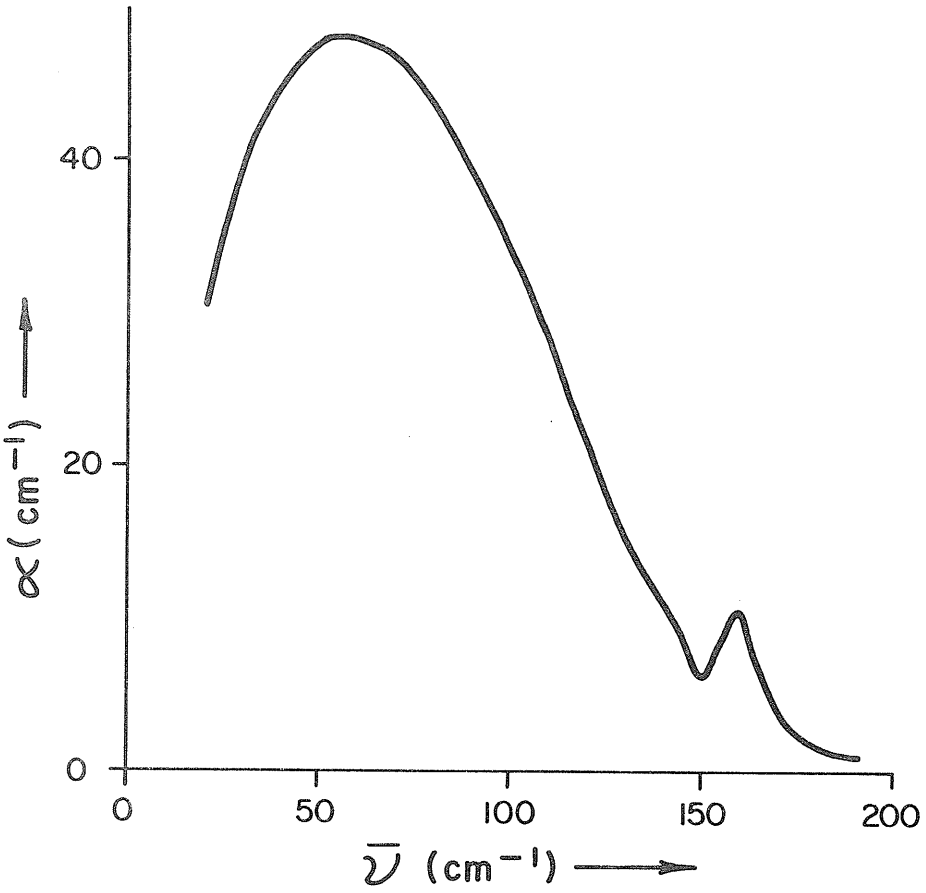

Figure V -3(a): Pure (8.515M) acetophenone at 302K.

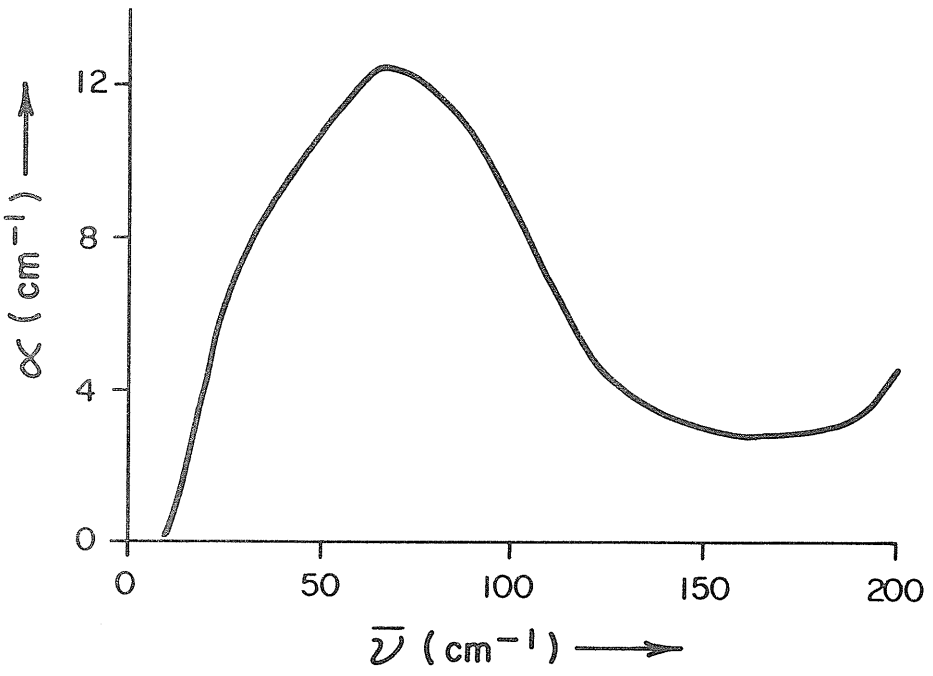

Figure V -3(b): 0.880M acetophenone in cyclohexane at 302K.

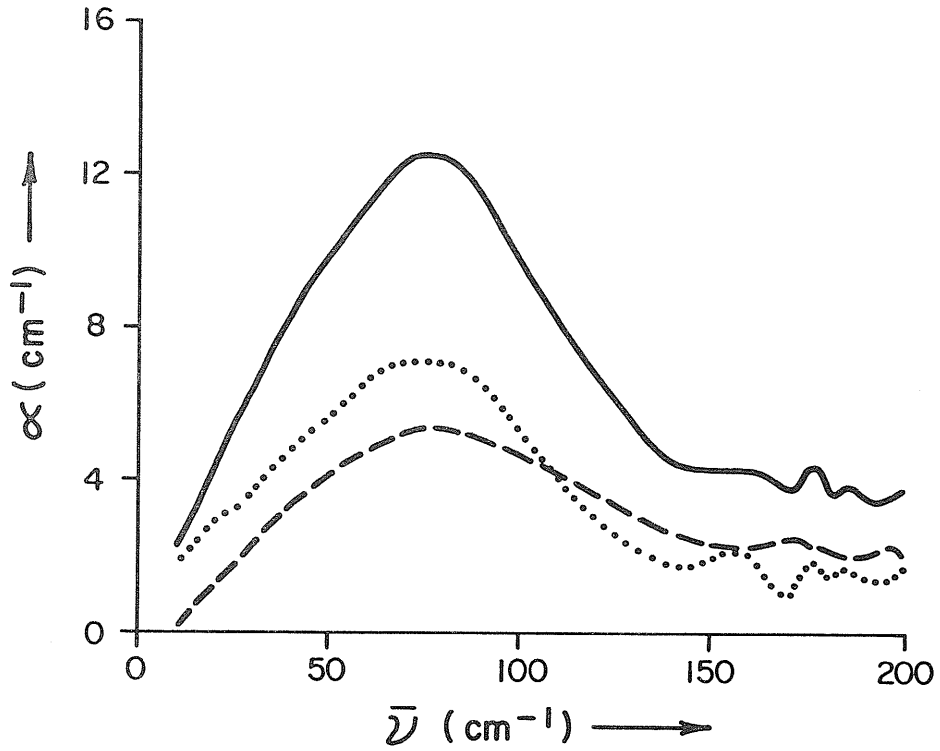

Figure V -3(c): 0.440M acetophenone in benzene at 302K.
——solution; — — benzene; ····· difference

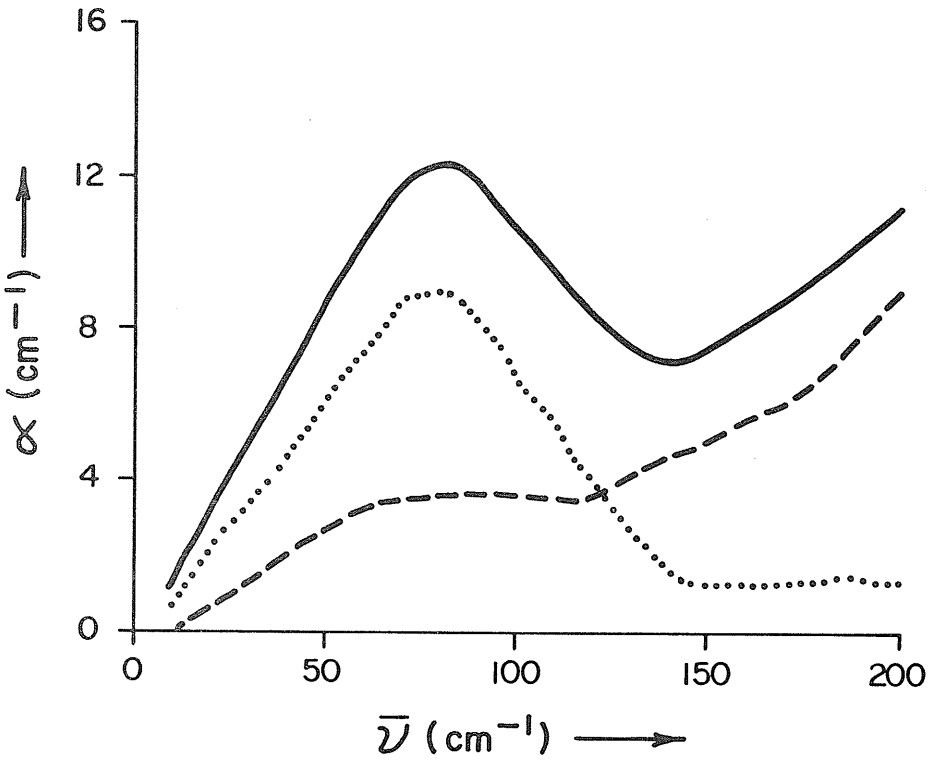

Figure V -3(d): 0.880M acetophenone in polystyrene at 302K.
——matrix; — — polystyrene; ····· difference

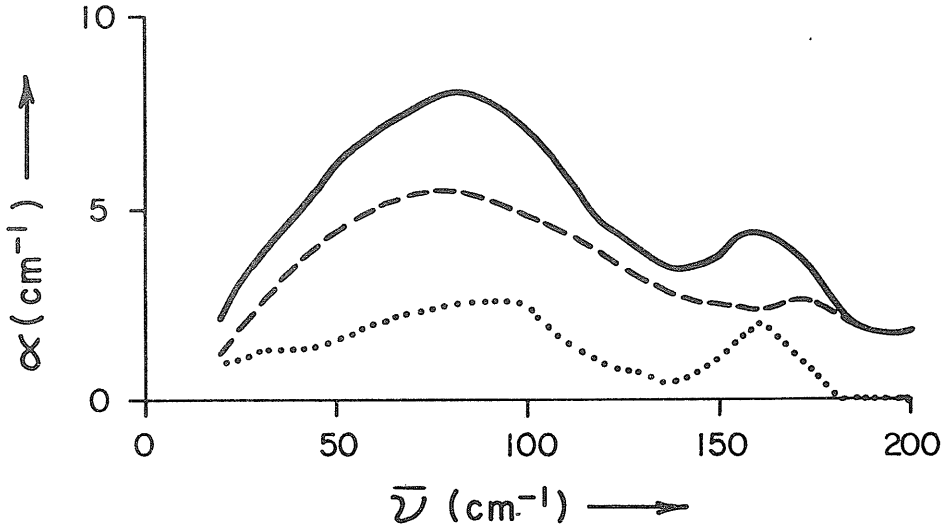

Figure V -4(a): 0.123M 1,4-diacetylbenzene in benzene at 302K.
——— solution; — — benzene; ····· difference

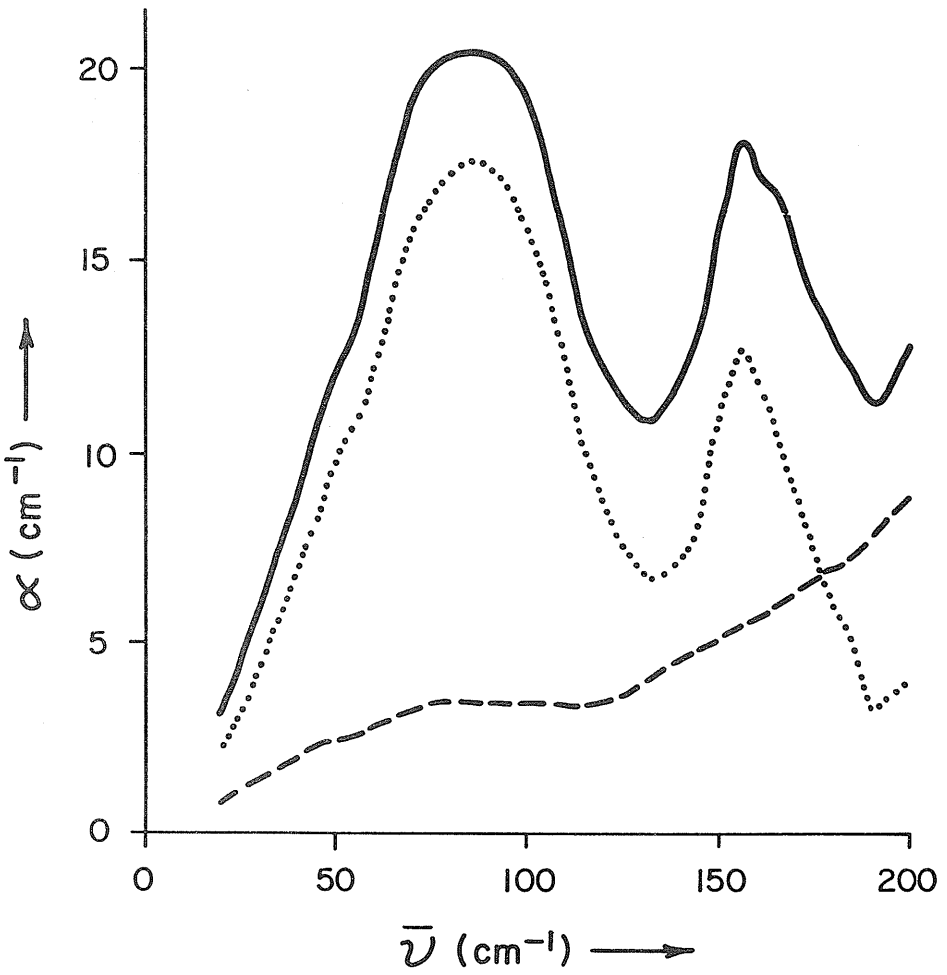

Figure V -4(b): 0.652M 1,4-diacetylbenzene in polystyrene at 302K.
——— matrix; — — polystyrene; ····· difference

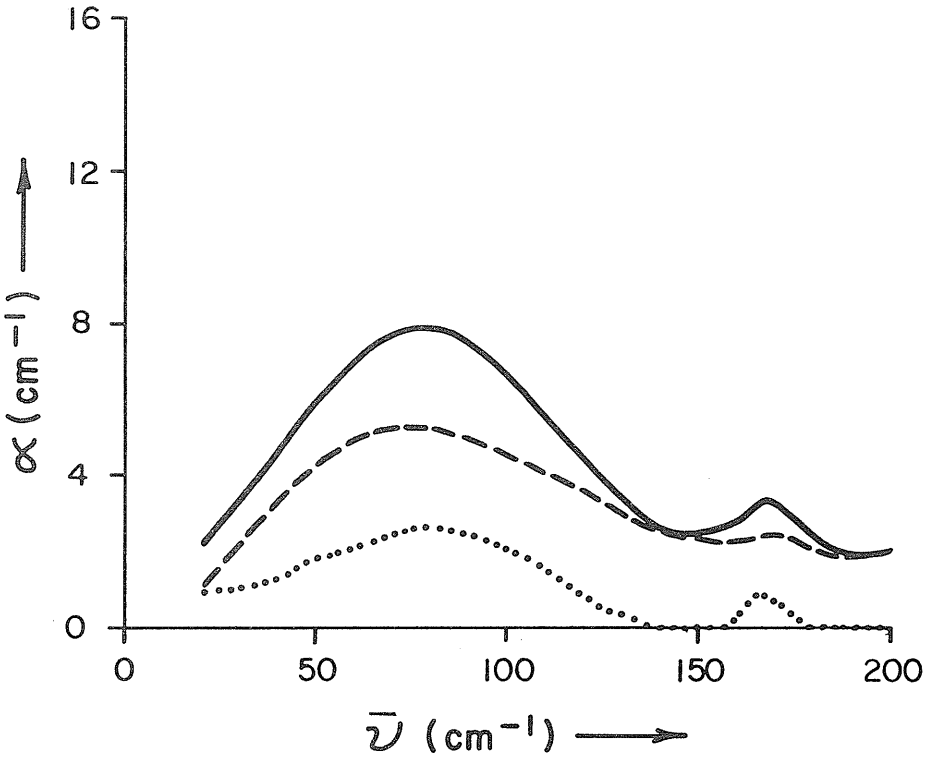

Figure V -5(a): 0.214M 4-acetylbiphenyl in benzene at 302K.
——solution; —— benzene; ····· difference

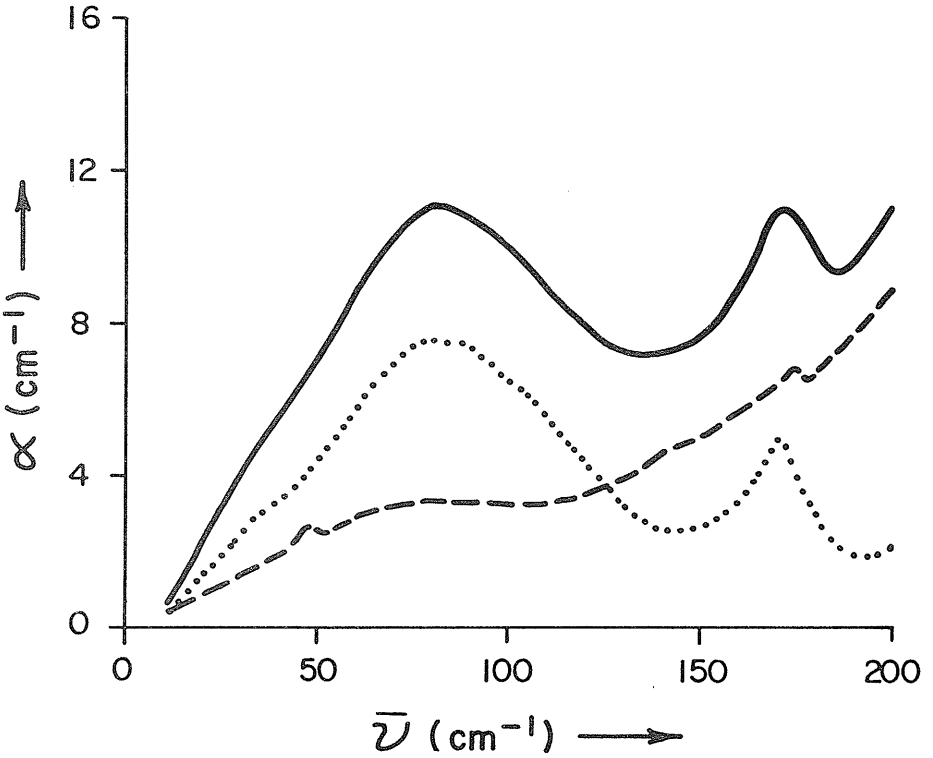

Figure V -5(b): 0.533M 4-acetylbiphenyl in polystyrene at 302K.
——matrix; —— polystyrene; ····· difference

the benzene solution value was less reliable since the solute concentration was low.

Thus, the spectra of acetophenone, 1,4-diacetylbenzene, and 4-acetylbiphenyl all appear not to have been altered by changing from benzene liquid solutions to polystyrene matrices. Yet, the molecular relaxation process in 4-acetylbiphenyl was very much slower in polystyrene than in benzene, and a similar although less pronounced effect was expected for the molecular relaxation in acetophenone. In 1,4-diacetylbenzene no molecular relaxation process was expected to contribute to its dielectric absorption. Further, it is expected that the rate and extent of molecular translational motions of these molecules are similarly decreased in polystyrene as compared to benzene solutions.

If the changes in the rates of molecular motions on passing from benzene to polystyrene solutions produced no discernible effect on the far-infrared absorption spectra of these solutes, one must ask whether the absorptions may be due solely to the acetyl groups which are rotating. But again, it is clear that the rates of rotation of the acetyl groups in polystyrene solutions are markedly slower than in benzene solutions. Despite this, the far-infrared absorptions appear unaffected by the change of solvent.

To test whether group relaxation alone might be involved in the far-infrared broad band absorption of a polar solute

in polystyrene matrix solution, the large rigid molecule 4-nitrobiphenyl was examined in this solvent system and in benzene solution. The spectra obtained are shown in Fig. V -6. It is clear that there is a broad band absorption in both solvent systems despite the large difference in molecular relaxation times between the two. However, there are differences in the frequency and intensity of the broad low-frequency absorption band, as Table V -1 shows. Whether these differences are genuine or just experimental error is difficult to say. The problem lies in the benzene solution spectrum. The solubility of 4-nitrobiphenyl in benzene is not very high, with the result that the difference between solution and solvent absorptions is rather small. Other solvents were tried in an attempt to circumvent this problem but without success. The problem was compounded by the uncertainty in the concentration of the benzene solution. The solution used was saturated, and its concentration was obtained by evaporation of the solvent from measured aliquots. This has provided the approximate concentration given in Table V -1, but there may be much larger error in this value than was the case for other solute concentrations which were not in saturated solutions. Therefore it is possible, although not certain, that the intensity of the broad band absorption of 4-nitrobiphenyl was reduced in polystyrene matrix compared to that in benzene solution. What is of greater interest, however, is that there actually was a broad band absorption for this rigid molecule even when the molecular relaxation time was vastly longer than in liquid solution.

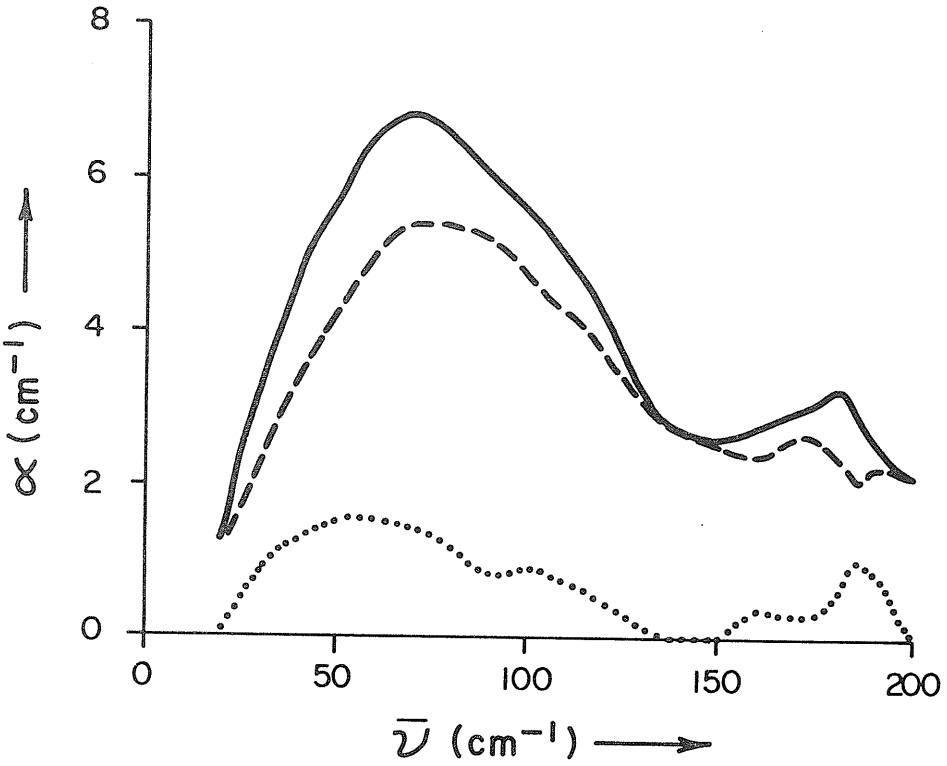

Figure V -6(a): 0.127M 4-nitrobiphenyl in benzene at 302K.
——solution; — — benzene; ····· difference

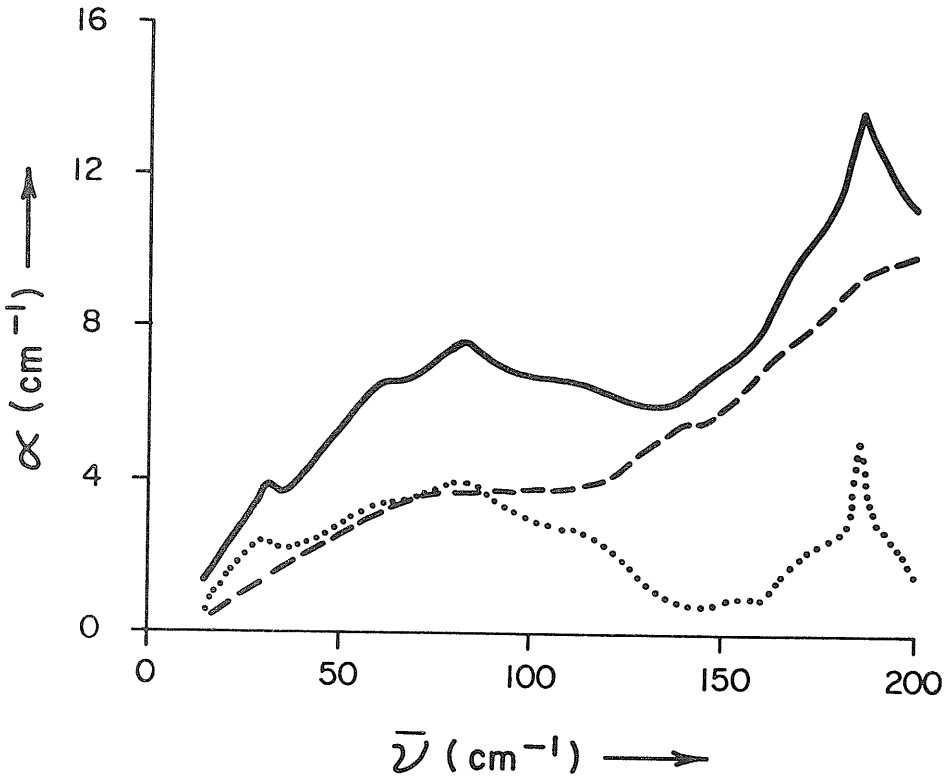

Figure V -6(b): 0.539M 4-nitrobiphenyl in polystyrene at 302K.
——matrix; — — polystyrene; ····· difference

As this thesis was being written, a new cell system was designed and constructed for the Grubb-Parsons interferometer. It allows sample temperature to be controlled within ± 1 C^{o} about a set-point anywhere in the range from about -160^{o}C (113K) to +70^{o}C (343K). A spectrum of the polystyrene matrix solution of 1,4-diacetylbenzene was recorded at 124K, and the solvent-corrected curve is shown in Fig. V -7 along with the spectrum at 298K for comparison. The relaxation times for acetyl group relaxation are indicated by the data in Chaper IV to be about 10^{-10} s at 298K and about 5 x 10^{-3} s at 124 K.

The two spectra shown in Fig. V -7 do not differ greatly. At the lower temperature, the broad band peak occurs at 93 cm^{-1} frequency, compared to 90 cm^{-1} at 298K. This difference is of the order of experimental error, and is less than the resolution (approximately 7 cm^{-1}) at which the spectra were recorded. The maximum intensity of the 93 cm^{-1} band is about 10% greater at the lower temperature, whereas very much larger changes of both peak height and frequency have been reported in pure liquid and rotator solid phases of other materials.[4,5,9,10] Perhaps the most important point is that on the low-frequency side of the broad band there does not appear to be any large difference in absorption intensities. Since the decreased sample temperature would reduce any contribution from

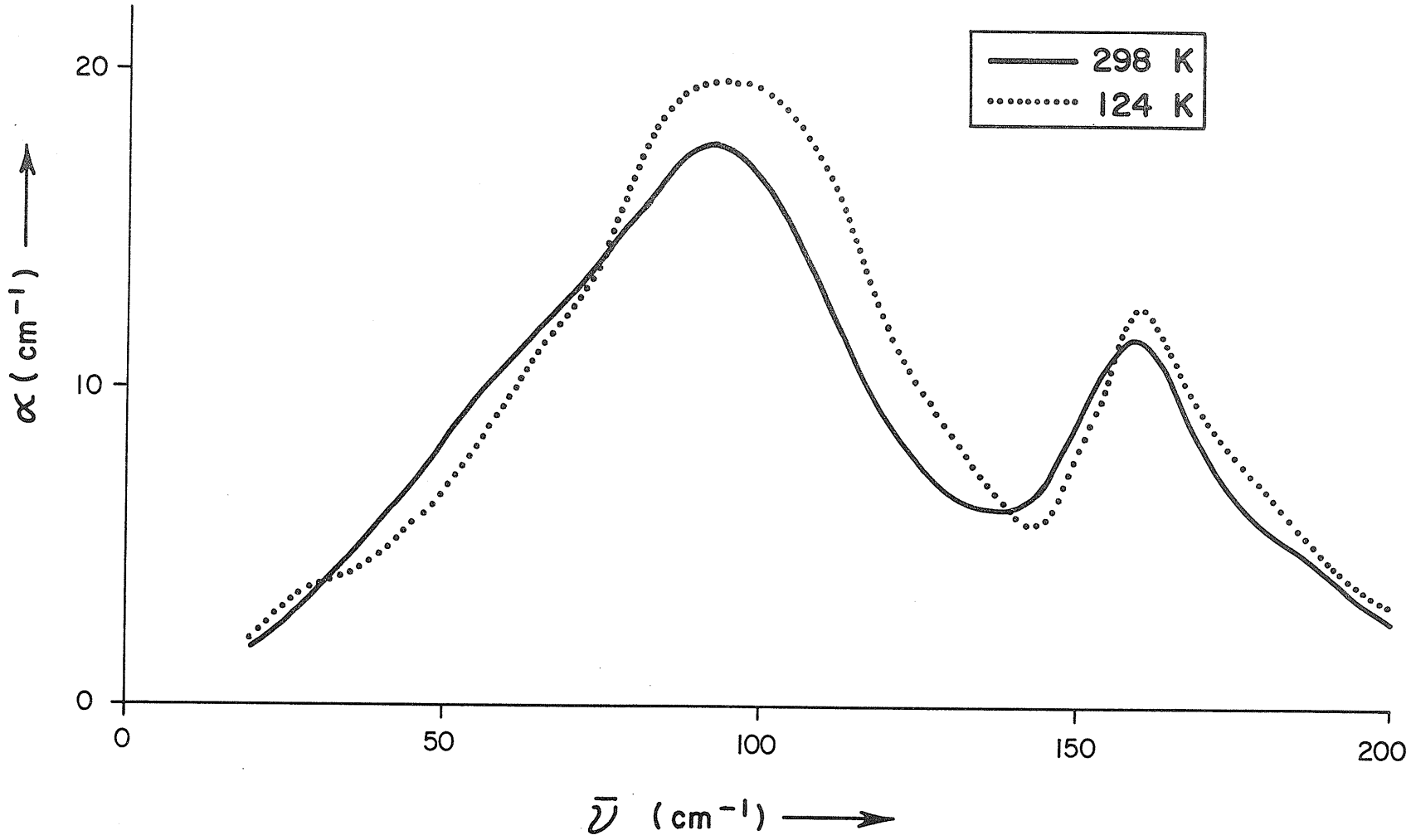

Figure V -7: 0.652M 1,4-diacetylbenzene in polystyrene at two temperatures as indicated.

dielectric absorption, it has been suggested that this might produce noticeable changes at low far-infrared frequencies.[6,11-13] The dielectric absorption maximum has been shifted to lower frequency by a factor of about 10^7 at 124K compared to 298K, and yet the frequency, intensity and shape of the broad band do not appear to have been altered. Thus, the existence of this broad band absorption appears not to be due simply to rapid motion of the acetyl substituent group.

The development of the low temperature cell provided another opportunity to examine the effect of decreasing the rate of molecular relaxation. Copeland and Denney[14] have reported dielectric absorption data for pure n-propylbenzene in the supercooled liquid state. This material has a freezing point of 173K.[15] Fig. V -8 shows the far-infrared spectra of n-propylbenzene at five temperatures, and the numerical data derived from these are included in Table V -1. Since it is difficult to estimate accurately the density, and thereby the concentration, of the supercooled liquid phase, the absorption cross-section, σ, has been calculated only for the spectrum obtained at 298K.

The three spectra at 298K, 203K (30 degrees above the melting point) and 178K (5 degrees above the melting point) show an increase of the intensity of the broad band near 80 cm^{-1} as temperature is decreased, which is typical of broad band spectra. The broad band intensity at 178K is more than double that at 298K, which factor is much greater than any

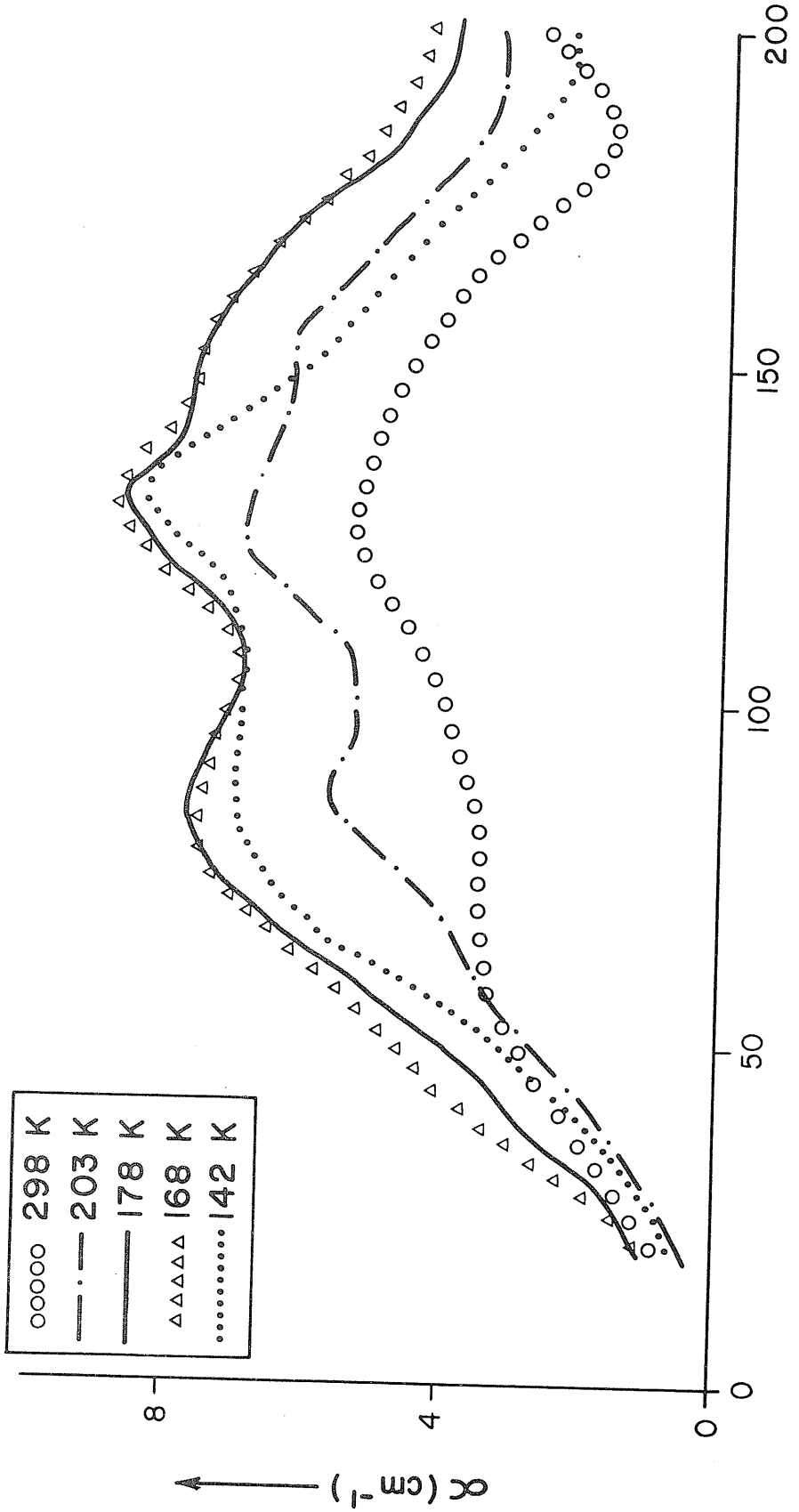

Figure V -8: Pure n-propylbenzene at five temparatures as indicated.

change in the density of the liquid over this temperature range. The intensity of the intramolecular band near $\bar{\nu}$ = 125 cm^{-1} also appears to increase, but it seems likely that this is merely because it is overlapped by the low-frequency broad band. The 125 cm^{-1} band also appears to be unusually broad for an intramolecular band. On the lower-frequency side this is undoubtedly due to overlap with the broad band. On the higher-frequecny side the spectrum at 203K suggests the presence of an overlapping peak near $\bar{\nu}$ = 153 cm^{-1}.

The two spectra at 168K (5 degrees below the melting point) and 142K (31 degrees below the melting point) were obtained on a supercooled liquid sample. The data of Copeland and Denney[14] show that the molecular relaxation times at these two temperatures are approximately 1.5 x 10^{-9} s and 6.7 x 10^{-5} s, respectively. That is, at 142K the rate of molecular relaxation is slower than that at 298K by approximately six orders of magnitude. Yet the far-infrared spectra of the supercooled liquid at both 168K and 142K are very similar to those of the liquid above the melting point. It is to be noted that in none of the low-temperature spectra is there any sign of a decrease of the intensity of the absorption below $\bar{\nu}$ = 50 cm^{-1} as compared to the spectrum at 298K. This is in agreement with the results obtained at low temperature for the polystyrene matrix solution of 1,4-diacetylbenzene.

To ensure that the samples investigated at 168K and 142K were, in fact, supercooled liquid phases of n-propylbenzene and not crystalline solid phases, a spectrum was recorded at 123K. The interferograms obtained were markedly different from any of those at higher temperatures. The final spectrum is shown as Fig. V -9, and numerical data have been included in Table V -1. This spectrum differs from those obtained at higher temperatures in two notable aspects. Firstly, the intensity of the absorption is considerably greater (by about 50%) than that at warmer temperatures. Secondly, all of the peaks appear to be somewhat sharper, and the broad band absorption is differentiated into two distinct peaks at $\bar{\nu}$ = 73 and 97 cm^{-1}. Although the exact shape of the 73 cm^{-1} band is uncertain because of an interfering absorption at 78 cm^{-1} due to the high-density polyethylene cell windows, its existence is clear. The intramolecular band appears to be split into two peaks at $\bar{\nu}$ = 127 and 135 cm^{-1} (the resolution was 3 cm^{-1}), and the shoulder at $\bar{\nu}$ = 160 cm^{-1} is now clearly present.

In summary, the spectrum of n-propylbenzene obtained at 123K has all the characteristics commonly found in the far-infrared absorption spectra of non-rotator crystalline solids[4,5] but is noticeably different from the spectra obtained at higher temperatures. This is a strong indication that the spectra obtained at 168K and 142K were not those of a crystalline solid but were rather those of a supercooled liquid.

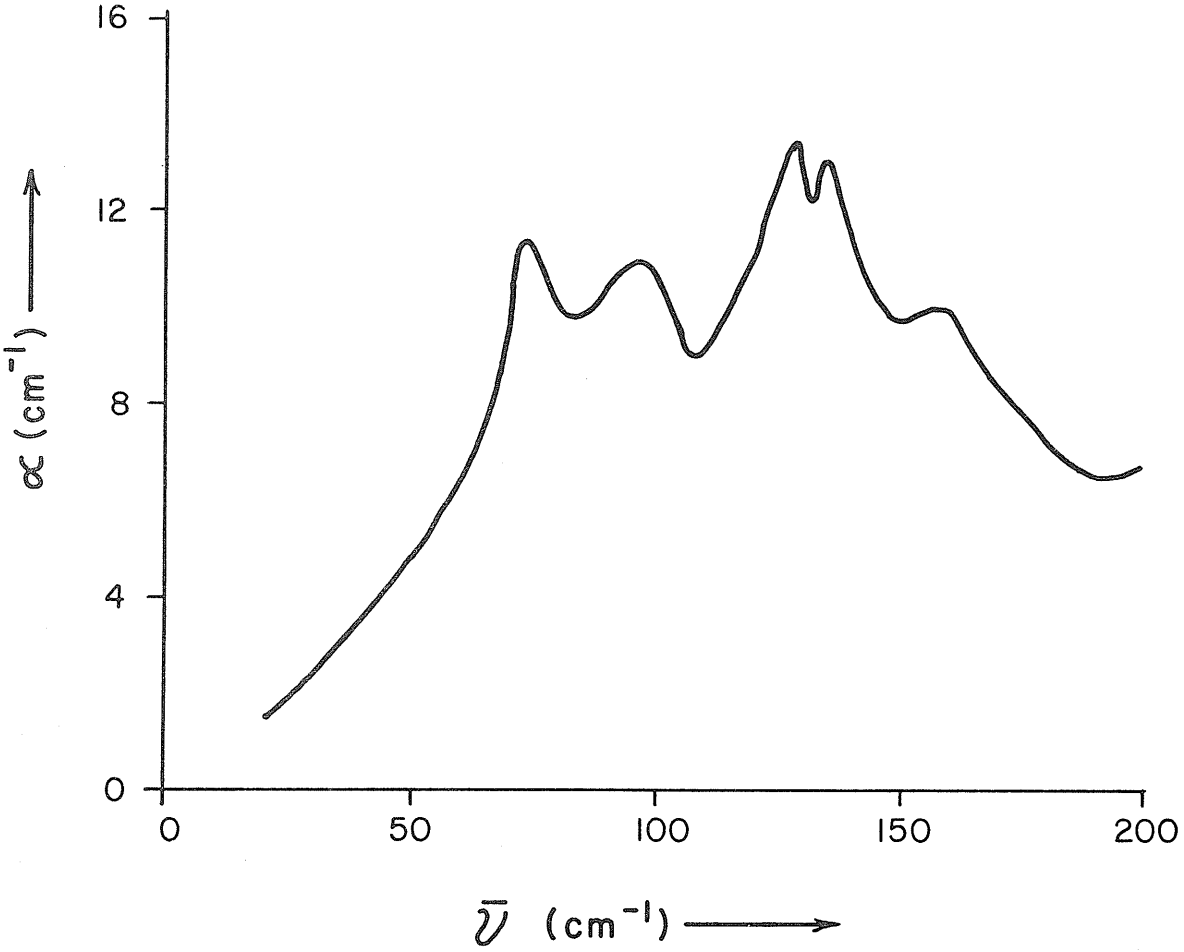

Figure V -9: Pure n-propylbenzene at 123K.

Chantry et. al.[16,17] have reported the existence of a broad band absorption near $\bar{\nu}$ = 70 cm^{-1} in some vinyl acetate-ethylene copolymers. Whereas pure polyethylene exhibits a sharp absorption peak in the range 72 to 78 cm^{-1} (dependent on temperature) due to crystalline lattice modes in the polymer, their copolymers exhibited an additional broad absorption band contributed by the polar acetate group. This broad band persisted even at liquid nitrogen temperatures. In the present work the rates of molecular and substituent group relaxations were decreased from those in liquid benzene solutions by dissolving the solute in the highly viscous solvent polystyrene, and in one case also by decreasing the temperature of the polystyrene solution. In the cases of the copolymers examined by Chantry et. al., relaxations of the polar vinyl acetate group are expected to be slowed by the viscosity of the copolymer and in addition by the fact that this group was chemically bonded to the polymer chain.

At this point it appears that five different procedures have been used to decrease the rates of molecular and intramolecular (i.e., substituent group) relaxation. Some pure liquids have been examined in crystalline solid phases which allow slow molecular rotations.[4,5,6] A polar group has been chemically bonded to a polymer chain.[16,17] In the present work, supercooled liquid n-propylbenzene has been examined, as well as polystyrene matrix solutions of several polar solutes. In addition, polymeric samples in this work and in that of Chantry et al.[16,17] have been examined

at low temperatures. In all of these cases the broad band absorption has been found in the far-infrared spectra below $\bar{\nu}$ = 100 cm^{-1} despite the slow rates of molecular rotation and translation. However, the spectrum of solid n-propylbenzene shown in Fig. V -9 and earlier work[4,5] has shown that, if molecular rotational motion is eliminated, the broad band is replaced by sharp, intense peaks due probably to lattice modes.

It is apparent that the rates of molecular and substituent group relaxation are not critical for the existence of a broad absorption band below a frequency of 100 cm^{-1} in the far-infrared region. Moreover, this broad band absorption appears to arise from some process which is completely separate from that of dielectric absorptions since a very great separation of these two processes in terms of frequency has not decreased the intensity of the broad band absorption; indeed, its intensity often increases as sample temperature is decreased.

DISCUSSION

The Hill model[3] postulated libration of molecules within potential energy wells provided by the surrounding molecules, with the possibilities that the molecule could jump from one well to another and that the wells might fluctuate rapidly due to molecular collisions. The present study was aimed at examining the far-infrared broad band absorptions when the rates of well fluctuation and inter-well jumping were reduced considerably.

It has been established that no broad band absorptions are apparent in the far-infrared region for rigid crystalline lattices which preclude molecular rotation, but that these absorptions are found if some molecular rotation is possible.[4,5,6] The present results indicate that the rate of this rotation is not critical.

Several theories have been advanced to account for the observed deviations of the dielectric parameters of pure liquids and solutions from the Debye theory both in the far-infrared region and at much lower frequencies. With respect to the latter, Copeland and Denney[14] recently considered the absorptions found in supercooled n-propylbenzene in the kilohertz frequency region. At room temperature the absorption occurs in the microwave region, but in the supercooled

liquid they suggest that the entire absorption is shifted to these much lower frequencies. They found that in the supercooled liquid the absorption could be described well by the Cole-Davidson skewed arc formulation which may be interpreted to indicate that the relaxation process involved co-operative intermolecular effects. They felt that the absorption process in the room temperature liquid was basically very similar to what occurs in the supercooled liquid. Since the latter process could be described by a mathematical function employing a single relaxation time, they suggested that even at room-temperature it was not necessary to invoke the existence of higher-frequency absorption processes such as intramolecular relaxation of the n-propyl substituent group.

Such a suggestion appears not to take into consideration two factors. Firstly, if the intramolecular relaxation did occur in the supercooled liquid (and it seems reasonable that it should), it is most unlikely that it could be seen to be separate from the broad distribution of relaxation times found for the molecular process which probably involves some co-operative motion in the supercooled liquid. Secondly, although the broad band absorptions of Fig. V -8 should make no measurable contribution to the data from supercooled n-propylbenzene, because the measurement frequencies for this system were very low, (10^2 to 10^4 Hz), this is no indication that a contribution from higher-frequency processes will not be found in data gathered at higher frequencies for room-temperature samples.

Citing previous results on alkyl halides, Copeland and Denney suggested that, although the temperatures at which the relaxation processes were observed in the supercooled liquid are much lower than those used for dilute liquid solution studies, "the basic character of the dispersion remains unchanged over a wide temperature interval."[14] The data of relaxation time as a function of temperature for supercooled n-propylbenzene was analyzed by the Eyring analysis computer program employed in the present work, yielding ΔH_E = 80 kJ mol^{-1} and ΔS_E = 406 J K^{-1} mol^{-1}. Similar analyses of data from pure alkyl benzenes above room temperature reported by Petro and Smyth[18] showed that ΔH_E ranged from 6.7 kJ mol^{-1} for toluene to 10.6 kJ mol^{-1} for iso-propylbenzene, while ΔS_E fell into the range 0 to -10 J K^{-1} mol^{-1}, being -3 JK^{-1} mol^{-1} for iso-propylbenzene. Thus, both the enthalpies and entropies of activation for molecular relaxation of pure alkyl benzenes at temperatures of the order of 300K were very much less than those found in supercooled n-propylbenzene. Such a difference in activation parameters suggests that the character of the relaxation processes does change over a wide temperature interval contrary to the view of Copeland and Denney. It would seem more reasonable to state that the differences between activation parameters reflect the differences in the environments surrounding the relaxing species, at widely different temperatures, and that the changes of environment should be gradual and continuous as the temperature of the liquid is altered.

Zwanzig[2] considered the interactions of point dipoles in a simple model of a rigid cubic lattice at high temperatures. Taken only to a first approximation, his equations predicted that dipolar interactions should give rise to a second absorption at frequencies higher than that of molecular relaxation whilst further terms should produce even higher-frequency absorptions. This approach could account for the existence of absorptions in the far-infrared region. However, Zwanzig pointed out that he had simplified the problem by ignoring the effects of the molecular moment of inertia. This meant that the theory indicates values of absorption greater than either the Debye theory or experimental data at frequencies above about 100 cm^{-1}. Further, the Zwanzig theory could not indicate a frequency at which a liquid sample might return to transparency. Therefore, it is not really applicable to the far-infrared region.

Minami and Ohno[11] and Higasi _et al._[12] have applied an autocorrelation function treatment of the Hill model[3] to absorptions in the far-infrared region by rod-like molecules. The model involves both libration of the molecule within potential energy wells and rotational diffusion of the molecule from one well to another. They assumed two different models for the shape of the wells. For a square well with rigid boundaries from which the librating molecule may rebound elastically it was possible to estimate the angles through which the molecule might rotate in its librational motion. These were found to be approximately 35^{o} for spherical molecules such as tert-butyl chloride,

30^{o} for 1,1,1-trichloroethane, 10^{o} for semi-planar iodobenzene, and 6^{o} for meta-dibromobenzene. Agreement with experimental data was not as good when a harmonic oscillator model was assumed for the librations within potential energy wells. However, the authors noted that their development used only one resonant frequency whereas a distribution of resonant frequencies would have been more reasonable. Since the choice of the distribution function would affect the results a great deal, it may be possible to achieve better agreement between theory and experimental data.

Haffmans and Larkin[6,13] have applied the auto-correlation function treatment to spherical molecules. They assumed that the librational motion in the pure liquid phase was limited to the rotational angle deduced from the known structure of the rotator solid phases. This angle was 0.62 rad, or about 36^{o}, in agreement with the results of the work by Minami et al. Its use allowed a reasonable fit of the spectrum predicted by their square well model to the observed data. This model indicated that, as temperature was increased, the total observed absorption would contain a larger contribution from the molecular relaxation process. Therefore, the band peak would appear to shift to lower frequencies even if the frequency of the librational motion were unchanged. If the potential energy wells became broader and/or shallower with increasing temperature, this apparent shift would be enhanced by a decrease in the librational motion frequency. Their consideration of Hill's

model, which they termed the "itinerant oscillator", led to similar indications of temperature effects.

In liquid phase near room temperature the absorptions due to molecular and intramolecular relaxation processes occur for simple small molecules at frequencies high enough that their contribution to the overall far-infrared absorption band may be appreciable. Therefore, it is not possible to examine whether the apparent shifts of the centre of the far-infrared broad band absorption are due solely to the changes in the dielectric absorption process. The present study of far-infrared absorptions by molecules dissolved in polystyrene and by those in a supercooled liquid suggest that the effects of temperature changes on the librational motion alone may now be investigated. Both techniques allow one to shift the molecular relaxation process to much lower frequencies and thereby to decrease its contribution to the lower-frequency side of the broad band.

An interesting point to be made in this regard is that the spectra obtained in this work for polystyrene matrix solutions suggest that, although the frequency of the dielectric relaxation process is altered by the viscous polymer matrix, the frequency of the librational process apparently is altered to a much smaller extent. The band centres found in the matrix solution samples were comparable to those in liquid benzene solutions. Similarly, the spectrum of 1,4-diacetylbenzene at 124K

was not very different from that at 298K. Likewise the broad band absorption was located near $\bar{\nu}$ = 85 cm^{-1} in all four of the cold liquid and supercooled liquid samples of n-propylbenzene. At 298K, this band appeared to be at 67 cm^{-1}, but whether this lower frequency value is correct is uncertain since at this temperature the intensity of the broad band was much less than at lower temperatures, with the result that its shape and location were somewhat distorted by the overlapping intramolecular band near $\bar{\nu}$ = 125 cm^{-1}.

To summarize, the prediction, that part of the apparent shift to higher frequency of the broad band absorption as temperature decreases may be due to the loss of the high-frequency tail of the dielectric absorption, has not been borne out by the present study. It is possible that the loss of this tail was more than compensated by the increase in the intensity of the broad band. This point certainly requires further experimental investigation.

Larkin[13] drew attention to the fact that his treatment of Hill's "itinerant oscillator" model predicted that there should be a separate absorption due to molecular relaxation at frequencies below 10 cm^{-1}. This frequency region is particularly difficult from an experimental viewpoint because of poor source output intensity and detector sensitivity. However, if the existence of such a low-frequency band

can be established, it would be interesting to examine what happens to it in a polystyrene matrix solution and in supercooled liquids. If it is due to molecular relaxation, its frequency under such conditions may be shifted to frequencies so low that it would not be observed with currently-available far-infrared equipment.

CONCLUSIONS

This study has shown that a typical broad band absorption is found for polar solute molecules dissolved in a polystyrene matrix. Neither the shape, the band centre, nor the maximum intensity of the band appeared to differ very much between liquid benzene solutions and the polymer solutions, with the possible exception of solutions of 4-nitrobiphenyl. Similarly, the broad band was found to exist in a cold polymer matrix solution and in a supercooled liquid. This clearly indicates that the broad band absorption is not merely a higher-frequency band due solely to the relaxation processes at frequencies in and below the microwave region. The broad band absorption must arise from some separate class of molecular motion such as has been proposed in theories involving a temporary "cage" surrounding a librating central molecule.

The existence of the broad band absorption found in the lower frequency region of far-infrared spectra and its characteristics of band centre, width, and height require that there be some freedom of the molecule to rotate. However, it is apparent from this study that the rate of this rotational motion and probably also the rate of molecular translational motion are not critical to the absorption process. It would appear that the major factor is that, over the entire sample, all possible orientations of polar molecules and surroundings may exist. In other words, if one uses the cage model to describe the structure of

the sample, it seems that what is important is not time-dependent fluctuations of local structure but rather the random distribution of such structures throughout the sample volume. This random quality appears to result primarily from the ability of the molecules to rotate, albeit slowly.

Far-infrared absorptions by large polar molecules under conditions of rapid and slow molecular rotations clearly require further study to establish whether decreased contributions from dielectric relaxation in the latter cases produce any appreciable changes in the lower-frequency side of the broad band absorption. Some current theoretical treatments suggest that these changes should be observed, whereas this does not appear to have been the case in the present study.

The polymer matrix solution technique would appear to provide a means by which one may investigate the effects of experimental parameters such as temperature on the absorption due solely to the processes (e.g., librational motions) responsible for the far-infrared broad band absorption. In addition, measurements are indicated on supercooled liquids and glasses, in which systems also the contributions from dielectric relaxations would be reduced in comparison with common liquid phases.

REFERENCES

1. A. Morita, Ph. D. Thesis, University of Salford, Salford, Lancs., England, (1974).

2. R. Zwanzig, J. Chem. Phys., 38, (1963), p. 2766.

3. N. E. Hill, Proc. Phys. Soc., 82, (1963), p. 723.

4. C. K. McLellan, M. Sc. Thesis, Lakehead University, Thunder Bay, "P", Ontario, Canada, P7B 5E1, (1971).

5. C. K. McLellan and S. Walker, J. Chem. Phys., 61, (1974), p. 2412.

6. R. Haffmans and I. W. Larkin, J. Chem. Soc. Faraday II, 68, (1972), p. 1729.

7. G. J. Davies, J. Chamberlain and M. Davies, J. Chem. Soc. Faraday II, 69, (1973), p. 1223.

8. G. Varsányi. "Vibrational Spectra of Benzene Derivatives", Academic Press, New York, N. Y., U. S. A. (1969), p. 319.

9. S. R. Jain and S. Walker, J. Phys. Chem., 75, (1971), p. 2942.

10. S. G. Kroon and J. van der Elsken, Chem. Phys. Lett., 1, (1967), p. 285.

11. R. Minami and A. Ohno, J. Phys. Soc. Japan, 35, (1973), p. 1730.

12. K. Higasi, R. Minami, H. Takahashi and A. Ohno, J. Chem. Soc. Faraday II, 69, (1973), p. 1579.

13. I. W. Larkin, J. Chem. Soc. Faraday II, 69, (1973), p. 1278.

14. T. G. Copeland and D. J. Denney, J. Phys. Chem., 80, (1976), p. 210.

15. R. C. Weast, (ed.), "Handbook of Chemistry and Physics", (49th ed.), The Chemical Rubber Co., Cleveland, Ohio, U. S. A., (1968).

16. G. W. Chantry, J. W. Fleming, E. A. Nicol, H. A. Willis and M. E. A. Cudby, Infrared Physics, 12, (1972), p. 101.

17. G. W. Chantry, J. W. Fleming, R. J. Cook, D. G. Moss, E. A. Nicol, H. A. Willis and M. E. A. Cudby, Infrared Physics, 13, (1973), p. 157.

SUGGESTIONS FOR FURTHER WORK

SUGGESTIONS FOR FURTHER WORK

The technique of examining the dielectric relaxations of a solute in an amorphous polymer matrix would appear very useful for investigations of energy barriers to intramolecular processes such as molecular inversion and substituent group rotation. Some work in this area is being carried out in this laboratory.

The present study has been confined to the use of atactic polystyrene as a solvent. Some preliminary results obtained by co-workers have indicated that the use of different polymers as a matrix material may affect molecular relaxation times more than intramolecular ones. Hence, the exact nature of the process observed may be clarified by studies in a variety of polymer solvents. These data could also provide information on the polymers themselves through their effects on the solutes in the matrices. It would be interesting, for example, to examine a large range of sizes of rigid solute molecules to determine whether there is an upper limit to the size of a molecule which may rotate in the polymer matrix.

Investigations of molecular relaxation in polymer matrices above the glass transition temperature could provide useful information. Such studies could yield values of the activation energy of the glass transition process itself and possibly shed some light on the nature of this process.

Steric hindrance, resonance, and inductive effects on intramolecular relaxation may be investigated conveniently through dielectric measurements on polymer matrix solutions. In these studies it would be preferable to use larger molecules so that there is a large separation of group and molecular relaxation processes. However, this restriction is not essential if other techniques are employed to clarify the origins of the dielectric absorptions. Information on these effects would be of interest to theoretical chemistry workers for comparisons of predicted values with those measured experimentally. It would also be of interest to compare these experimental values with those obtained through other experimental techniques.

In the far-infrared frequency region, investigations are indicated to examine further whether the broad band absorption is altered in polystyrene matrix solutions on the low frequency side of the band, for this effect does not appear to have been observed in the present study. In addition, if there is a separate absorption band below a frequency of 10 cm^{-1} in liquid solutions due to molecular relaxation, as predicted by one theoretical treatment, it would be interesting to see whether this band is affected by placing the molecule in a polymer matrix. Other techniques of reducing the rate of molecular relaxation, such as the use of low-temperature polymer matrices, supercooled liquids, and glassy states, should be employed also to examine their effects in the far-infrared region.

Some evidence in the literature suggests that the nature of the solvent employed for liquid solution samples does not affect the broad band absorption very much. This could be investigated further by employing a variety of polymers as solvents. Similarly, examination of a wide range of solute concentrations in polymer matrix solutions would be of interest in the far-infrared region, since information on dielectric relaxation suggests that this latter process is affected by concentration.

It may be possible to extend the use of the polymer matrix solution technique to other fields of investigation. For example, if it were possible to observe the n.m.r. absorption of the protons of a solute molecule superimposed on the absorptions due to the protons of the polymer solvent, this technique might alter the relaxation times for molecular and intramolecular processes.

APPENDIX I

Tabulated Dielectric Data

TABLE I - DIELECTRIC DATA FOR SIX PURE LIQUIDS

t(°C)	T(K)	ε'	ε"	Source Code*
		FLUOROBENZENE		
30.0	303.0	2.42	0.63	0
		2.76	0.95	0
		5.15 (ε_o)	0	0
		2.13 $(n_D)^2$	0	0
10.0	283.0	2.56	0.62	0
		2.75	0.90	0
		5.64 (ε_o)	0	0
		2.16 $(n_D)^2$	0	0
- 9.4	263.6	2.58	0.48	0
		2.74	0.82	0
		5.98 (ε_o)	0	0
		2.20 $(n_D)^2$	0	0
-29.9	243.1	2.62	0.42	0
		2.69	0.81	0
		6.37 (ε_o)	0	0
		2.22 $(n_D)^2$	0	0
		CHLOROBENZENE		
30.0	303.0	2.52	0.37	0
		2.54	0.61	0
		2.96	1.12	P
		3.41	1.43	P
		4.61	1.41	P
		5.43	0.59	P
		5.53 (ε_o)	0	P
		5.56 (ε_o)	0	0
		2.31 $(n_D)^2$	0	0

TABLE I - (continued)

t(°C)	T(K)	ε'	ε"	Source Code*
		CHLOROBENZENE-continued		
10.0	283.0	2.60	0.31	O
		2.56	0.56	O
		2.95	0.67	H
		2.99	1.08	P
		3.51	1.44	P
		4.54	1.65	P
		4.67	1.62	H
		5.65	0.79	P
		5.96 (ε_o)	0	P
		5.80 (ε_o)	0	H
		5.99 (ε_o)	0	O
		2.34 $(n_D)^2$	0	O
- 9.8	263.2	2.64	0.28	O
		2.56	0.50	O
		2.91	0.78	H
		2.92	0.94	P
		3.45	1.44	P
		4.30	1.87	P
		4.46	1.65	H
		6.10 (ε_o)	0	H
		6.27 (ε_o)	0	P
		6.26 (ε_o)	0	O
		2.37 $(n_D)^2$	0	O
-28.5	244.5	2.61	0.25	O
		2.58	0.47	O
		2.88	0.90	H
		4.10	1.56	H
		6.40 (ε_o)	0	H
		6.64 (ε_o)	0	O
		2.40 $(n_D)^2$	0	O

TABLE I - (continued)

t(°C)	T(K)	ε'	ε"	Source Code*
		BROMOBENZENE		
30.0	303.0	2.62	0.24	O
		2.54	0.37	O
		2.80	0.78	P
		2.82	0.76	H
		4.12	1.43	H
		4.12	1.36	P
		5.06	0.70	P
		5.32 (ε_o)	0	P
		5.32 (ε_o)	0	H
		5.27 (ε_o)	0	O
		2.42 $(n_D)^2$	0	O
10.0	283.0	2.67	0.23	O
		2.56	0.36	O
		2.82	0.64	H
		2.89	0.63	P
		3.19	1.10	P
		3.89	1.44	P
		5.13	0.96	P
		3.99	1.44	H
		5.64 (ε_o)	0	H
		5.61 (ε_o)	0	P
		5.68 (ε_o)	0	O
		2.45 $(n_D)^2$	0	O

TABLE I - (continued)

t(°C)	T(K)	ε'	ε"	Source Code*
		BROMOBENZENE-continued		
- 9.0	264.0	2.71	0.19	O
		2.58	0.30	O
		2.81	0.52	H
		2.81	0.50	P
		2.98	0.84	P
		3.61	1.41	P
		3.77	1.34	H
		5.89 (ε_o)	0	H
		5.90 (ε_o)	0	P
		5.93 (ε_o)	0	O
		2.48 $(n_D)^2$	0	O
-29.0	244.0	2.70	0.16	O
		2.58	0.24	O
		2.80	0.40	H
		3.47	1.10	H
		6.18 (ε_o)	0	H
		6.27 (ε_o)	0	O
		2.51 $(n_D)^2$	0	O
		IODOBENZENE		
30.0	303.0	2.88	0.25	O
		2.69	0.35	O
		2.82	0.39	H
		3.28	0.86	H
		4.46 (ε_o)	0	H
		2.58 $(n_D)^2$	0	O

TABLE I - (continued)

t(°C)	T(K)	ε'	ε"	Source Code*
		IODOBENZENE (continued)		
10.0	283.0	2.82	0.19	0
		2.73	0.33	0
		2.85	0.32	H
		3.13	0.71	H
		4.70 (ε_o)	0	H
		2.62 $(n_D)^2$	0	0
- 9.7	263.3	2.90	--	0
		2.78	0.28	0
		2.88	0.25	H
		3.04	0.56	H
		4.95 (ε_o)	0	H
		2.64 $(n_D)^2$	0	0
-29.3	243.7	2.94	--	0
		2.81	0.25	0
		2.90	0.19	H
		3.00	0.42	H
		5.20 (ε_o)	0	H
		2.67 $(n_D)^2$	0	0
		1,1,1 -TRICHLOROETHANE		
45.0	318.0	2.16	0.83	0
		3.00	1.92	0
		6.55	0.48	0
		6.59	0.09	0
		2.03 $(n_D)^2$	0	0
20.0	293.0	2.27	0.90	0
		2.67	1.61	0
		4.02	2.44	P
		5.20	2.42	P
		6.64	1.59	P
		7.28	0.69	0
		7.25	0.11	0

TABLE I - (continued)

t(°C)	T(K)	ε'	ε"	Source Code*
		1,1,1-TRICHLOROETHANE (continued)		
20.0	293.0	7.2 (ε_o)	0	P
		7.17 (ε_o)	0	0
		2.07 $(n_D)^2$	0	0
-20.0	253.0	2.51	0.90	0
		2.78	1.37	0
		8.33	0.17	0
		2.11 $(n_D)^2$	0	0
		BENZONITRILE		
50.0	323.0	3.20	1.24	0
		3.48	1.90	0
		23.12	1.63	0
		23.09 (ε_o)	0	0
		2.29 $(n_D)^2$	0	0
35.0	308.0	3.34	0.99	0
		3.44	1.85	0
		24.16	2.02	0
		24.31 (ε_o)	0	0
		2.32 $(n_D)^2$	0	0
21.0	294.0	3.14	0.97	0
		3.38	1.69	0
		3.99	3.07	P
		4.64	4.29	P
		7.17	7.98	P
		9.39	9.65	P

TABLE I - (continued)

t(°C)	T(K)	ε'	ε"	Source Code*
		BENZONITRILE (continued)		
		25.23	2.81	0
		25.63 (ε_o)	0	0
		2.33 $(n_D)^2$	0	0
5.0	278.0	3.15	1.03	0
		3.54	1.50	0
		26.65	3.65	0
		27.09 (ε_o)	0	0
		2.36 $(n_D)^2$	0	0
-10.0	263.0	3.34	1.35	0
		28.31	5.14	0
		28.60 (ε_o)	0	0
		2.38 $(n_D)^2$	0	0

*Source Code:

O - Own data
P - van Eick and Poley, reference 2, Chapter III
H - Mallikarjun and Hill, reference 9, Chapter III

TABLE II - LIMITING HIGH-FREQUENCY DIELECTRIC CONSTANTS AND SQUARED REFRACTIVE INDICES FOR SIX PURE LIQUIDS

t(°C)	T(K)	ε_∞	$(n_D)^2$	$\Delta\varepsilon$	Source Code
		FLUOROBENZENE			
30.0	303.0	2.33	2.13	0.20	0
10.0	283.0	2.45	2.16	0.29	0
- 9.4	263.6	2.52	2.20	0.32	0
-29.9	243.1	2.53	2.22	0.31	0
		CHLOROBENZENE			
30.0	303.0	2.47	2.30	0.17	P
		2.46	2.31	0.15	0
10.0	283.0	2.71	--	--	H
		2.63	2.34	0.29	P
		2.51	2.34	0.17	0
- 9.8	263.2	2.64	--	--	H
		2.66	2.37	0.29	P
		2.59	2.37	0.22	0
-28.5	244.5	2.60	--	--	H
		2.58	2.40	0.18	0
		BROMOBENZENE			
30.0	303.0	2.51	--	--	H
		2.55	2.41	0.14	P
		2.58	2.42	0.16	0
10.0	283.0	2.74	--	--	H
		2.72	2.45	0.27	P
		2.67	2.45	0.22	0
- 9.0	264.0	2.82	--	--	H
		2.73	2.48	0.25	P
		2.71	2.48	0.23	0
-29.0	244.0	2.89	--	--	H
		2.72	2.51	0.21	0
		IODOBENZENE			
30.0	303.0	2.69	--	--	H
		2.78	2.58	0.20	0
10.0	283.0	2.81	--	--	H
		2.82	2.61	0.21	0
- 9.7	263.3	2.87	--	--	H
		2.89	2.64	0.25	0
-29.3	243.7	2.90	--	--	H
		2.91	2.67	0.24	0

TABLE II - continued

$t(^{o}C)$	T(K)	ε_{∞}	$(n_D)^2$	$\Delta\varepsilon$	Source Code*
		1,1,1-TRICHLOROETHANE			
45.0	318.0	2.03	2.03	0	0
20.0	293.0	2.09	2.07	0.02	0
-20.0	253.0	2.41	2.11	0.30	0
		BENZONITRILE			
50.0	323.0	3.25	2.29	0.96	0
35.0	308.0	3.30	2.32	0.98	0
21.0	294.0	3.20	2.33	0.87	0
5.0	278.0	3.25	2.36	0.89	0
-10.0	263.0	3.25	2.38	0.87	0

NOTE: Estimated error on ε_{∞} values is ± 0.05 for all except benzonitrile, for which it is ± 0.10. Since the errors on squared refractive indices are much smaller than this, the same error estimates apply to $\Delta\varepsilon$.

*Source Code:
0 - Own data
P - van Eick and Poley, reference 2, Chapter III
H - Mallikarjun and Hill, reference 9, Chapter III

TABLE III RESULTS OF COMPUTER ANALYSES OF DIELECTRIC DATA FOR SOME SMALLER MOLECULES

T (K)	τ (μs)	log $f_{max.}$	Error* $\pm$	β	$\Delta\varepsilon''$ (max.)	ε_∞	μ (D)
			0.2649M Acetophenone in polystyrene				
143	966	2.217	.044	.187	.01139	2.646	1.208
149	377	2.625	.016	.188	.01184	2.640	1.255
153	161	2.995	.014	.194	.01222	2.636	1.275
159	75.1	3.326	.020	.195	.01269	2.631	1.321
163	39.8	3.602	.031	.205	.01309	2.628	1.327
168	18.01	3.946	.056	.213	.01349	2.625	1.342
172	10.74	4.171	.056	.221	.01374	2.622	1.347
192	1.191	5.126	.061	.235	.01370		
199	0.669	5.376	.041	.231	.01396		
202	0.425	5.573	.048	.249	.01434		
207.5	0.300	5.725	.049	.248	.01468		
213	0.187	5.930	.032	.258	.01506		
			0.263M Acetophenone in polystyrene				
141.5	641	2.395		.184	.01612	2.631	1.426
146	291	2.738		.188	.01645	2.627	1.454
150	118.1	3.129		.188	.01700	2.621	1.503
154.5	65.4	3.386		.199	.01734	2.621	1.499
158.5	40.2	3.597		.204	.01783	2.618	1.529
162.5	20.4	3.893		.211	.01837	2.614	1.551
168.5	10.65	4.175		.220	.01888	2.609	1.566
			0.193M 1,4-diacetylbenzene in polystyrene				
133	875	2.260		.154	.00610	2.624	1.091
141.5	154.6	3.013		.163	.00666	2.612	1.153
150	50.1	3.502		.168	.00700	2.605	1.209
158.5	11.41	4.144		.184	.00753	2.596	1.239
168.5	2.70	4.771		.207	.00829	2.585	1.267

TABLE III - continued

T (K)	τ (μs)	log $f_{max.}$	Error* ±	β	Δε" (max.)	ε_∞	μ (D)
		6.85M (pure) 1,4-diacetylbenzene					
137.5	681	2.369	.043	.691	.00436	2.941	0.070
146	148.2	3.031	.028	.684	.00420	2.930	0.072
154.5	50.2	3.501	.083	.607	.00405	2.919	0.078
162.5	14.97	4.027	.035	.670	.00400	2.903	0.076
		0.194M 2,4,6-trimethylacetophenone in polystyrene					
139.1	716	2.347	.078	.282	.00843	2.605	0.987
145.8	338	2.673	.081	.268	.00880	2.597	1.061
149.4	190.2	2.923	.047	.281	.00901	2.593	1.062
152.2	140.5	3.054	.054	.274	.00923	2.599	1.097
156.2	88.4	3.255	.054	.272	.00945	2.583	1.131
160.0	51.3	3.492	.044	.283	.00978	2.576	1.144
165.8	27.4	3.764	.078	.277	.01026	2.577	1.204
168.6	20.57	3.889	.066	.284	.01044	2.568	1.213
178.0	7.50	4.327	.070	.285	.01088	2.566	1.271
185.5	3.34	4.678	.035	.294	.01149	2.559	1.314
187.9	2.67	4.776	.045	.353	.01135		
202.2	1.210	5.119	.040	.350	.01220		
214.5	0.471	5.528	.031	.370	.01334		
222.8	0.254	5.797	.027	.380	.01399		
236.9	0.122	6.114	.021	.393	.01499		
		0.1623M 4-acetylbiphenyl in polystyrene					
146	279	2.756	.122	.175	.00241	2.604	0.751
150	103.6	3.187	.094	.182	.00252	2.599	0.770
154	75.4	3.325	.064	.167	.00259	2.597	0.831
158.5	39.8	3.602	.035	.156	.00276	2.590	0.896
167	9.13	4.241	.076	.158	.00301	2.582	0.953
172	5.40	4.470	.080	.139	.00326	2.576	1.064

TABLE III - continued

T (K)	τ (μs)	log $f_{max.}$	Error* ±	β	Δε" (max.)	ε_∞	μ (D)
		0.161M 4-acetylbiphenyl in polystyrene					
311.3	756	2.323	.075	.199	.00807	2.606	1.893
314.8	606	2.419	.066	.194	.00815	2.604	1.934
317.2	484	2.517	.028	.198	.00821	2.603	1.932
320.0	363	2.642	.021	.200	.00826	2.602	1.937
323.9	272	2.767	.025	.196	.00830	2.600	1.975
326.9	203.8	2.893	.053	.190	.00833	2.597	2.017
331.4	153.6	3.015	.039	.188	.00839	2.595	2.053
		5.85M (pure) 4-acetylbiphenyl					
154.5	2691	1.772	.170	.404	.00058	2.814	0.040
162.5	639	2.397	.068	.435	.00059	2.801	0.040
172	149.0	3.029	.091	.489	.00061	2.790	0.040
182	55.2	3.460	.122	.565	.00065	2.771	0.039
192	13.55	4.070	.173	.239	.00063	2.748	0.062
		0.5381M 4-nitrobiphenyl in polystyrene					
294.5	699	2.358	.074	.194	.05595	2.581	2.560
295.5	585	2.434	.063	.199	.05654	2.584	2.549
298.9	422	2.577	.060	.192	.05763	2.567	2.631
302.5	297	2.729	.066	.188	.05924	2.560	2.713
305.4	216	2.868	.049	.185	.06086	2.550	2.782
308.6	135.0	3.071	.038	.185	.06284	2.541	2.835
312.5	82.1	3.287	.044	.178	.06540	2.520	2.964

TABLE III - continued

T (K)	τ (μs)	log $f_{max.}$	Error* ±	β	Δε" (max.)	ε_∞	μ (D)
		0.1999M N-acetylindole in polystyrene					
192	617	2.412	.118	.142	.00570	2.594	1.332
202	130.6	3.086	.099	.141	.00608	2.587	1.418
212	42.1	3.577	.091	.138	.00641	2.573	1.513
222	8.32	4.282	.120	.124	.00688	2.566	1.686
		0.1539M 2-acetylfluorene in polystyrene					
158.5	413	2.585	.120	.194	.00245	2.593	0.776
162.5	246	2.811	.045	.183	.00255	2.588	0.829
172	65.9	3.383	.055	.182	.00274	2.587	0.887
177	27.9	3.757	.073	.168	.00285	2.579	0.957
		0.1539M 2-acetylfluorene in polystyrene					
317	363	2.642	.039	.177	.00711	2.563	1.966
322	232	2.836	.065	.179	.00727	2.564	1.990
327	149.9	3.026	.064	.176	.00739	2.557	2.042
332	89.5	3.250	.051	.170	.00750	2.551	2.112
337	44.3	3.555	.073	.176	.00757	2.548	2.104
		4.06M (pure) 2-acetylfluorene					
212	418	2.580	.120	.184	.00239	3.947	0.137
222	138.9	3.059	.133	.213	.00264	3.959	0.137
232	70.9	3.351	.131	.229	.00283	3.963	0.140
242	36.2	3.643	.073	.263	.00307	3.969	0.139

TABLE III - continued

T (K)	τ (μs)	log $f_{max.}$	Error* ±	β	$\Delta\varepsilon''$ (max.)	ε_∞	μ (D)
			0.224M 4-methylacetophenone in polystyrene				
177	425	2.574	.019	.159	.01369	2.625	1.742
182	274	2.765	.050	.151	.01405	2.618	1.839
187	142.5	3.048	.013	.155	.01433	2.614	1.859
192	62.9	3.403	.050	.154	.01476	2.609	1.918
199	26.9	3.772	.044	.162	.01536	2.604	1.944
202	18.50	3.935	.044	.163	.01556	2.604	1.967
			0.192M 4-nitroacetophenone in polystyrene				
212	563	2.452	.151	.131	.00930	2.611	1.878
222	250	2.804	.065	.137	.00975	2.607	1.929
232	91.7	3.240	.067	.145	.01018	2.602	1.959
242	41.1	3.588	.088	.158	.01057	2.601	1.958
252	14.42	4.043	.077	.161	.01096	2.597	2.018
			0.2533M 1-acetylcyclohexene in polystyrene				
133	560	2.454	.110	.207	.01234	2.660	1.156
137.5	383	2.618	.111	.185	.01292	2.647	1.275
141.5	171.3	2.968	.073	.183	.01331	2.642	1.325
146	63.4	3.399	.078	.170	.01359	2.636	1.413
150	46.0	3.540	.052	.176	.01394	2.630	1.432
154.5	26.4	3.781	.049	.175	.01422	2.624	1.479
158.5	12.98	4.089	.039	.168	.01475	2.614	1.561

TABLE III - continued

T (K)	τ (μs)	log $f_{max.}$	Error* ±	β	Δε" (max.)	ε_∞	μ (D)
		0.2047M bromocyclohexane in polystyrene					
236.9	1177	2.131	.164	.665	.00413	2.683	0.568
240.3	802	2.297	.057	.712	.00410	2.681	0.551
244.2	526	2.481	.023	.773	.00405	2.679	0.530
248.4	355	2.651	.016	.783	.00394	2.677	0.524
253.5	231	2.838	.017	.788	.00375	2.675	0.515
258.7	151.6	3.021	.043	.729	.00362	2.672	0.532
264.5	91.8	3.239	.033	.739	.00343	2.669	0.520
273.0	42.5	3.574	.026	.767	.00310	2.666	0.493
281.7	21.8	3.864	.023	.790	.00292	2.661	0.480
292.2	11.14	4.155	.057	.710	.00265	2.653	0.492
294:5	10.58	4.177	.201	.694	.00271	2.649	0.506
302.6	3.69	4.635	.160	.516	.00241	2.643	0.561
		0.2335M 4-methoxybenzaldehyde in polystyrene					
194.6	505	2.499	.031	.206	.02026	2.617	1.906
200.0	257	2.793	.044	.206	.02089	2.613	1.961
205.2	138.8	3.059	.043	.220	.02134	2.613	1.945
210.4	88.5	3.255	.040	.216	.02175	2.609	2.009
216.0	46.9	3.530	.042	.227	.02228	2.608	2.010
220.8	27.0	3.771	.055	.219	.02289	2.601	2.095
225.6	18.86	3.926	.047	.228	.02341	2.605	2.098
233.2	10.23	4.192	.093	.231	.02409	2.601	2.154
237.0	5.57	4.456	.081	.218	.02441	2.590	2.251

* The error estimate quoted is the 95% confidence interval calculated by computer from the experimental data's fit to the best straight line on a Fuoss-Kirkwood analysis graph.

NOTE:

A blank space indicates that the information was not available.

TABLE IV RELAXATION PARAMETERS FOR SEVERAL SMALLER MOLECULES IN A POLYSTYRENE MATRIX (ps) OR AS PURE SOLIDS (pure)

Molecule	T (K)	ΔH_E (kJ mol^{-1})	ΔS_E (JK^{-1} mol^{-1})	ΔG_E(kJ mol^{-1}) 150K	225K	300K	τ(μs) 150K	225K	300K
Acetophenone (ps)	143-213	30	26	26	24	22	2.8×10^{2}	6.9×10^{-2}	9.8×10^{-4}
(ps)	141-168	29	28	25	23	21	1.4×10^{2}	4.1×10^{-2}	6.4×10^{-4}
1,4-diacetyl-benzene (ps)	133-168	29	36	23	21	18	41	1.3×10^{-2}	2.0×10^{-4}
(pure)	137-162	27	16	24	23	22	87	4.7×10^{-2}	9.9×10^{-4}
2,4,6-tri-methylaceto-phenone (ps)	139-237	23	-12	25	26	27	1.8×10^{2}	0.23	7.7×10^{-3}
4-acetylbi-phenyl (ps)	146-172	30	35	25	22	20	1.3×10^{2}	2.9×10^{-2}	4.0×10^{-4}
(ps)	311-331	68	33	63	61	58	3.0×10^{15}	2.6×10^{7}	2.2×10^{3}
(pure)	154-192	33	21	29	28	26	5.5×10^{3}	0.61	5.9×10^{-3}
N-acetyl-indole (ps)	192-222	48	70	38	32	27	3.7×10^{6}	6.6	8.2×10^{-3}
2-acetyl-fluorene (ps)	158-177	32	28	28	26	24	1.9×10^{3}	0.22	2.3×10^{-3}
(ps)	317-337	89	100	74	66	59	1.6×10^{19}	5.3×10^{8}	2.8×10^{3}
(pure)	212-242	32	-24	36	38	40	1.1×10^{6}	1.2×10^{2}	1.2

TABLE IV continued

Molecule	T (K)	ΔH_E (kJ mol^{-1})	ΔS_E (JK^{-1} mol^{-1})	ΔG_E(kJ mol^{-1}) 150K	225K	300K	τ(μs) 150K	225K	300K
Iodobenzene (ps)	129-163*	16	-43	22	25	29	19	0.18	1.6×10^{-2}
4-bromo-toluene (ps)	174-264*	30	- 0.8	30	30	30	7.6×10^{3}	1.8	2.6×10^{-2}
4-nitrobi-phenyl (ps)	294-312	86	110	70	62	54	5.7×10^{17}	4.5×10^{7}	3.7×10^{2}
4-bromobi-phenyl (ps)	295-335*	60	21	57	55	54	1.8×10^{13}	1.3×10^{6}	3.3×10^{2}
4-methyl-acetophenone	177-202	37	32	32	30	28	5.4×10^{4}	1.8	9.8×10^{-3}
4-nitro-acetophenone (ps)	212-252	39	0.9	38	38	38	7.5×10^{6}	1.7×10^{2}	0.73
(pure)	133-314	no dielectric relaxation observed							

TABLE IV continued

Molecule	T (K)	ΔH_E (kJ mol^{-1})	ΔS_E (JK^{-1} mol^{-1})	ΔG_E(kJ mol^{-1}) 150K	225K	300K	τ(μs) 150K	225K	300K
1-acetyl-cyclohexene (ps)	133-158	25	13	23	22	22	44	3.4×10^{-2}	8.8×10^{-4}
2-furan-aldehyde (ps)	230-294	38	-17	41	42	43	4.5×10^{7}	1.2×10^{3}	5.4
Bromocyclo-hexane (ps)	237-303	47	13	45	44	43	2.1×10^{9}	4.4×10^{3}	5.9
4-methoxy-benzalde-hyde (ps)	194-237	38	15	35	34	33	6.7×10^{5}	19	9.3×10^{-2}

* Data provided through the courtesies of A. Lakshmi, A. Khwaja, and Mr. B. K. Morgan of this laboratory.

APPENDIX II

Diagrams of Molecular Structures

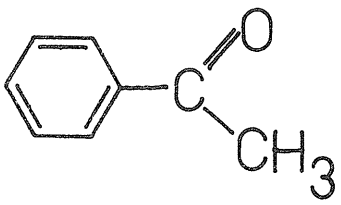

Acetophenone

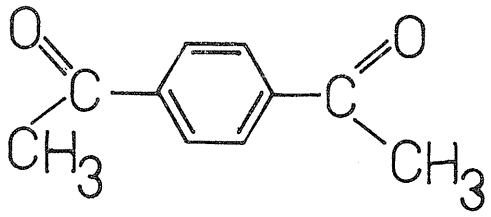

1,4-diacetylbenzene

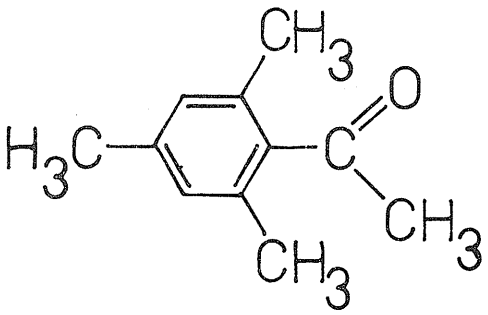

2,4,6-trimethylacetophenone

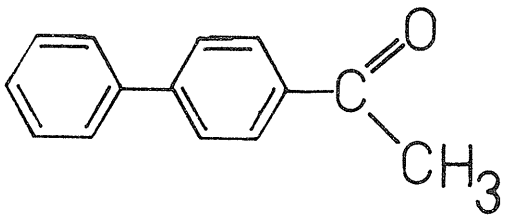

4-acetylbiphenyl

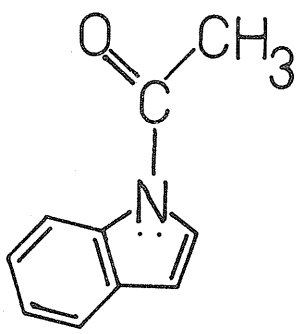

N-acetylindole

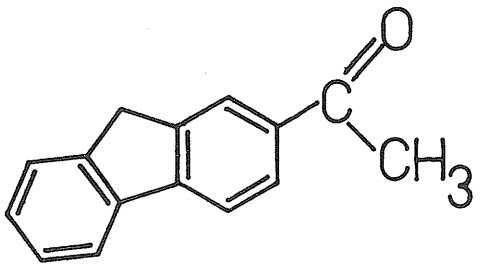

2-acetylfluorene

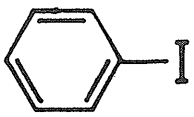

Iodobenzene

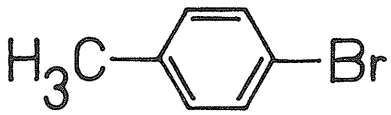

4-bromotoluene

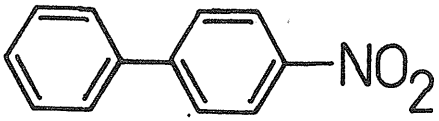

4-nitrobiphenyl

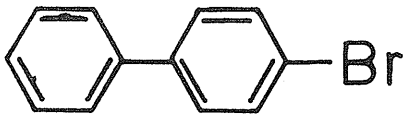

4-bromobiphenyl

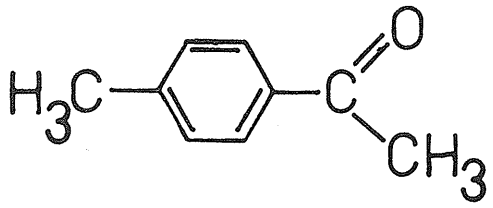

4-methylacetophenone

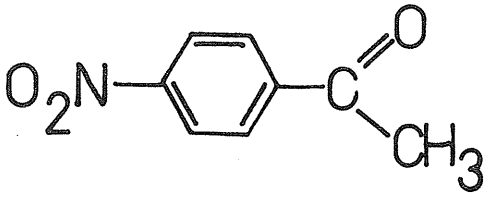

4-nitroacetophenone

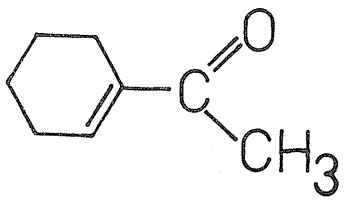

1-acetylcyclohexene

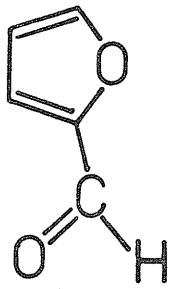

2-furanaldehyde

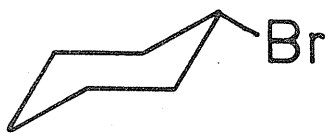

Bromocyclohexane

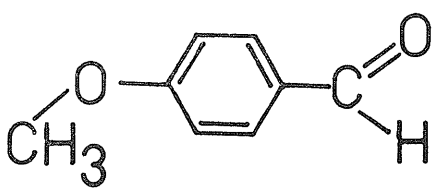

4-methoxybenzaldehyde